DRONES AND SATELLITES IN ESWATINI

2021

A Framework for Use of Unmanned Aerial Vehicles (UAVs) and Satellite Remote Sensing Technologies in Crop Monitoring

CTCN
CLIMATE TECHNOLOGY CENTRE & NETWORK

Framework and Case Study Report, the Kingdom of Eswatini.

This report was prepared by the Regional Centre for Mapping of Resources for Development (RCMRD) following the implementation of a Technical Assistance provided to the Eswatini National Disaster Management Agency (NDMA). Funding for this implementation was provided by the UNFCCC Climate Technology Centre and Network (CTCN). Opinions, expressions and representations provided in this report do not reflect the official position of the CTCN.
October, 2021.

Contents

Executive Summary

Overview: The Kingdom of Eswatini is experiencing an upward trend in mean annual temperature across the different parts of the country, as well as increased drought and flood incidences. Coupled with an increase in pests and diseases, and exacerbated by unemployment and increasing food commodity prices, major constraints have been placed on food security. The country's vulnerability assessment information still relies on pre-planting and post-harvest assessments, and oftentimes the annual National Agricultural Survey which aims to provide information on cropped area through questionnaires and field surveys is not consistently conducted due to resource and technology constraints. As a result, the country lacks continuous crop growth monitoring and assessment tools and technologies for quick and early detection of undesirable threats and occurrence of risks and hazards to food security. With Unmanned Aerial Vehicles (UAV) technology and satellite earth observations, it is expected that such assessments can be done with minimal human resources and during any phase of crop growth in order to deliver timely interventions. The Climate Technology Centre and Network (CTCN) implemented a Technical Assistance activity in the country through the Regional Centre for Mapping of Resources for Development (RCMRD) and national stakeholders to demonstrate the benefits of using UAVs and satellite remote sensing for crop growth monitoring using a case study approach.

Objective and Data collection: The main objective of this activity was to develop framework and case study is to enhance the capacity of national agencies in Eswatini to monitor agricultural performance through the use of UAVs and satellite remote sensing technologies. Four pilot sites were selected for the case study development namely Gege, Sidzakeni, Sigangeni and Mpolonjeni. Three types of drones were used: DJI Phantom 4, DJI Matrice 200 and WingtraOne fixed-wing drone. Data were collected from the four sites in April 2021 with the leadership of the National Disaster Management Agency (NDMA). In addition to the UAV data, satellite imagery from Sentinel-2 was also acquired for the same areas over the same period to aid in land cover mapping with a focus on demonstrating methods for generating cropland extents over the entire country using a combination of UAV and satellite data. Several vegetation indices were also acquired from the MODIS satellites and used as predictor variables for a yield prediction framework. Lastly, a gender analysis was conducted through an analysis of existing literature on how

gender aspects are incorporated in agricultural technologies and gaps that exist in Eswatini that can be strengthened to reduce gender disparities.

Outcomes: The first part of this report covers key areas that serve as a guide to national stakeholders to successfully initiate an operational crop monitoring program. Specifically, it demonstrates the vital importance of identifying the right combination of stakeholder participation, timing for monitoring activities and coordination amongst implementing partners. Further, it also provides the required type of UAVs in order to optimize data collection and complementary data from satellite sources that can supplement data collected in the field using drones. It also details data and methods for gender analysis with a focus on agricultural technologies that may have gender dimensions that are necessary to consider, especially outcomes that are intended to improve gender participation in the development and implementation of agricultural technologies. The second part covers the case stakeholder consultations, data collection and data analysis case study. Several products were generated from the case study.

First, methods were developed to merge UAV and satellite data through fusion techniques. These methods were implemented in the R programming tool which has several advantages as an open-source tool. Secondly, methods were also developed to generate vegetation indices from UAV imagery. The case study focused on the Normalized Difference Vegetation Index (NDVI) which is widely used in crop growth monitoring. Thirdly, methods were developed for generating crop extents from UAV, satellite and fused UAV-satellite products through the use of image classification techniques. Lastly, a statistical yield prediction algorithm was developed that uses crop growth indices from satellite data and yield statistics from field surveys. This model was applied on the maize crop nationally for the year 2020. A climate analysis using historical data and projected climate model data, as well as a detailed gender analysis were done to support the case study. Finally, an overview of early warning systems that are focused on crop condition monitoring using satellite data was also completed with demonstrations of how these can be used in Eswatini for risk assessments to crop growth and for risk forecasting. It is hoped that outputs from this activity shall serve as an important resource for improving climate resilience in Eswatini through the enhancement of existing efforts that target agricultural monitoring in the country.

List of Figures

List of Tables

1. Introduction

1.1 Purpose of the Framework

The Kingdom of Eswatini is experiencing an upward trend in mean annual temperature across the different parts of the country, as well as increased drought and flood incidences. Coupled with an increase in pests and diseases, and exacerbated by unemployment and increasing food commodity prices, major constraints have been placed on food security. The country's vulnerability assessment information still relies on pre-planting and post-harvest assessments, and oftentimes the annual National Agricultural Survey which aims to provide information on cropped area through questionnaires and field surveys is not consistently conducted due to resource and technology constraints. As a result, the country lacks continuous crop growth monitoring and assessment tools and technologies for quick and early detection of undesirable threats and occurrence of risks and hazards to food security. With Unmanned Aerial Vehicles (UAV) technology and satellite earth observations, it is expected that such assessments can be done with minimal human resources and during any phase of crop growth in order to deliver timely interventions.

The National Disaster Management Agency (NDMA) and the National Designated Entity (NDE) of Eswatini; the Eswatini Meteorological Service requested support for technical assistance from the Climate Technology Centre and Network (CTCN) with the overall objective to strengthen Eswatini's climate resilience, disaster risk reduction and vulnerability assessments in the agricultural sector. This strengthening would be achieved by building capacity on the application of UAV technology and remotely sensed imagery for crop monitoring and early warning systems. This technical assistance aimed to:

i enhance the capacity of national stakeholders, including the National Disaster Management Agency, on the application of UAV technology and remotely sensed imagery for crop monitoring and provision of timely early warning data to farmers
ii make available a set of baseline data for agricultural indicators in support of vulnerability assessments and decision-making, and
iii improve the country's readiness to seek GCF funding for up-scaling of technologies

This framework is expected to strengthen the country's capacity to identify, plan for and respond to climate-induced vulnerabilities and food insecurity situation in the country.

It will allow for more effective data management and decision making around vulnerability assessment, food security and response, and enhance the use of climate information to increase resilience to broader climate change impacts and shocks for populations at risk of acute food insecurity in the country. The framework has several components that address stakeholder engagement, description of key agricultural monitoring indicators that can be measured using UAVs and satellites, and data sources for these indicators. It also addresses key data and tools necessary for an operational crop health monitoring program across the country, including specifications of UAV technologies required to support crop monitoring (type of drones, supporting infrastructure and skills). A detailed description of these requirements is provided in the first section of the framework while the case study sections provide a use-case of how a combination of UAV and satellite remote sensing technologies were piloted in the country as broadly illustrated in the flow chart in Figure 1. Lastly, detailed step-by-step guidelines are provided in the Annexes providing descriptions of how the case study was implemented using open-source analytical tools that are freely available over the web.

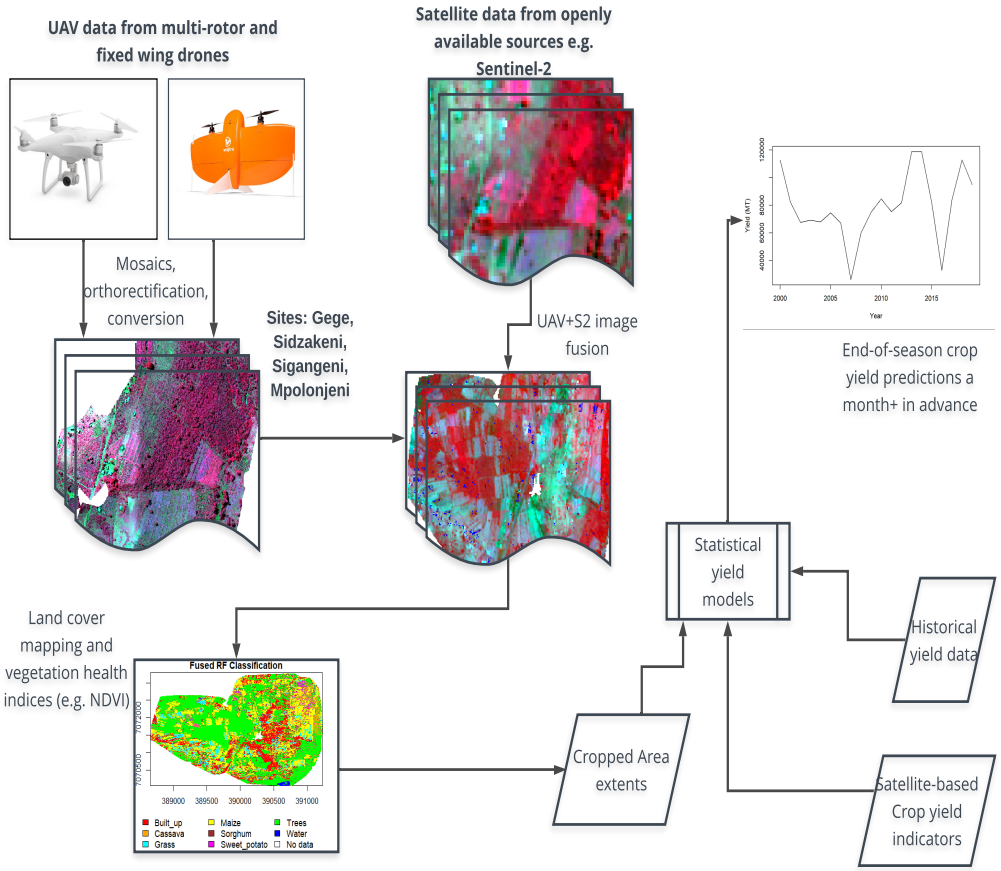

Figure 1: A flowchart illustrating general processes for merging UAV and satellite imagery to map crop health indicators, cropland extents and end-of-season yield forecasting.

1.2 Target Audience/Users

This framework was written with the intention of assisting stakeholders working at the national and sub-national levels optimize the use of new and innovative technologies that have benefits that can improve climate resilience in Eswatini. It is assumed that the audience may have little or no prior knowledge of the use of drones or UAVs and satellite remote sensing technologies in crop monitoring, but needs to understand how to use such technologies in the identification of risks to crop health and production in the most cost-effective approaches so that appropriate decisions and interventions can be designed and implemented to improve food security preparedness in the country. Broadly, such interventions would rely on a combination of data from UAVs and satellites, as well as an effective coordination amongst stakeholders working in the agricultural sector.

The intention of this framework is to provide a useful reference for data collection, analysis and synthesis, and communication of information to various users in the country in such ways as to provide early warning information for preparedness purposes. Such information would also serve to provide insights about threats to crops from climate and non-climate related risks with the goal of improving agricultural policy development to increase the resilience of the country's population and guarantee food security. It is expected that this framework will serve as a support tool to existing national programs that are focused on food security and agricultural vulnerability assessments.

Box 1

UAV imagery provides very high spatial resolution imagery at local scales than most freely available satellite data. On the other hand, satellites provide high spectral resolution imagery, wider spatial coverage and higher temporal resolution than UAVs. A combination of the two sources through merging techniques draws from the advantages of both types of imagery making regular crop health monitoring, extent mapping and yield forecasting possible.

1.3 Institutional Mapping

Planning for climate-resilient societies is not a singular event and is not a task for one particular institution or sector nor is it a one-time or infrequent exercise. Even more, activities that improve the collection and use of agricultural monitoring data and information is a multi-agency undertaking. Given the nature of information required to make decisions that impact food security for millions of people in Eswatini, and the diversity of skills, knowledge, logistics, power, influence and roles in the food security sector, it is recommended that a number of institutions are involved during the implementation of interventions that promote coordination and cooperation in assessing crop conditions, climate risks and providing early warning information to decision makers.

Although this framework was developed based on the technical assistance requested through the NDE and NDMA, a number of stakeholders are key to ensuring an operational crop monitoring and assessment program using UAVs and satellite data. These stakeholders are listed below with their envisaged roles:

i **National Disaster Management Agency:** NDMA works under the Office of the Prime Minister whose mandate is to prevent and substantially reduce the impact of

disasters by promoting an integrated and coordinated system of disaster management focused on decreasing vulnerability, increasing preparedness and mitigation capacity. NDMA has acquired drones that can be deployed for disaster response and this framework and case study was accomplished through use of these drones. This framework was developed with the intention of building the capacity of NDMA and other stakeholders to optimize the use of drones and satellite technologies and it is expected that the agency would take a leading role in the operationalization of these technologies.

ii **Ministry of Agriculture:** MoA is the agency through which the government coordinates all agricultural related activities and programs. The primary mandate of MoA is to ensure household food security and increased sustainable agricultural productivity through diversification and enhancement of commercial agricultural activities. The ministry is also responsible for the development and promotion of appropriate technologies and efficient extension services while ensuring stakeholder participation and sustainable development and management of natural resources in the country. A range of activities that target agricultural monitoring are coordinated by MoA. As such, the critical role of determining, planning and coordination of the timing of data collection using drones, data analysis and information dissemination would be the role of MoA assisted by NDMA and other relevant stakeholders.

iii **Eswatini Meteorology Service:** The meteorological service is the primary institution mandated to collect, analysis and disseminate weather and climate information to the public. For a successful monitoring of existing, emerging and future climate risks to the agricultural sector, EMS is a key partner in the implementation of the proposed technologies. Besides monitoring crop conditions using drones and UAVs, meteorological information such as rainfall and temperature forecasts are vital for the determination of risks to in-season and out-of-season environmental conditions that may impact crop production.

iv **Eswatini Civil Aviation Authority:** ESWACAA is an administrative and commercial body corporate mandated to provide, in an economically viable manner, air transport services and regulation of civil aviation activities in Eswatini; in accordance with international standards. UAVs operation approvals fall under ESWACAA and permission to operate any type of UAV or Remotely Piloted Aerial Systems (RPAS) must be sought before the operation of such equipment in the field. The authority has released advisories to concerned members of the public and a list of documents that need to be filled are available from the authority.

v **Eswatini Central Statistical Office:** CSO's mission is to effectively coordinate the National Statistical System, provide high quality statistical data and information required for evidence-based policy, planning and decision-making for national socio-economic development, administration, accountability, and to promote a culture of using statistics. A comprehensive climate risk assessment requires biophysical and socio-economic data. Much of the socio-economic data are collected by CSO through period agricultural and household surveys. Such data are important for early warning systems. For example, a robust end-of-season crop yield forecast will depend on good quality yield data collected from past agricultural surveys. Likewise, inorder to estimate number of people under risk of food insecurity at any given point, household surveys and census surveys are important sources of such data, and these are usually collected by the CSO.

vi **Academia and research institutions:** Research institutions are critical in training, knowledge generation and transfer of technologies. Introduction of new technologies

like the use of UAVs and satellites will require a skilled pool of technicians who are able to carry out data analysis and generate information that is relevant for decision making. It is thus important to make such institutions an important stakeholder for training and retraining of drone pilots, remote sensing data analysts and other skills required to successfully deploy technologies to support agricultural development.

vii **Regional and International Organizations:** A number of regional and international agencies working with and support food security programs in Eswatini. They include United Nations agencies like the Food and Agicultural Organization (FAO), the World Food Programme (WFP) amongst others. These agencies are critical to promoting agricultural development and food security in the country, and as such, are important stakeholders in the development and implementation of digital agricultural technologies in the country.

viii **Farmer groups and organizations:** There are a number of community based organizations and groups that support rural farming and promote gender participation in agricultural activities in Eswatini. A good example is the Women Farmer Foundation which strives to empower and develop women and youth in the agricultural sector in Eswatini, in the process uplift their low social and economic status. Such farmer-based organizations are critical in building awareness, training and piloting of agricultural technologies that aim is to improve gender participation and equality.

ix **Private sector:** UAVs are to a large extent being developed and manufactured by private companies. It is expected that this trend will continue to exist due to the sector's expertise in engineering technologies that are otherwise not readily available in public institutions. It is imperative to consider integrating drone manufacturers in the stakeholder engagements as drone technologies continue to improve and expand into developing regions. Adaptation of such technologies will often face challenges that include amongst others, repair and replacement of drone components like sensors etc. Involving private companies can ensure regualar support when implementing UAVs-supported services in Eswatini.

1.4 Timescales

Agencies working on the use of UAV technology for crop health monitoring must be aware of key timelines that may have an influence on decisions that should be made across the monitoring period. UAV technology can be used in various stages of crop growth including early emergence, stand and gap monitoring, scouting for crop pests and nutrient deficiency as well as during the critical period when crops begin flowering and seeding as illustrated in Figure 2. In Eswatini, crop calendars for major crops need to be taken into account when planning when to deploy UAVs. Taking the maize crop as an example, the main season begins sometime in the month of October and ends in May of the following year. The main growth period is between December and April (Figure 3).

When thinking about in and out-of season monitoring, it is recommended to leverage freely available satellite imagery to monitor out of season conditions, especially soil moisture and evapotranspiration trends as those may have an impact on early stages of crop growth (emergence). This would be the period between May and September. As the start-of-season approaches, rainfall and temperature would then become a key parameter to introduce in the monitoring plan, with data coming from satellite products and/or in-situ data from the meteorological services. Upon sowing and emergence, drones can then be deployed to monitor germination rates and to identify any potential gaps that may require farmers to

replant if environmental conditions allow.

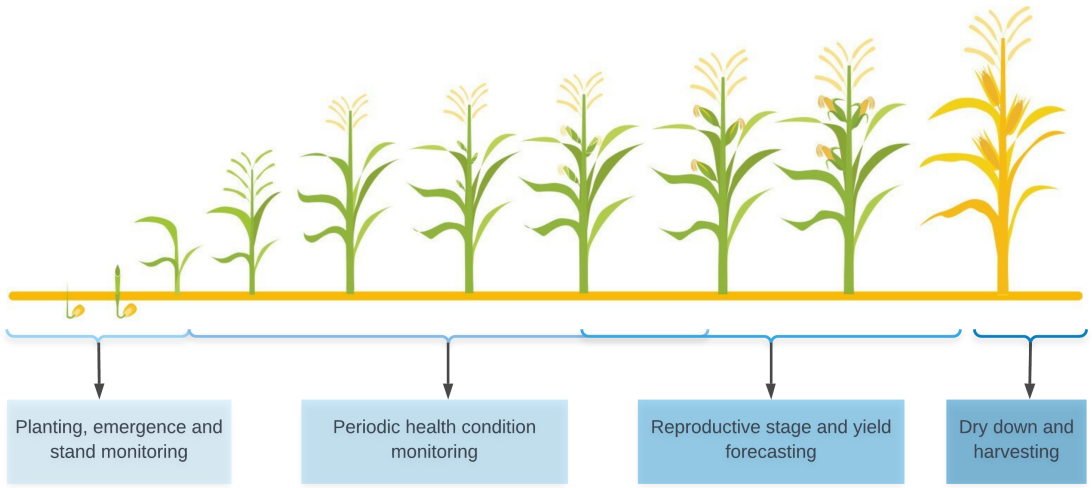

Figure 2: An example of UAV use in main growth stages for maize crop. UAV technology adds value throughout the growing season, from emergency and early growth assessments through to pre-harvest yield prediction.

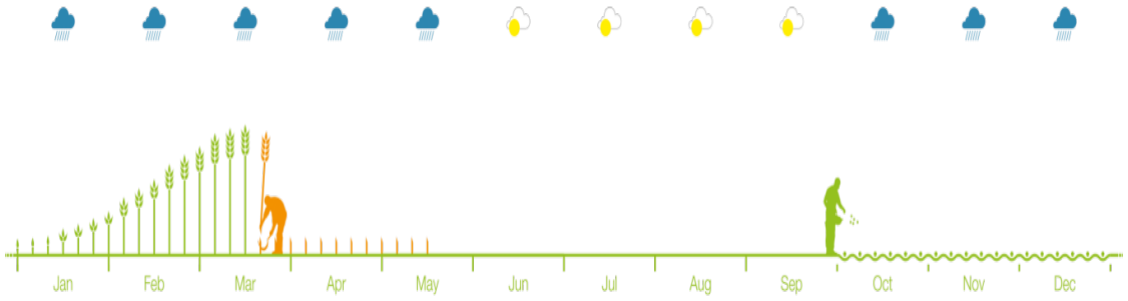

Figure 3: Eswatini cropping calendar. Source: FAO.

Active monitoring for biomass growth and the health of crops then follows the early stages where vegetation condition monitoring, in addition to environmental parameters (rainfall, temperature, evapotranspiration, soil moisture among others) is important. This can be achieved by a combination of UAVs and satellites. The latter would provide very quick outlooks of crop health over vast areas and where hotspots or areas of particular concern are observed (e.g., vegetation die down, nutrient deficiency observed through vegetation indices like Normalized Difference Vegetation Index (NDVI) etc.), then UAVs can be deployed to investigate conditions on the ground with high spatial details. Such a combination of data sources would present a cost-effective approach because only when there are concerns that warrant further investigation would it be necessary to deploy UAVs like shown in Figure 4. A critical stage where the scale of UAV use should be optimized is the main reproductive stages. This stage involves flowering and seeding and would have the most robust crop biomass. It is expected that vegetation monitoring indices such as NDVI would be most effective at this stage and recommendations are made to deploy UAVs to collect ground truth data for crop or planted area mapping during this stage. From a timing perspective, this would be the period between late November/early December and late February/March.

Additionally, this stage is appropriate for yield modeling and forecasting. Vegetation indices from satellite imagery such as NDVI, Leaf Area Index (LAI), Gross Primary

Productivity (GPP), Enhanced Vegetation Index (EVI), Soil Adjusted Vegetation Index (SAVI), Soil Moisture Index (SMI), and rainfall indices such as Standardized Precipitation Index (SPI) or Z-scores, among others should be gathered and prepared for such an analysis. It would be important to have a good historical context that relates production (yields) and these environmental indices that are known to influence crop growth and end-of-season production. Most predictions rely on statistical modeling such as regression models which are usually linear regressions but a significant effort is being dedicated to develop mechanistic models that apply a range of assumptions of how environmental parameters interact with other factors of production such as farming practices (e.g., fertilizer application, pest management, irrigation, tillage practices among others) and cultivars.

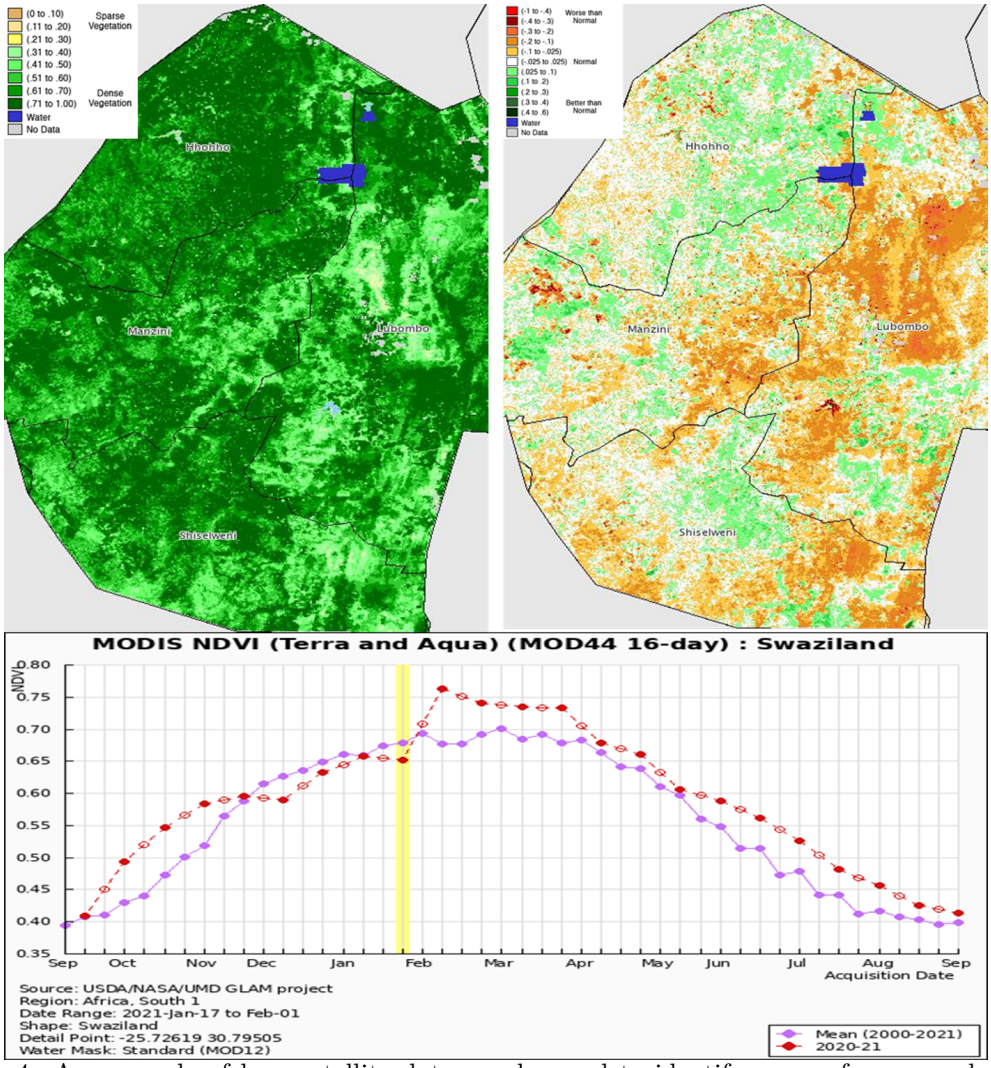

Figure 4: An exmaple of how satellite data can be used to identify areas of concern during a growing season. The two maps in this figure show current NDVI status (left) and an anomaly status (right) for the same period compared with the longterm expectation. As it can be seen here, and also in the graph below the maps, there are areas in the eastern provinces where vegetation performance for the period of interest (January-February 2021) was below expectation or "below normal". UAVs can be deployed to investigate the situation on the ground. Data source: `https://pekko.geog.umd.edu/usda/apps/`.

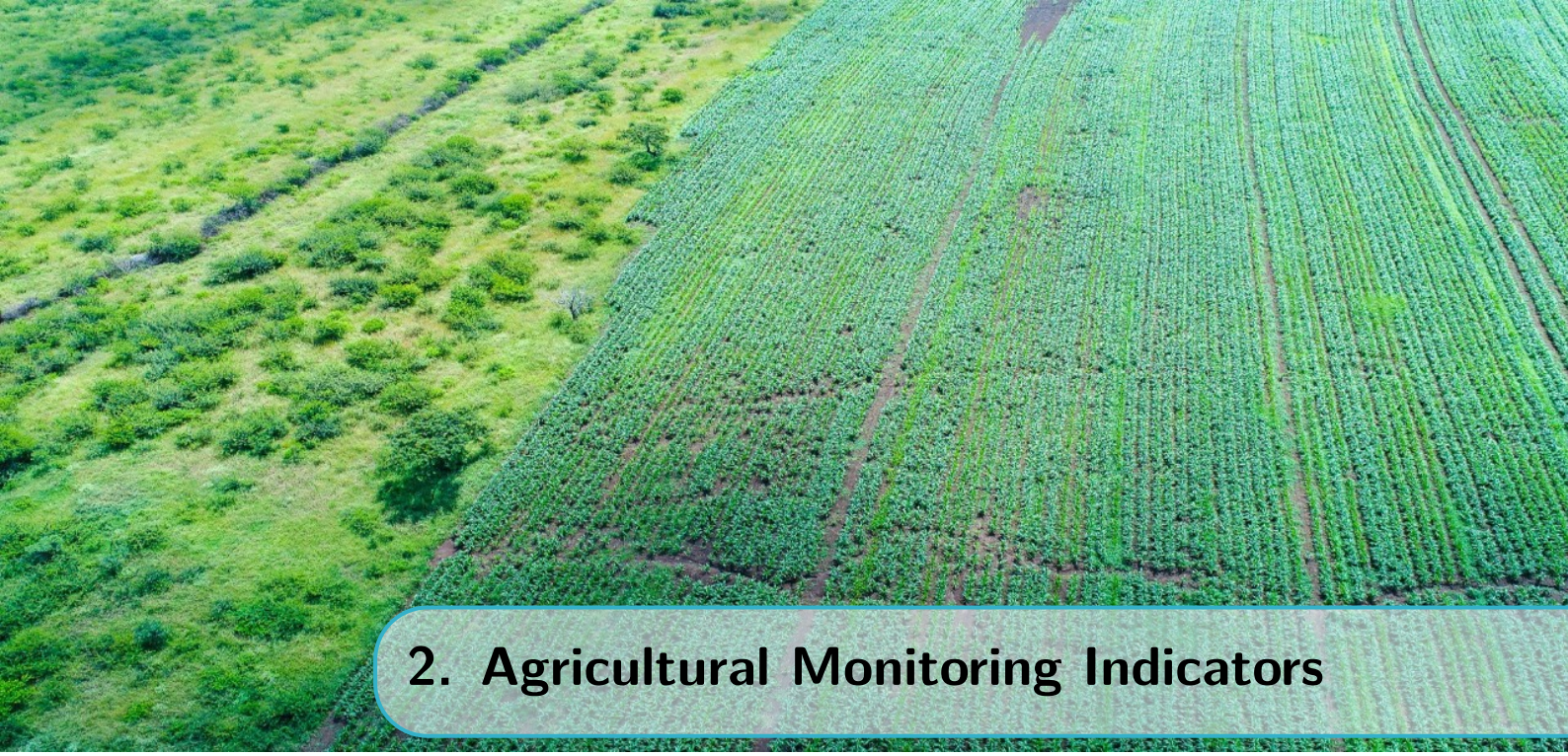

2. Agricultural Monitoring Indicators

2.1 Overview

A truly comprehensive agricultural monitoring program will track a variety of indicators including, generally; production, markets and prices, utilization and access, among others. This framework is however developed to focus only on indicators that may impact production, and which can be monitored using UAVs and satellite remote sensing. There are three broad categories which are discussed in this section namely climatic, vegetation health, crop production indicators.

2.2 Climatic Indicators

Climatic indicators have the greatest impact on crop growth conditions in regions which are dependent on rainfed agriculture. Rainfall is especially important as all crops require water to survive and develop. A regular rainfall pattern is critical to healthy crops but too much or too little of it can be harmful or even devastating to crops. Drought can kill crops, while floods or overly wet weather can provide an enabling environment for crop diseases. Therefore, rainfall is one of the more important meteorological parameters to consider when monitoring crops. Rainfall anomalies provides information about the deviation of the average rainfall from the long-term rainfall over that same period for a particular location. Negative deviations indicate rainfall of the period has been lower than the long term average values or the "normal expectation", suggesting drought conditions. Positive deviations indicate rainfall amount higher than the long term average, pointing to flooding events or an intense rainy season. Both situations have a direct effect on crop health and phenological cycle. It is therefore vital to provide information about the rainfall performance of a season.

Temperatures affect the rate of agricultural crop development through biological and chemical processes that take place in crops and soils, and due to the fact that these two are connected with air temperature. Crops grow within limits of minimum and maximum temperature and fluctuations below or above these limits can have devastating effects on crop development consequently affecting yields. Much like rainfall, anomalies can be used

to track temperature patterns over space and time. Anomalies (temperature increase or decrease of a certain period over the long term average of the same period) indicate that the deviation of temperatures was sustained over time and could therefore point to regions where crops may be susceptible to alterations in phenology cycle or adverse effects on crop health.

Soil moisture is another important variable for crop growth. It is expressed as the volume of water content stored on the surface of soil particles as well as in the pores between individual soil particles. The amount of soil moisture is dependent on meteorological conditions (rainfall, temperature, exposure to radiation, and wind), runoff, soil type and vegetation cover type. Crop roots take up water in the soil and if the water is less, then the crop will grow under stress. If this persists, the crop will wilt and eventually die. Excess soil moisture can also suffocate crops if pores in the soil are oversaturated with water and oxygen levels are restricted. This can ultimately be detrimental to crop survival. Soil moisture conditions are monitored by comparing current conditions to historical conditions over the same period. Such comparisons will generate information about where and when crops are under water stress due to insufficient soil moisture. This is often used in agricultural drought monitoring as soil moisture deficits are preceded by meteorological deficits.

Other climatic related parameters include evapotranspiration, Standard Precipitation Index (SPI) and surface runoff that have an impact on crop performance. These are products generated from rainfall, temperature, soil moisture and other meteorological and land surface parameters.

2.3 Vegetation Condition Indicators

Vegetation indices are important indicators of biomass in vegetation and are vital in crop monitoring [1]. Some most widely used indices include the Normalized Difference Vegetation Index (NDVI), Vegetation Condition Index (VCI), Enhanced Vegetation Index (EVI), SPI, Leaf Area Index (LAI), and Soil Adjusted Vegetation Index (SAVI). NDVI is particularly useful as it measures the difference between near-infrared and red light and can reveal crop conditions that cannot be visible by human eyes. Healthy vegetation will usually appear green and in the NDVI scale (-1 to 1), the values will be closer to 1. Lower values close to or below zero indicate less vegetation or bare soil. This way, by using NDVI, it is possible to estimate the state of vegetation of a particular location. Like all other indicators, an NDVI anomaly will give the difference between average NDVI over a given time period over the long term average of the same period for the same location. In agricultural monitoring, negative values can be an indicator of poor crop conditions or a slower growth rate of the crop due to a variety of environmental conditions such as droughts.

2.4 Crop Production Indicators

Crop production data is a vital indicator of yield for a given crop for a particular season. This data is often required to develop yield prediction models and it is a factor of area planted and other crop growth indicators. Yields are the basis upon which decisions are made to either supplement deficits or plan for reserves during surplus seasons. For a particular crop type, yield is forecast before harvesting and subsequently revised after harvest using the above method. Forecasts use actual data up to the time of the forecast

and "average" data between the time of the forecast and harvest; post-harvest estimates use only actual current season data.

2.5 Data Sources

All indicators discussed above can be monitored using ground and airborne instruments. Climatic indicators are traditionally collected and provided by meteorological services. However, advances in remote sensing have made it possible to acquire data for these indicators using indirect measurement methods, and there are a number of freely-available products generated from merging ground observations and satellite estimates (an example is shown in Figure 5). The advantage of such merged products are numerous but among them, the ability to correct errors from satellite estimates using ground observations not only provides us a consistent product but also a higher resolution product that can provide more details and variability across space than would ground observations. On the other hand, vegetation conditions indicators are generally monitored through the use of satellites and UAVs. Few ground observations of soil moisture are available regionally but these products can be accessed from either satellites or from land surface models that assimilate land and atmospheric variables mechanistically to estimate water and energy fluxes. Crop production indicators are available from the ministry of agriculture and/or the national statistics offices, or international agencies such as FAO. Some of the open-source data portals that provide EO data are listed below:

i RMCRD Early Warning eXplorer (EWX): `https://data.rcmrd.org/ewx-viewer/`
ii Famine Early Warning System Network (FEWSNET): `https://earlywarning.usgs.gov/fews/search/Africa`
iii GEO Global Agricultural Monitoring (GLAM): `https://cropmonitor.org/index.php/eodatatools/eodata/`
iv SERVIR ClimateSERV: `https://climateserv.servirglobal.net/`
v Copernicus Global Land Service: `https://land.copernicus.eu/global/products`

Crop production data can also be accessed from FAO: `https://www.fao.org/faostat/en/#country/209`.

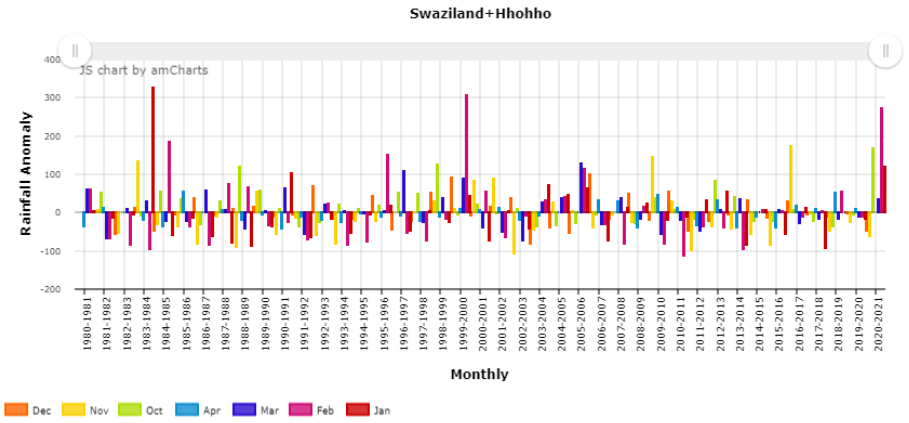

Figure 5: A timeseries graph of interannual rainfall anomaly (mm) from gridded satellite-rainfall product averaged over Hhohho province between 1981-2021 for the growing season. Caveat: This graph was extracted from the current version of the EWX which still references the country as Swaziland.

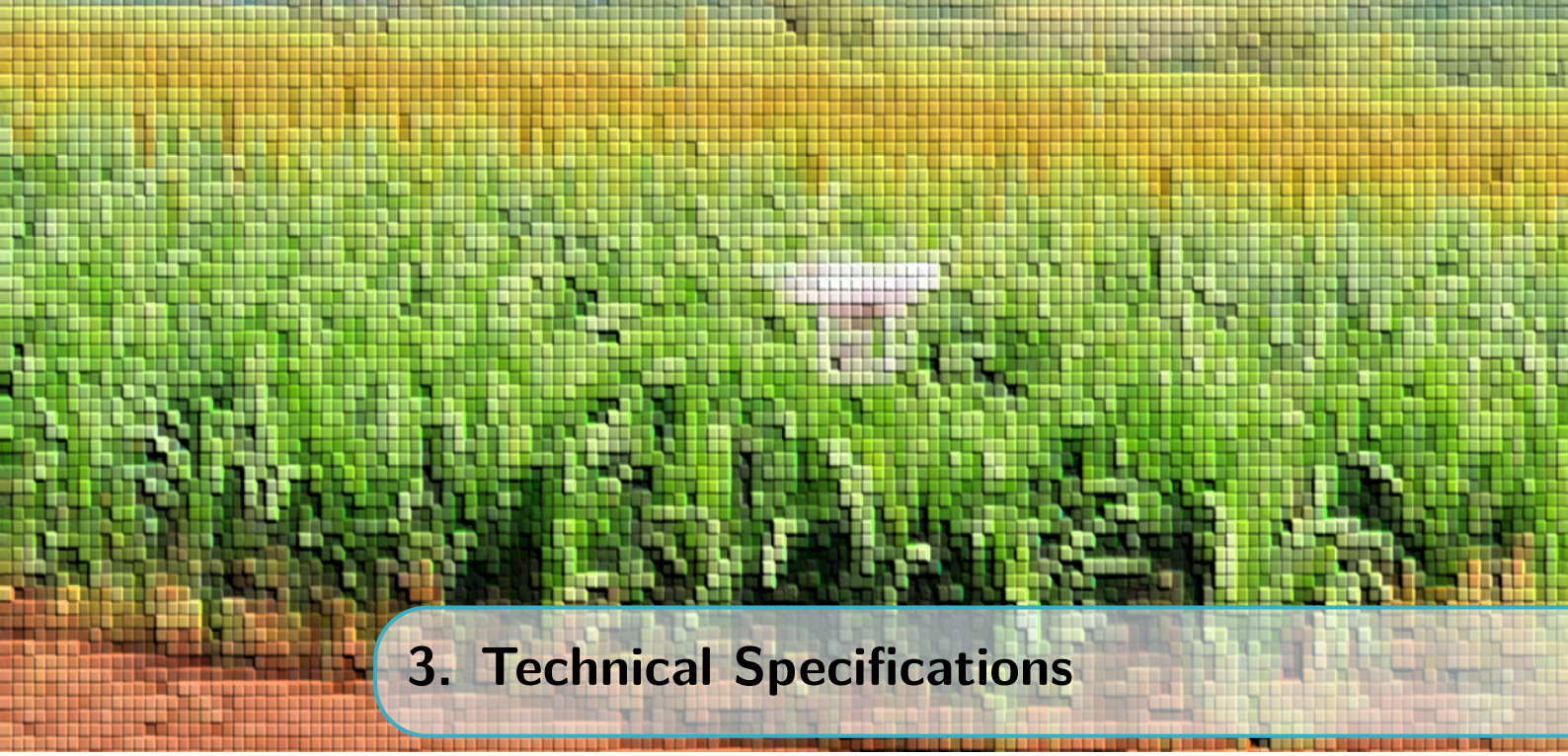

3. Technical Specifications

3.1 Overview

The adoption and use of Unmanned Aerial Vehicles, also known as unmanned aerial systems (UAS) and drones, in agricultural monitoring has increased in the recent decade due to a number of factors. First, UAV prices have been steadily decreasing due to the proliferation of drone making companies and the rise in demand across the world. These prices have been matched by growth in affordable drone image processing and navigation software. Second, there has also been a progress change in general civil aviation environment from overly strict regulations toward drones that have civilian focuses to a balance between safety and humanitarian good. Third, the growth in adoption, particularly in rural areas where most agriculture is practised has stemmed partly from the need to reduce costs associated with ground surveys that are expensive and time consuming, and the need to increase scouting frequency during a growing season. Fourth, imaging sensors have evolved considerably in the last decade. As a result, images with resolutions much higher than those offered by satellites can be obtained even with the UAVs flying at high altitudes. This makes it possible to detect risks to crops before they become widespread. Lastly, UAVs have become much easier to operate and image processing tools have evolved to a point where information from an image can be extracted fast to aid decisions that have an implication on farm management [2].

It is important to have the right combination of UAV technology, satellite data and data management tools to ensure maximum benefits. This chaper discusses some of these considerations that would aid decision making on the choice of appropriate technologies for agricultural monitoring by stakeholders in Eswatini.

3.2 Classification of UAVs

Unmanned Aerial Vehicles in agriculture can be categorized into two broad types: rotor and fixed wing UAVs. Both types have their own benefits and limitations as summarized in Table 1. Rotary wing drones exhibit low-speed flights for shorter duration but are able to land anywhere due to their hovering ability. Fixed wing drones offer high-speed flights

for longer duration but require a specified areas for take-off and landing. Both types of UAVs can be operated remotely through a console. Most UAvs have the following basic components that aid in navigation and image capture [2, 3]:

i Frame
ii Brush-less motors
iii Electronic Speed Control (ESC) modules
iv A control board
v An Inertial Navigation System (INS) and Global
vi Navigation Satellite System (GNSS)
vii Payload sensors (i.e., Light Detection and Ranging LiDAR systems, thermal camera, multispectral camera, RGB camera etc.) and altimeter (i.e., ultrasonic sensor, laser altimeter, barometer etc.)
viii Transmitter and receiver modules

Table 1: Differences between four types of drones that are commonly used in agricultural monitoring. Source: `https://guide.directindustry.com/choosing-the-right-drone/`.

Drone type	Advantages	Disadvantages
Fixed-wing drone	Long range	Impossible to hover
	Faster	Vertical takeoff impossible
	Heavier loads	
	Fly at higher altitudes	
	Use less energy, therefore better flight endurance	
Rotary-wing drone	Very maneuverable	Low endurance
	Can hover	Reduced speed and load
	Vertical takeoff and landing possible	Regular maintenance required
Multirotor drone	Greater manoeuvrability	Even lower endurance
	Can hover	Reduced speed and load
	Vertical takeoff and landing possible	Regular maintenance required
		Sensitive to weather conditions
Hybrid drone	High endurance	Impossible to hover
	Fast	
	Heavier loads	
	Vertical takeoff and landing possible	

3.3 Choosing an Appropriate UAV

Numerous UAVs with various features are currently available in the market. The choice of the right type of UAV depends on the objectives of the entity planning to acquire the equipment. For example, for large scale crop monitoring, it is recommended that drones that have longer flight times on a single battery charge are acquired. With the intention of using a drone for crop monitoring, a drone should be capable of flying according to waypoints definition, controlling its flight altitude, landing automatically given the battery status, sensing and avoiding the obstacles during its flight, and acquiring stabilized images. The WingtraOne fixed wing drone is an example of such drones. This Vertical Take Off and Landing drone has twice the flight time as multi-rotor drones such as DJI Phantoms and DJI Matrice 200. It can map areas that are more than 10 times the area mapped by multi-rotor drones for the same Ground Sampling Distance. Some drones carry sensors of various capabilities. This is what is commonly known as "Payload". A basic drone comes with a digital camera along with different filters. For agricultural monitoring purposes, drones with cameras that carry multi-spectral cameras that are capable of imaging the visible spectrum (Red, Green and Blue) are a minimum requirement. Computation of commonly-used

vegetation indices for plant health monitoring will, however, require cameras that have the Near InfraRed and Red-Edge sensors. Some commonly used multi-spectral cameras are Micasense, Sentera among others. Something else to put into consideration is the cost of a drone and its payload, availability of spare parts and factory support when malfunctioning drones require repair. It is also important to consider the ease-of-operation of a drone before purchasing it. Just like other air crafts, all drones will require trained personnel to operate and different types of drones may require different sets of skills [4].

3.4 Flight Planning and Data Collection

Flight planning is an important and preliminary step for quality data acquisition. Most drones will have an accompanying flight control board that is integrated with a flight planning software to design and send the designed flight plan to the drone, a process known as downlinking [5]. Similarly, applications can also be used on smartphones and tablets, for the same purpose, facilitating mission planning ahead of flight. These applications and software act as ground control stations (GCS) for drones. An example is shown in Figure 6.

Figure 6: An example of a flight mission plan using a DJI drone.

The other important factors to consider when flight planning include identification and estimation of flight area and surroundings, identification of potential hazards, preparation and configuration of equipment and weather conditions. Weather conditions such as wind speed can highly influence drone flight time and endurance. Drone flights during high winds will consume more energy. Similarly, the presence of poles, trees, windmills, nearby roads, vehicles and populated areas are also considered before flying drones in addition to local and national laws regulating the drones flights.

Another important consideration is the image overlap to ensure the accuracy and quality of the data. Image overlaps ensure images do not contain gaps where flight paths do not align. However, larger overlaps increase the image capturing time that further result in higher amounts of point cloud and therefore extended processing time. Some

studies like Siebert and Teizer [6] recommended at least 70 and 40% longitudinal and transverse coverage areas respectively. The need for a greater amount of overlap should be evaluated depending upon the respective drone used and its application. The flight plan, once completed, should be saved and by connecting a tablet or phone with the drone's remote control, the desired mission can be executed.

3.5 Image Processing and Software

Using UAVs and satellite data in agricultural monitoring enables data analyst to place objects or phenomenon that relate to crop health in both space and time. This ability of generating spatial information from both types of imagery is possible because of computer programs and software that are able to handle such data. Various open source and commercial software are in the market for pre-processing of images and automatic assembly of the orthomosaic and even facilitate a person with no prior expertise to extract meaningful information, in a shorter time as compared to conventional photogrammetry, of Digital Elevation Model (DEM), orthomosaic and Digital Surface Models. While this framework does not intend to go into details of some of these software, Pix4D, WebODM and Agisoft are some of the available photogrammetry software that have been shown to have good capability to handle large volumes of drone imagery. Pix4D is a commercial software while WebODM and Agisoft are open-source software that can be downloaded and run successfully with relative flexibility. At the core of these software is the ability to pre-process raw drone images which are often stored as tiles into orthomosaic images that cover an entire area of mission.

Spectral information in raw drone images is often stored in Digital Number (DN) formats and for post-processing analysis, DNs need to be converted into Surface Reflectance. Along this conversion, several other pre-processing procedures have to be done such as atmospheric, radiometric and geometric corrections, and there are openly available materials that can aid data analysts in doing these corrections. Finally, when the drone images have been pre-processed, it is possible to bring in other data from satellites and to fuse or combine the two sources for analysis. For a detailed analysis of the different available commercial and open-source drone mapping software, their advantages, disadvantages and cost, see this link: `http://www.50northspatial.org/uav-image-processing-software-photogrammetry/`.

On the other hand, satellite imagery can be accessed in formats that are ready for use thus reducing pre-processing time. In some cases, it may be necessary to download or access raw satellite imagery and process them in the same way as the drone imagery inorder to have quality products to work with. Several satellite image processing and analysis software are available. Commonly used commercial photogrammetry software include ESRI ArcGIS, ERDAS, ENVI and IDRISI, while the QGIS software is one of the most popular open-source software available to data analysts who cannot afford commercial licenses. While other tools like R and Python are not particularly developed for image processing, they have packages that are very powerful for such purposes but require intensive programming skills. One advantage about R and Python is that it is possible to automate processes ensuring routine tasks such as pre-processing. it is also important to have sufficient data storage and a high performance computing infrastructure. Drone imagery is voluminous and it is likely that benefits from UAVs and satellites would not be realized without having this infrastructure. Minimum requirements would be a computer with more than 32 GB memory coupled with more than 5 Terrabytes of storage space.

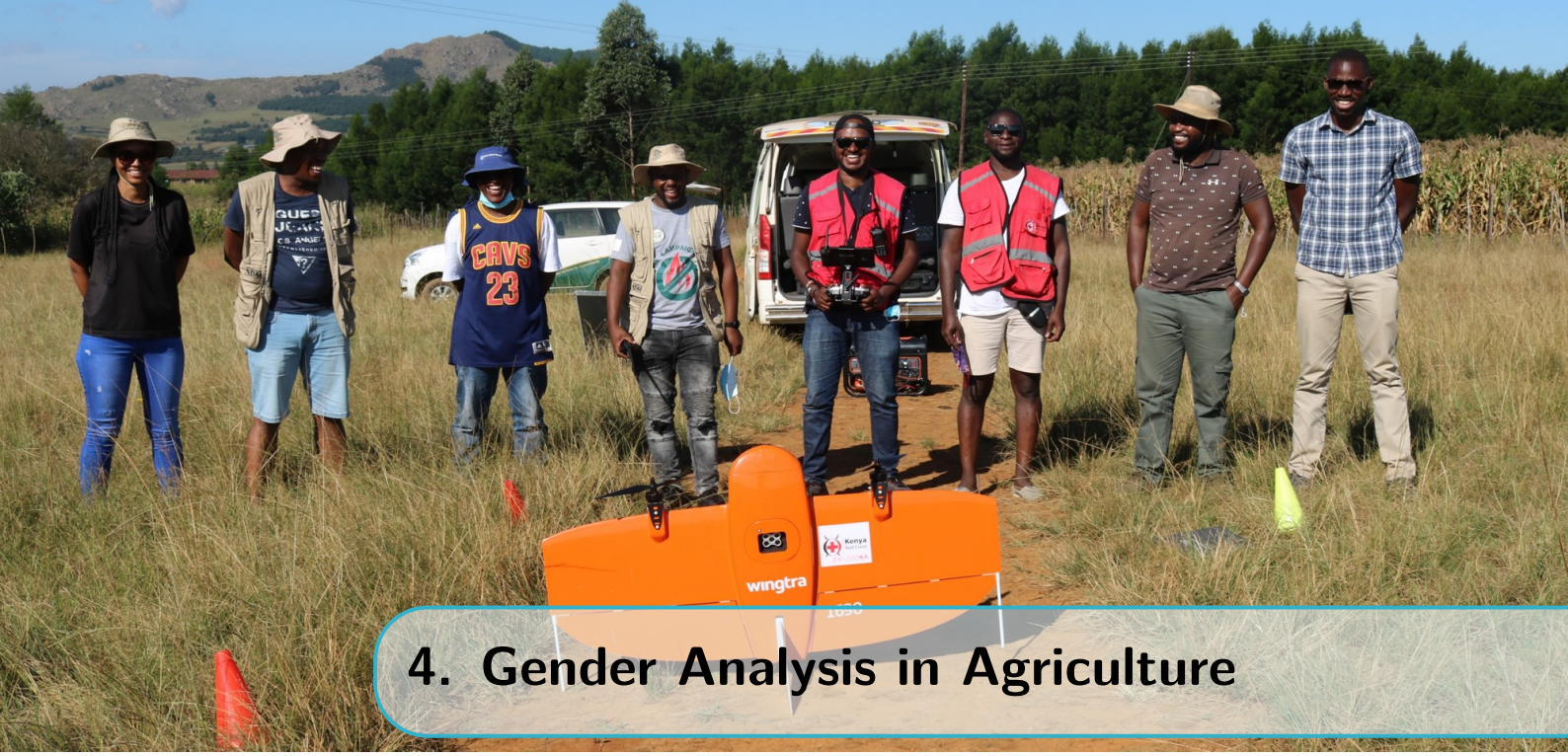

4. Gender Analysis in Agriculture

4.1 Overview

Inequalities between men and women in their access to productive resources, services and opportunities are one of the causes of under-performance in the agriculture sector, and contribute to deficiencies in food and nutrition security, economic growth and overall development. These inequalities are costly and undermine the effectiveness of international development efforts and the impact of development cooperation [7]. At a global level, there has been renewed emphasis on the importance of gender issues in climate change debates. This emphasis has been advanced through the international environmental treaty – the United Nations Framework Convention on Climate Change (UNFCCC).

During the 2005 Conference on the Parties (COP 11), NGOs noted that more women should have representation in climate change discussions. This suggestion was put into action a decade later in 2015, when the Women's Earth & Climate Action Network (WECAN International) played an active role in the exercise to form a global agreement to confront climate change through COP 21. Rural women in particular are reported to be at high risk of negative impacts from climate change [8, 9]. This is because their household responsibilities such as childcare and the collection of firewood and water can make women particularly climate-sensitive, because they are taking on more agricultural work as men migrate for labour, because they have less access to agricultural resources such as land, extension services and inputs with which to adapt to variability and change, and because gendered social norms and roles can inhibit women's adaptive capacity [10, 11, 12, 13, 14].

On the other hand, the increasing role that rural women are playing in smallholder agriculture provides an important opportunity to positively impact food production and security in a changing climate [15]. It has been estimated that if rural women had the same access to agricultural resources as men, yields could increase by 20–30% and the total number of hungry people around the world reduced by 12–17% [11]. The year 2020, marking the twenty-fifth anniversary of the Beijing Platform for Action, was intended to be ground-breaking for gender equality. Instead, with the spread of the COVID-19 pandemic, even the limited gains made in the past decades are at risk of being rolled back. The pandemic is deepening pre-existing inequalities, exposing vulnerabilities in social,

political and economic systems which are in turn amplifying the impacts of the pandemic. A new UN study shows that the COVID-19 pandemic has had far-reaching and diverse effects on women and girls in East and Southern Africa, and will set back global efforts to achieve most gender-related Sustainable Development Goals (SDGs) targets, especially those relating to SDG 3 and SDG 5.

Agricultural development programs in developing countries are seen as vehicles for poverty alleviation, nutrition, and food security as well as agricultural growth. However, while significant research has been done to determine the role of gender inequalities in agriculture on human well-being outcomes, especially those that relate to women, significant gaps still exist in regard to technological advances that are aimed at improving yields for smallholder agriculture that is still dominated by women [16, 17]. Several frameworks have been developed to guide gender analysis in agriculture. A recent FAO supported report titled "Gender in Agriculture: closing the knowledge gap" [16] provides a detailed description of data and methods requirements for a comprehensive analysis. This framework borrows from the FAO report and is not meant to be a replica of that report but materials are summarized to provide a brief description of important considerations when undertaking a gender analysis.

4.2 Data and methods for gender analysis

4.2.1 Introduction

It is now well documented that gender relations are complex and context-specific. There is a diversity of gender characteristics across cultures and contexts. These differences stem from the fact that men and women have varying distributions of rights, resources and responsibilities, and these are a product of social factors [18]. Consequently, understanding the consequences of interventions,- including those that relate to agricultural development technologies-, requires a robust set of qualitative and quantitative indicators. There are numerous data collection tools available to researchers interested in understanding gender dynamics in agriculture. Traditionally, these tools have focused on either:

i. Biological factors such as yields, disease resistance, and plant and animal growth. This information is mostly collected by agricultural research centers.
ii. Agricultural statistics bureaus that collect information about labour, markets, production by crop, cropping patterns and agricultural income by aggregate measures such as households, per capita etc.
iii. Farmer characteristics, access to resources and input, insurance, agricultural productivity etc. are collected via household surveys which are coordinated by statistics bureaus or departments of agriculture

In all these approaches to data collection, a particular emphasis is now being paid on collecting sex and gender disaggregated data in household surveys using either qualitative methods or mixed-methods. Qualitative data refer to a broad range of textual or visual information derived from interviews, observations, documents or records. These data are traditionally acquired from individuals (e.g. Key informants) or a group of individuals, often repeatedly, and in their natural environment [19]. Quantitative data may derive from official statistics and surveys. Survey-based methods involve structured interviews of a representative household sample to obtain information on a range of questions, and pre-formulated, closed-ended, and codifiable questions are usually asked to one household member (often the head) during one or two visits, although modifications of the standard

interview approach can be used to get more detailed information on gender relations [18].

New agricultural technologies such as the use of Unmanned Aerial Systems (UAV) commonly referred to as drones is revolutionizing the agriculture sector by providing a more efficient and less-costly options to monitor crop growth, crop residue, drainage and soils, and even to map cropped areas. Traditionally, these activities have been undertaken through costly approaches that make it impossible to have repeated monitoring. Additionally, the use of drones has also made it possible to monitor emerging risks in agricultural production such as pests and diseases. Complementary to drones, satellites such as Landsat and MODIS have also been widely used to provide crop health monitoring data where it is impossible or cost-effective to sample through ground observations. These new technologies, coupled with traditional methods of crop monitoring are making it possible to target crop management interventions (e.g. sowing, fertilizer application, harvesting etc.) more effectively [20].

Gender dynamics can affect the adoption of new agricultural technologies. Taking into account gender roles and responsibilities may not be adequate to realize positive outcomes. However, project designs should make considerations of these roles and responsibilities to ensure that the impact of new technologies is not detrimental to intended outcomes. Women, especially in rural Africa, have been shown to have lower rates of uptake of new agricultural technologies, but are not generally opposed to them. Concerns have been raised on the impact of mechanized agriculture on labor. It is believed that many rural women depend on agriculture for household nutrition and food security, and a majority still derive paying labour from involvement in agriculture. The introduction of drones should consider these facts and regulatory policies or interventions take into account the overall goal of making agriculture more sustainable, profitable as well as provisioning for rural labor [21]. When considering the introduction of drones in agricultural value-chains and their impact or relation to gender outcomes, it is important to keep in mind the following issues that all contribute to overall agricultural production:

4.2.2 Gender Roles

i. *Productive work*: this is work that produces goods and services for consumption by the household or for income and is performed by both men and women. Women's productive work is often carried out alongside their domestic and childcare responsibilities (reproductive work) and tends to be less visible and less valued than men's productive work.
ii. *Reproductive work*: this work involves the bearing and rearing of children and all the tasks associated with domestic work and the maintenance of all household members. These tasks include cooking, washing clothes, cleaning, collecting water and fuel, caring for the sick and elderly. Women and girls are mainly responsible for this work which is usually unpaid.
iii. *Community roles*: women's community activities include provisioning and maintenance of resources which are used by everyone, such as water, healthcare, education. These activities are undertaken as an extension of their reproductive role and are normally unpaid and carried out in their free time. In contrast it is mainly men who are involved in politics at the community level. This work may be paid or unpaid but can increase men's status in the community.

4.2.3 Gender Needs Assessment

A gender needs assessment is an important tool that should be implemented before the roll-out of a new technology to understand a diversity of factors that may affect its success. These factors may include gender roles (inputs) discussed earlier and would have an impact on outputs, outcomes and impacts. For example, when considering the impact of technology on women farmers, two perspectives need to be considered in a gender needs assessment exercise:

i. *Practical needs*: women may identify safe water, food, health care, cash income, as immediate interests/needs that they must meet. Meeting women's practical gender needs is essential in order to improve living conditions, but in itself it will not change the prevailing disadvantaged (subordinate) position of women. It may in fact reinforce the gender division of labor.
ii. *Strategic needs*: these may include changes in the gender division of labour (e.g. women may take on work not traditionally seen as women's work or men may take more responsibility for child care and domestic work), legal rights (e.g. property and land rights) , an end to sexual and domestic violence, equal wages and women's decisions over their reproductive roles.

It is also important to identify factors that determine or contribute to gender differences in agriculture. These factors can be categorized as: i) political, economic and cultural, ii) community norms and social hierarchies, iii) training and education, iv) community attitudes towards external development workers, v) past and present influences, vi) opportunities and constraints. Additionally, climate change has a significant impact on agricultural production. It is counterproductive to conduct a gender assessment or analysis without considering the impact of climate change especially in identifying vulnerabilities and capacities that exist in a technology implementation area or location. The main focus of such an assessment is on people's existing strengths (strengths) and weaknesses (vulnerabilities) and how new technologies could affect the intended beneficiaries.

The following questions should be considered (but are not exhaustive):

Physical capacities and vulnerabilities

i. What are the ways in which men and women in the community were/are physically or materially vulnerable?
ii. How does climate change affect women and men?
iii. How can women contribute to climate change action?
iv. What productive resources and skills exist?
v. Who has access and control over resources?

Social/Organizational Capacities and Vulnerabilities

i. What is the social structure of the community and how does it serve women /men in the face of Climate Change?
ii. How do climate change measures affect women?
iii. What factors lead to women headed households?
iv. What is the impact of climate change on the social organization?
v. What is the level and quality of participation of men and women in these structures?
vi. Will a proposed technology-driven project improve the welfare of vulnerable and marginalized groups or communities?
vii. What climate risks and resistance to gender equity would affect the implementation

of the project?

Motivational/Attitudinal Capacities and Vulnerabilities

i. How do men and women in the community view themselves and their ability to deal effectively with their social/political environment?
ii. What are the people's beliefs and motivations to respond to Climate Change beliefs about gender roles and relations?
iii. Do people feel they have the ability to shape their lives? Do men and women feel they have the same ability?

Roles and Power in Decision Making

i. How does the law and customs perpetuate gender inequality?
ii. How does marital power contribute to discrimination of women?
iii. For what purpose do you use the money that is generated from crop sale and who decides how to use this money?
iv. If it is the husband, to what extent do you (as a wife) agree on how the money is spent?
v. To what extent is the wife free to use the income and resources that she generates?
vi. To what extent do women participate and negotiate in decision-making inside the household?
vii. Who is responsible for expenses on items in Table 2?

Table 2: Gendered roles and responsibilities on household expenditure.

Expense	Men	women	Joint
Children's education			
Health			
Clothing			
Daily food items			
Inputs related to land			

Stakeholder Analysis

i. Who is directly responsible for decisions on issues important to the project (women/-men)?
ii. Who holds positions of responsibility in interested organizations (W/M)?
iii. Who is influential in the project area (both thematic and geographic areas) (W/M)?
iv. Who will be affected by the project (W/M)?
v. Who will promote/support the project, provided that they are involved (W/M)?
vi. Who will obstruct/hinder the project if they are not involved (W/M)?
vii. Who has been involved in the geographic area in the past (W/M)?
viii. What strategies can we use to involve women and other marginalized groups?
ix. Who has the capacity to contribute to gender equality in the project?
x. Who has the capacity to hinder efforts at gender equality in the project?

Technology Needs Assessment

i. What is the level of digital technology coverage in the Kingdom of Eswatini?
ii. What is the ratio of women to men utilizing digitized technologies?
iii. What are the challenges women face in accessing digitized technologies?
iv. Why and in what ways do agricultural technologies typically exhibit gender-differentiated

effects?

v. How can technology support women's competitiveness and integration in agricultural value chains?
vi. In what ways can sustainable production practices support women's empowerment?
vii. What are the key explanatory factors behind gender gaps in the adoption of technologies?
viii. How can research and development and extension become gender-sensitive?
ix. What are some examples of initiatives aiming to tackle the gender-based constraints that impinge on women's adoption of technology?
x. What measures could national policies consider to help women benefit from technological changes?

Box 2

The introduction of agricultural technologies that use UAVs and satellite remote sensing needs to consider several factors before their implementation. On one hand, data collection will require the right combination of skills, knowledge, equipment and software. Other other hand, information generation and dissemination needs to put into consideration who the target audience is as different audience may require different forms of data packaging. If the intention is for decision makers, for example, information packaging should be in such a way that it makes the most impact using easy-to-understand language. If it is for farmers, considerations should be made as to what format best suits such an audience. The timing of such information is also key as different decisions are needed to be made at different levels at different times. Lastly, it is imperative to consider the impact of new digital technologies on outcomes of interest and to ensure that such technologies do not disadvantage sections of the population who may not have a conducive type of environment for their introduction due to various social, economical, cultural, natural or technological factors.

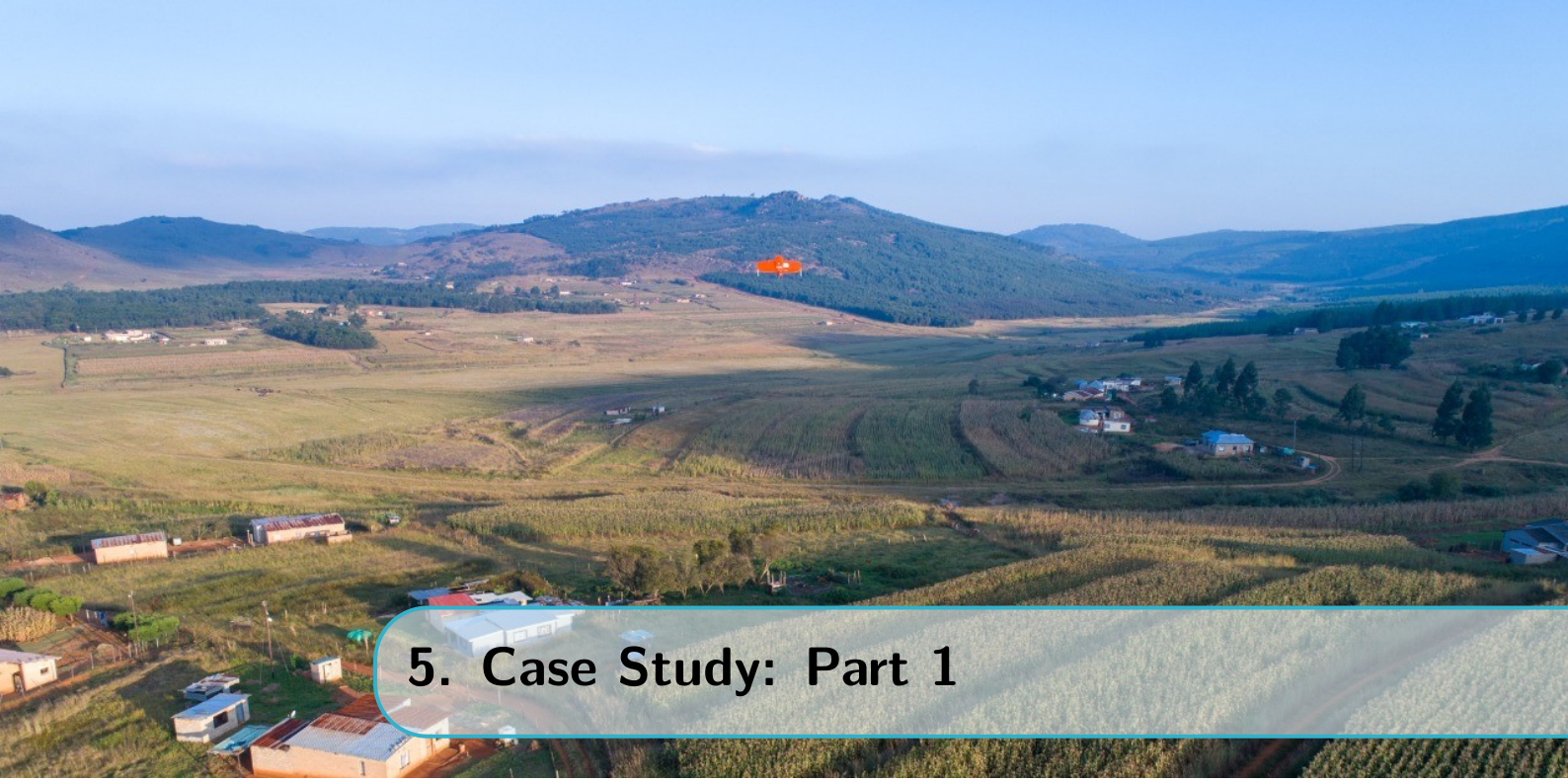

5. Case Study: Part 1

5.1 Stakeholder consultations

Introduction

Stakeholder consultations are important inputs before and during the implementation of a new technology. For the purpose of this Technical Assistance (TA) by the Climate Technology Centre Network (CTCN), the Regional Centre for Mapping of Resources for Development (RCMRD) held a half-day consultation with key stakeholders in Eswatini on 5th March 2021 to build consensus on planned activities and agree on key crop monitoring indicators to be covered used drones and satellite imagery. Participants were drawn from a range of sectors including agriculture, disaster management, weather services and security and UN agencies. The main agencies that will work closely with the RCMRD team are the National Disaster Management Agency (NDMA) as well as the National Designated Entity of Eswatini. From these consultations, it was apparent that there was need to bring more stakeholders on board for wider consultations and update them on the TA.

The specific objectives were;

i. to introduce stakeholders to the CTCN TA on UAV and Remote Sensing technologies for agricultural monitoring project
ii. to discuss and agree on indicators to be monitored using drones and satellite data to support agricultural vulnerability assessments
iii. to hold discussions on partner roles and responsibilities

NDMA played the critical role of identifying and inviting stakeholders from Eswatini, while RCMRD led the virtual workshop. A total of forty-three participants (43) from various institutions attended the workshop (Table 3). The following agencies were represented the in the workshop: The Climate Technology Centre Network (CTCN), Regional Centre for Mapping of Resource for Development (RCMRD), the Kenya Red Cross Society (KRCS), the National Disaster Management Authority (NDMA), Eswatini Water and Agricultural Development Enterprise (ESWADE), University of Eswatini (UNESWA), Eswatini National Trust Commission (ENTC), Eswatini Civil Aviation Authority (ESWACAA), His Majesty's

Correctional Services (HMCS), Umbutfo Eswatini Defence Force (UEDF), Ministry of Agriculture (MOA), Deputy Prime Minister's Office (DPMO), Central Statistical Office (CSO), Department of Meteorology and MM Geomatics Surveys. The workshop was officially opened with remarks from Mr. Russel Dlamini, the NDMA Chief Executive Officer. In his remarks, Mr. Dlamini expressed his appreciation that this TA was underway and that the proposed activities will contribute to food security monitoring in the country. He offered his support to ensure that proposed activities are implemented successfully.

Outcomes

In regards to the first objective, a presentation was made by the project technical lead from RCMRD outlining the technical assistance and the expectations in the development of a case study from a combination of drone and satellite data. This presentation further highlighted the progress made so far which included development of planning and communication documents and a structured stakeholder engagement. Introductions to the technical assistance team from RCMRD, KRCS and key points of contacts from collaborating agencies in Eswatini, and discussions about the key outcomes of the TA were provided. It was explained that the development of the case study in this project, the results thereof and experience shall be used to put together a proposal to solicit funding from the Green Climate Fund (GCF) for scaling up of piloted technologies.

Three presentations were made on the second objective. The first focused on the operations of a drone for image collection. Participants were taken through the process workflow; from flight planning to image analysis. This presentation was made by one of the drone pilots and GIS officer at the KRCS. Some of the considerations that were highlighted in this presentation include the need to acquire the right drone and cameras as these vary by purpose and efficiency. There are two main types of cameras: those that collect true colour images (Red, Green and Blue channels) and those that collect multispectral images (Red, Green, Blue, Near-InfraRed, RedEdge channels). The presentation also highlighted technical preparations that are required before carrying out a drone mission including the development of flight plans/surveys and standard operation procedures. In general, the essential process checks involved in drone mission planning are: equipment and supplies checklist, pre-site survey, safety, security and emergency plans, weather conditions, crew briefing and in-flight checklist. Lastly, some examples of how the KRCS has used drones in Kenya were showcased (Figure 7).

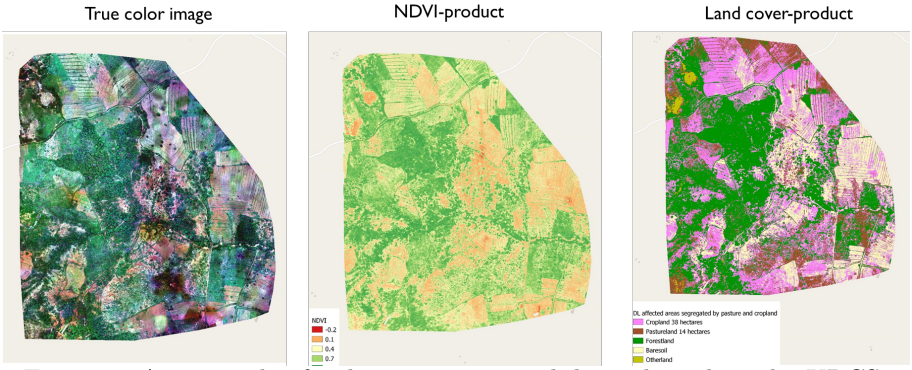

Figure 7: An example of a drone imagery and derived products by KRCS.

The second presentation covered applications of drones in agriculture. It was noted that this is one of the emerging areas under which drone technology is being used to improve

agricultural yields. Drones have been used in almost all phases of crop growth: soil analysis, gap analysis during crop emergence stages, monitoring growth and harvest stages (crop scouting, health, irrigation demand and optimization as well as yield estimations), review of end of season maps and planning for the next season. In this TA, the case study will be developed focusing primarily on monitoring growth and end of season/harvesting stages. The key parameters that will be included will be crop health through the development and tracking of vegetation greenness/biomass, and prediction of end of season yields through the use of UAV and satellite-based indicators. These indicators will include vegetation indices such as the normalized difference vegetation index- NDVI and cropped area, complemented by other biophysical indicators that impact yields especially rainfall, temperature and soil moisture (Figure 8).

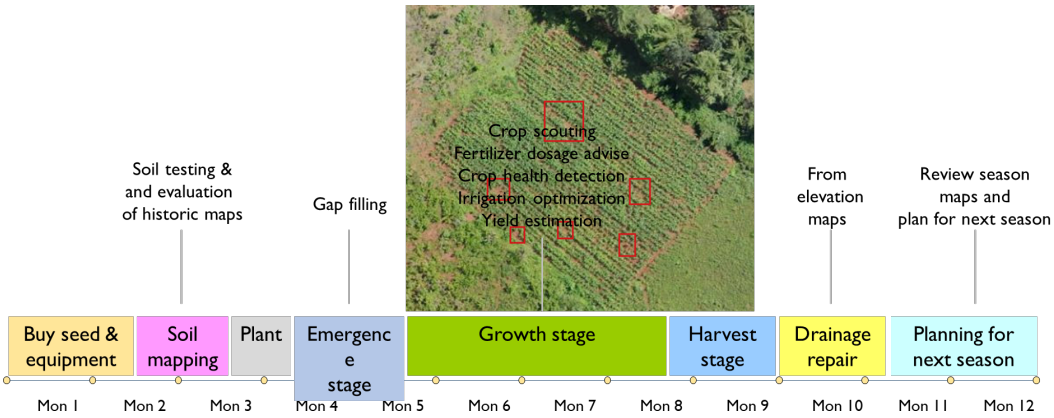

Figure 8: An illustration of UAV use during a cropping season.

The third presentation focused on methods for fusing or combining UAV and satellite data. The presenter explained that the objective of this technique is to take advantage of the very high spatial resolution imagery from drones to combine with relatively courser resolution satellite imagery in order to improve on the quality of the information contained in the output image. Drones can collect data from smaller areas than freely available satellites and that a combination of these two types of images can improve crop monitoring across larger areas that cannot be mapped using drones. It is expected that image fusion will result in: extended range of operation, spatial and temporal coverage, reduced uncertainty and increased reliability, and compact representation of information. Three types of fusion techniques will be explored: pixel-based, feature-based and decision-based fusion. Crop indices that will form a core part of the case study development will benefit from this fusion because while the focus is on a small geographical area, methods developed will be scaled up nationally.

Following these presentations, several responses and questions emerged. First, Mr. Russel Dlamini (CEO, NDMA) pointed out that the presentations provided an understanding of how NDMA and other national agencies can take advantage of drones and associated analysis to improve early warning systems and decision making in agriculture. Outputs from this technical assistance would be applicable in anticipatory planning processes by NDMA and that the data that will be collected can be fed into the drought monitor. In response to this, it was also noted that a complementary service that the country could explore is the establishment of a national crop monitor.

Participants sought to know whether there exists a sensor to monitor soil, to which participants debated in and it was generally agreed that with the current technology soil properties can be measured indirectly and further scaled up through modelling. Additionally,

Mr Rajiv Garg of CTCN elaborated that with the use of high-resolution satellite imagery and Artificial Intelligence (AI), measurement of soil properties was achievable. ICRAF, Kenya has done intensive work on soils and thus more information can be obtained from their website. This TA will not cover this aspect but this will be explored as part of the GCF proposal that will be submitted at the end of the technical assistance.

It was further noted that current regulations and policy need to be streamlined and harmonized in order to promote the use of UAV technologies for humanitarian purposes and other activities that are intended to improve livelihoods such as the proposed technical assistance. It was noted that the current regulations are very restrictive and laborious with approvals required by a number of agencies. This issue would be addressed in the GCF proposal and a synthesis of the current regulations and possible challenges that are being experienced will be provided.

Lastly, discussions were held on partner roles and responsibilities. It was agreed that the point of contact for the teams would be: RCMRD (Denis Macharia), NDMA (Mr. Eric Seyama and Mr. Sibusiso) and NDE (Mr. Bafana Nicholus Simelane). The NDMA and NDE team would coordinate all in-country activities (field data collection, training) while also giving feedback and providing advice to the RCMRD team on various tasks that may require their input. Specifically, it was agreed that the NDMA and NDE teams would work with their counterparts from the ministry of agriculture to identify sites where drones would collect data for the case study development as well as provide assistance in the approval of drone importation from Kenya. Participants emphasized on the need to have contingency plans given that the COVID-19 pandemic might disrupt some of the planned activities. It was elaborated that NDMA has a drone pilot licensed by Eswatini and that he could help in data collection. Further, it was agreed that in case of unforeseen circumstances, the scheduled one-on-one training could take place virtually. It was also agreed that several sites would be identified for data collection.

5.2 Flight Planning and Execution

The mission for data collection was conducted over a period of 16 days (30th March - 14th April). Mission planning was informed and guided by procedures already in place at the KRCS. An initial step is to set up the team responsible for the data collection missions. This includes a Pilot-In-Command (PIC) who is a certified drone pilot, two visual observers (VOs) and a GIS and IT support team that would help with the imagery processing. For this particular mission, the PIC and VO1 were from the KRCS, while the VO2 was part of the RCMRD team. The GIS and IT support teams were from the KRCS based in Nairobi, Kenya.

This task was undertaken together with technical capacity building in UAV use for crop vulnerability assessments in Eswatini by showcasing to the NDMA the processes to be undertaken in order to:

i. Adequately prepare for a UAV/drone flight missions
ii. Carry out a test flight mission to collect imagery for identified parameters
iii. Carry out flight missions for mapping of identified crop conditions parameters like vegetation indices and cropped area. This task also included the development of flight plans, standards of operations (SoPs) and capturing of multispectral imagery using a Red, Green, Blue and Near infrared (NIR) enabled drone to collect data for the development of a case study (Pilot mission).

Table 3: The list of participants who attended the inception workshop.

Name	Institution	Name	Institution
Denis Macharia	RCMRD	Nozakhele Dlamini	NDMA
Anastasia Wahome	RCMRD	Ntabeni Msibi	NDMA
Benson Kenduiywo	RCMRD	Pitsoe Ndlandla	UEDF
Bonokwakhe Sukati		Precious Ncamsile Mdluli	Mdluli - NDMA
Celinhlanhla Magagula	ESWADE	Robison Mugo	RCMRD
Daniel Dhladhla	MOA	Rusell Dlamini	NDMA CEO
Eric Seyama	NDMA	Sabelo Simelane	CSO
Felix Mamba	UNESWA	Sacolo Sanele	DPMO
Gcebile Dlamini	NDMA	Samukelisiwe Myeni	DPMO
Fred Onyango	RCMRD	Siboniso Mavuso	NDMA
Israel Mduduzi Simelane		Sibusiso Ginindza	NDMA
Judith Mugambi	CTCN	Sibusiso Mdluli	CSO
Ken Kasera	RCMRD	Sizwe Mabaso	UNESWA
Lucky Shongwe		Sonia Dupont	ESWACAA
Majahonke Mamba	NDMA	Taariq Twaha	KRCS
Martin Murimi	RCMRD	Zakhe Dlamini	ENTC
Mbonane Nobuhle	NDMA	Zandile Mavuso	DPMO
Nosizo Mthupha	DPMO	Zinhle Motsa	ESWADE
Mdumiseni Wisdom	UNESWA	Rajiv Garg	CTCN
Michael Otieno	KRCS	Stephen Sande	RCMRD
Mkihwa Maseko	HMCS	Manqoba Mabuza	MM Geomatics
Mbuso Vilakati	Vilakati		

The tools used in the mission planning included desktop and mobile Geographic Information System (GIS) applications: Google Earth, QGIS, OsmAnd as well as Google maps. The PIC worked with the GIS team to upload a mission plan for the areas of interest which are mostly in Google Earth KML format onto the drone's WingtraPilot application. These were subject to customization dependent on the drone landing zones that were later established as the crew conducted onsite surveys once in Eswatini. Further to the technical planning, the KRCS in coordination with the RCMRD & NDMA teams, was able to seek approval from the Eswatini Civil Aviation Authority (ESWACAA) to fly within the Eswatini airspace. This included submitting an approval request with; the drone specifications, the KRCS drone unit Standard Operating Procedures (SOPs), the pilots' bio data as well as mandatory requirements as required by the regulator.

While conducting the missions, the team ensured the following were available on site to support with coordination and safety, data capturing and storage:

i. Radios - VHF and Airband
ii. Modem/ Wifi connection
iii. External hard disk
iv. Pylon marking cones
v. Landing zone
vi. Diesel powered generator to recharge drone batteries, remote controller, drone tablet and radios
vii. Tent as a temporary work station
viii. Electrical power cables

This is a recommended list and can be adjusted for every mission.

5.3 Data Collection

One WingtraOne fixed-wing drone was used to collect data in large scale due to its strengths in having longer flight time and data quality. This drone was complemented by two DJI multi-rotor drones from NDMA: DJI Phantom 4 and Matrice 200. Rotary drones and fixed-wing drones are two types of UAVs that each bring distinct advantages. A rotary system, such as a quadcopter or multicopter, is ideal for mapping and inspecting small areas, thanks to its ability to take high resolution imagery at closer range, using mm per pixel resolution. The take-off and landing area can also be very small, which suits more urban areas. In contrast, a fixed-wing drone is often more suitable and beneficial for agricultural applications, where mapped areas are usually large and take-off and landing space is not limited.

WingtraOne drone endurance and high cruising speed allows a greater area of land to be mapped up to 2.6x faster, with an object resolution of cm/inch per pixel, and users also benefit from its ability to withstand high wind resistance – an important factor when mapping large areas of open land –, as well as reduced labor costs. A hybrid of the two was utilized by the KRCS team, the WingtraOne is a vertical take-off and landing (VTOL) drone that brings the best of the two drones, with a vertical takeoff and landing component it can take off from a small area, and then transition into fixed wing mode to cover larger areas faster with less battery consumption.

Data collection was done in four sites namely; Gege, Sidzakeni, Sigangeni and Mpologeni. A total of 19.57 KM^2 of imagery was collected by the WingtraOne drone while the DJI drones mapped an area of 5.1 KM^2. Table 5 shows the data collection outcomes for WingtraOne drone for each of the four sites. The WingtraOne drone carried the MicaSense RedEdge-M camera which is a five-band multispectral camera that is used to capture RGB, NDVI, and advanced vegetation bands in a single flight. This camera has the Blue, Green, Red, RedEdge and Near InfraRed sensors. The MicaSense RedEdge camera workflow includes: i) Configuring flight plan parameters in a separate user interface opened in a browser. These parameters include target altitude and frontal image overlap, ii) Flight parameters are set and, iii) Camera is calibrated to get reliable information by placing a reflectance tag that comes with the drone levelled on the ground, then taking a picture before and after the flight, and iv) Images are directly geo-tagged using a GPS receiver attached to the camera.

5.4 Data Processing

Drone images captured during flights were backed up on locally available resources such as memory cards, laptops and external hard disks. A memory card reader was used to facilitate the transfer. Drone images captured using the MicaSense payload are already tagged with GPS metadata and therefore no further processing of the images is required before having them move the next process steps. Image Processing was done using the Pix4D software but open-source options like the WebODM and Agisoft are available for use. In most instances it was not practical to transfer the images over the internet to a storage server in the office due to the large quantity and sizes of drone images, and weak internet connection in areas where missions were carried out. Files were backed up and stored on a storage server for further analysis. The backups should remain untouched in case something goes wrong during processing and there is a need to revert to the original files. It is recommended to maintain several copies of all files at every stage of the process.

Drone Type	Features	Sample
WingtraOne Fixed-wing Drone	Vertical take-off and landing (VTOL) drone used in conducting small & largescale drone surveys, designed to cover long distances with a maximum flight time of 55 minutes.	
DJI Phantom 4 Multi-rotor Drone	Equipped with intelligent modes, obstacle avoidance and a camera that shoots 4K ultra-high definition with an estimated flight time of 28 minutes.	
DJI Matrice 200 Multi-rotor Drone	Known as the ultimate aerial tool, built for industrial inspections and public safety operations, has an estimated flight time of 24 minutes and known for its versatility and accessories/payloads available for use.	

Table 4: Drone types used in this pilot case study, and their features.

Images collected from each of the flights were combined and saved in a single folder and then processed, but it is a best practice to run smaller batches with every processing task if computing resources do not allow large area processing. This prevents the entire large batch from failing and then having to be re-run. Some of the issues that come up during processing can be averted but this becomes clearer as the team develops the experience and then customises its process to suit them. The KRCS team recommends to keep folders for each processing task to approximately 250 images each for best results in terms of speed of

Table 5: Number of missions and total mapped area using WingtraOne fixed-wing drone in four pilot sites.

Site	**Mission**	**Ha**	**Km2**
Sidzakeni	Mission 1	103.52	1.0352
	Mission 2 (flight1)	129.17	1.2917
	Mission 2 (flight 2)	56.29	0.5629
	Mission 3	109.82	1.0982
	Mission 4	71.33	0.7133
Mpolonjeni	Mission 1	100.75	1.0075
	Mission 2	68.04	0.6804
	Mission 3	114.39	1.1439
	Mission 4	94.48	0.9448
	Mission 5	125.21	0.9448
Sigangeni	Mission 1	92.85	0.9285
	Mission 2	137.22	1.3722
	Mission 3	119.35	1.1935
	Mission 4	82.92	0.8292
	Mission 5	93.42	0.9342
Gege	Mission 1	75.33	0.7533
	Mission 2	109.35	1.0935
	Mission 3	72.94	0.7294
	Mission 4	106.08	1.0608
	Mission 5	125.21	1.2521
Total area covered		**1987.67**	**19.57**

processing and minimizing failures. The results from the processing (e.g. orthomosaic in Figure 9) can then be combined in GIS software such as QGIS.

Figure 9: A sample RGB orthomosaic image after processing UAV images from multiple flight missions.

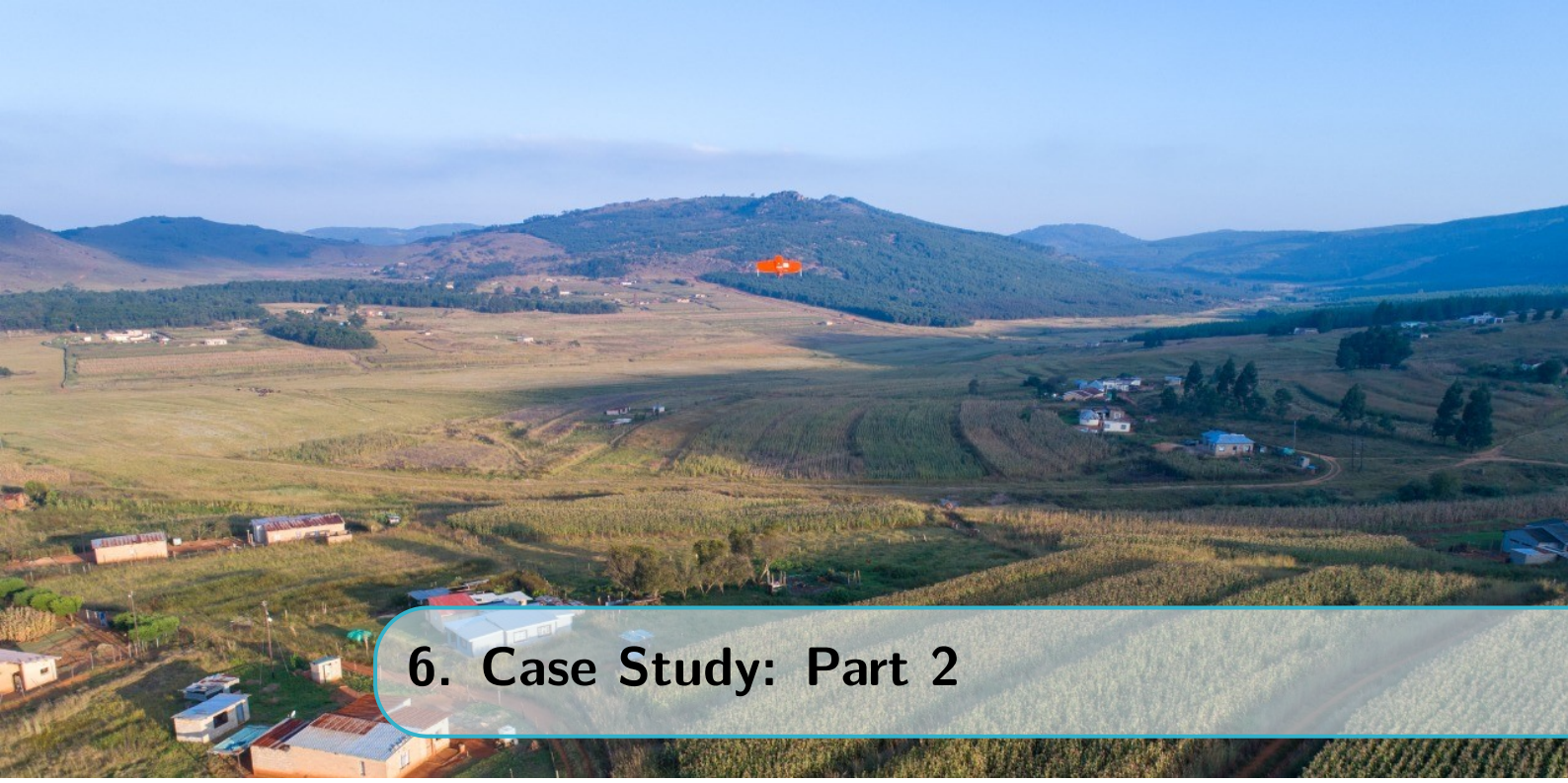

6. Case Study: Part 2

6.1 UAV and Satellite Data Fusion

6.1.1 UAV and Satellite Data Pre-processing

UAV images were processed using five virtual workstations installed with Pix4D drone image data processing software. Using virtual workstations running on servers allows for tasks to run uninterrupted, overnight, and not have any other work being done on the same workstations. This allows for quick turnaround time in processing the imagery. Pix4D processes images in the following process: pre-processing entailed initial processing, extraction of point cloud and mesh and extraction of Digital Surface Models (DSM), Orthomosaics and spectral indices with both digital numbers and surface reflectance for all the missions. The micasense camera has a calibration panel that utilises spectral values. To be able to compare the results further with Remote Sensing data, it was required to convert the digital numbers to surface reflectance values which are comparative with Sentinel 2– the satellite imagery source chosen for this pilot. This improves the image interpretability as surface reflectance values take into account the atmospheric conditions and time. This provides better information extraction through image classification and spectral indices.

6.1.2 UAV and Satellite Data Fusion

Remote sensing techniques used in precision agriculture and farming that apply imagery data obtained with sensors mounted on UAV platforms became more popular in the last few years due to the availability of low-cost UAV platforms and low- cost sensors. Data obtained from low altitudes with low-cost sensors can be characterised by high spatial and radiometric resolution but quite low spectral resolution, therefore the application of imagery data obtained with such technology is quite limited and can be used only for the basic land cover classification [22]. To enrich the spectral resolution of UAV imagery data acquired from low altitudes over the four pilot sites in Eswatini using Sentinel-2 imagery (Figure 10), several image fusion techniques that have been applied elsewhere for vegetation and land cover monitoring purposes were evaluated. These were: i) Pixel fusion, ii) Feature Map fusion, iii) Decision fusion and, iv) Image indices fusion. The fusion was based on the pansharpening process, that aims to integrate the spatial details of the high-resolution

panchromatic image from the WingtraOne and DJI drones with the spectral information of lower resolution multispectral imagery from Sentinel-2 satellite to obtain multispectral images with high spatial resolution. The key of pansharpening is to properly estimate the missing spatial details of multispectral images while preserving their spectral properties [22].

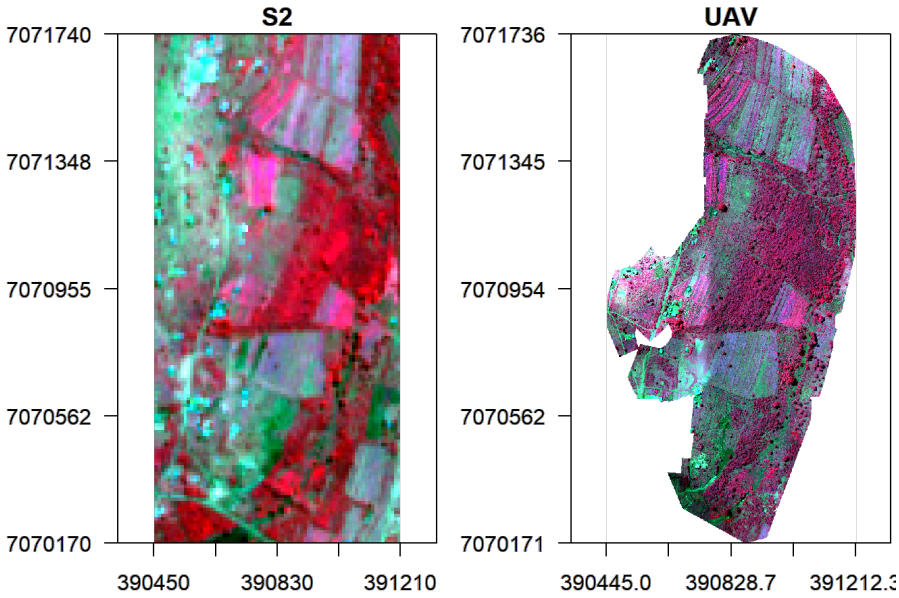

Figure 10: Raw Sentinel-2 and UAV images for Mpolonjeni site, Eswatini.

Data fusion (Figure 11) is a formal framework which provide the means and tools for the alliance of data originating from different sources. It aims at obtaining information of greater quality; the exact definition of "greater quality" will depend upon the application [23]. The principal motivation for image fusion is to improve the quality of the information contained in the output image in a process known as synergy. A study of existing image fusion techniques and applications shows that image fusion can provide us with an output image with an improved quality. In this case, the benefits of image fusion include:

i. Extended range of operation
ii. Extended spatial and temporal coverage
iii. Reduced uncertainty
iv. Increased reliability
v. Robust system performance
vi. Compact representation of information

In the pixel fusion method, multiplication, mean and the approach proposed by [25] which normalizes the multispectral image with the low-pass UAV single band image and multiplies the result with the original UAV single band image. The results are shown in Figure 12. In the feature based method, NDVI from the UAV and S2 imageries were fused using an averaging technique (Figure 13). Both fusion methods used an upsampled UAV image, meaning that this imagery was matched to the S2 spatial resolution which is 10 m. While this upscaling reduces the spectral variability of the UAV imagery, it destroys its spatial resolution, making it coarser and difficult to differentiate between features. A different approach is to downsample the S2 imagery to match the UAV spatial resolution before fusion (1 m). This results in a product that has improvements in both spatial and

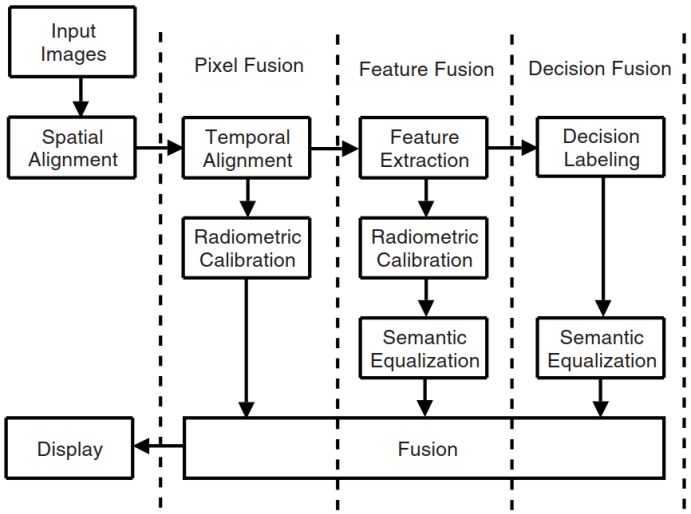

Figure 11: The generic image fusion processing chain. It consists of 4 principal blocks: (1) Multiple Input Images, (2) Common Representational Format, (3) Fusion, &, (4) Display. [24].

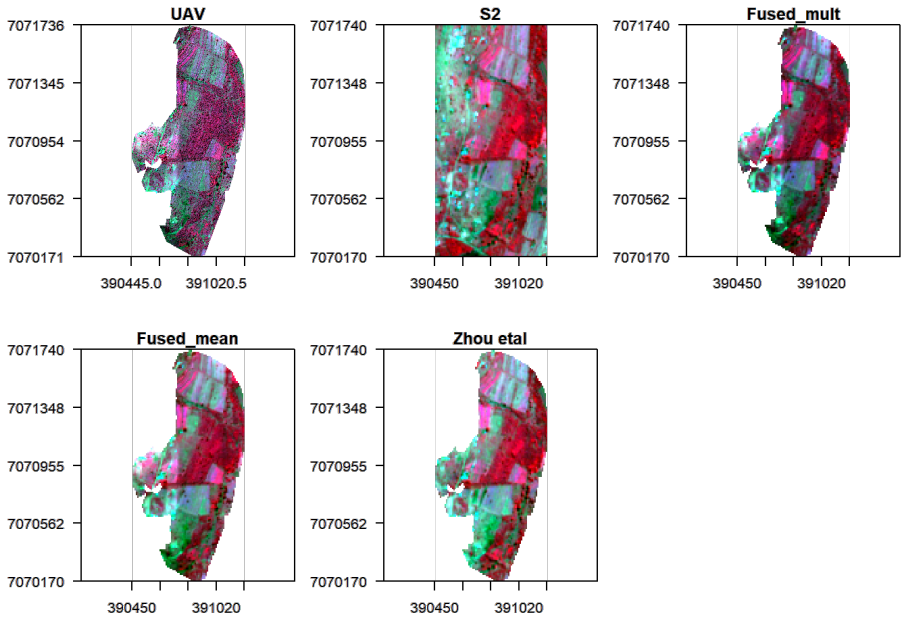

Figure 12: Fused multispectral image outputs from the pixel fusion methods: multiplication, mean and the Zou method. The first two images are the raw UAV and Sentinel-2 (S2) images, respectively.

spectral information of S2, and the spectral information from the UAV imagery. Here, sampling points (Figure 14) created from the S2 original resolution (10 m) and the upscaled UAV imagery (10 m) were used to develop a model that can predict S2 reflectance at the UAV resolution of 1 m.

The spectral fusion method used spectral information extracted from the UAV and S2 images using the sampling points created in Figure 14. Models were created using linear (LM), Random Forest (RF) and Support Vector Machine (SVM) algorithms. In this case, models were developed using a sample of the validation points to predict spectral information for S2 bands using UAV bands (Figure 15). Validations done using outputs from the three models showed that RF gives better prediction because it had lower Mean

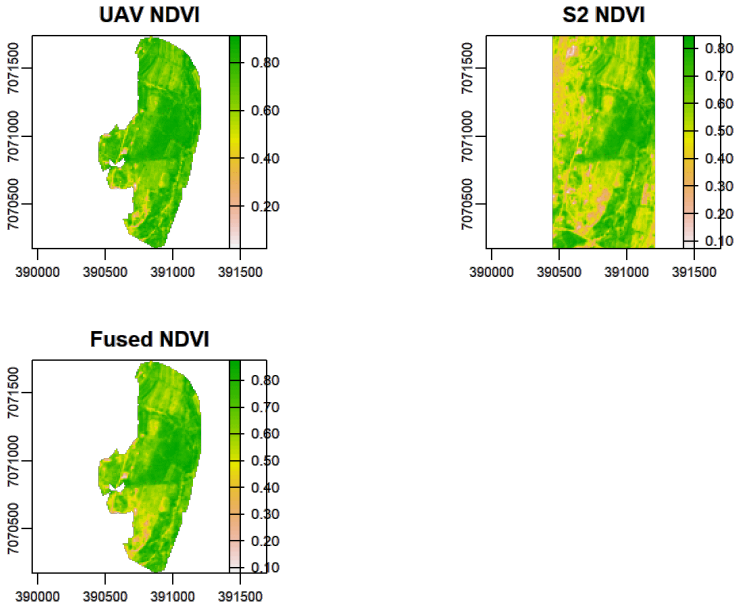

Figure 13: NDVI based feature fusion using S2 and UAV imagery.

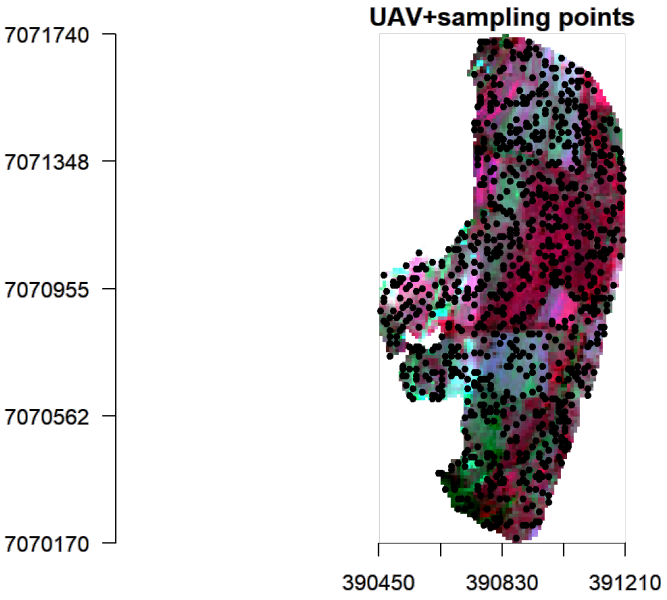

Figure 14: Sampling points for predicting S2 reflectance at a resolution of 1 m to match the UAV resolution.

Absolute Percentage Error (MAPE) and Root Mean Square Error (RMSE). SVM had twice the error (MAPE) given by RF. The resulting fused image using Zou's approach [25] is shown in Figure 16.

Lastly, a Principal Component Analysis (PCA) spectral fusion (or Gram-Schmidt fusion) was also tested. This method follows steps that are detailed in Metwalli et al. [26] and Zhao et al.[27]. First, a panchromatic band is computed by taking the mean of UAV RGB bands following Jenerowicz et al. [22]. Secondly, the S2 multi-spectral image bands are transformed by the PCA transformation, and lastly, the first PCA of the multi-spectral

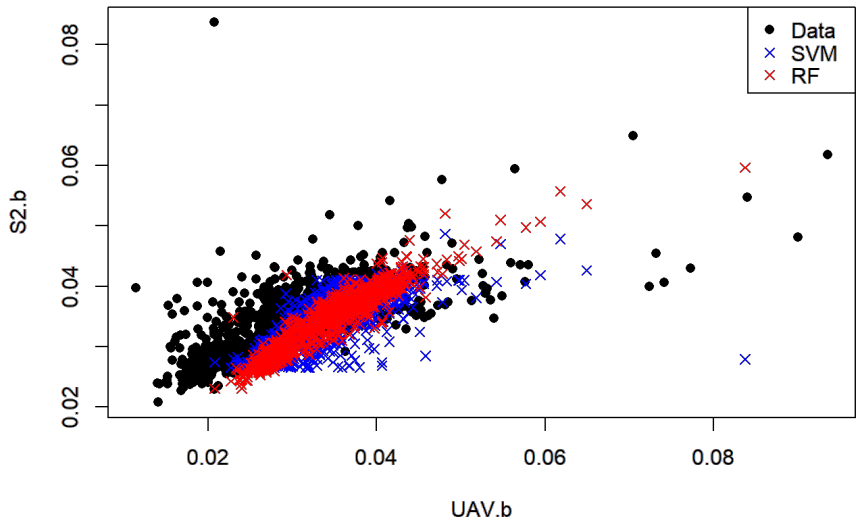

Figure 15: A plot showing UAV and S2 relationships for the Blue spectral band for two models (SVM and RF).

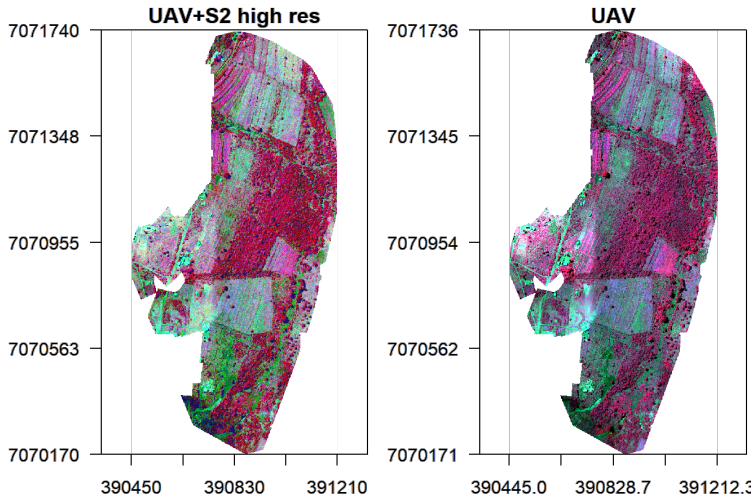

Figure 16: Fused UAV and S2 images using predicted S2 bands and UAV bands following Zou et al. [25] approach.

image is replaced by the histogram matched panchromatic imagery. The new PCA-based fused multi-spectral imagery (Figure 17) was obtained by computing the inverse of the principal component transformation.

Following the successful fusion of UAV and S2 imagery for the Mpolonjeni site, crop mapping was undertaken using two image classification techniques. This mapping was done inorder to demonstrate the benefits of using UAVs to aid decision making, especially in cropped area and production (yield) estimation in Eswatini. The following section provides details of how this was achieved. First, a pilot cropland mapping was done using the three sets of images (UAV, S2 and fused UAV+S2 images) for areas that were mapped using drones, and secondly, the mapping was scaled up across the entire country using S2 images

and insights derived from the pilot cropland mapping.

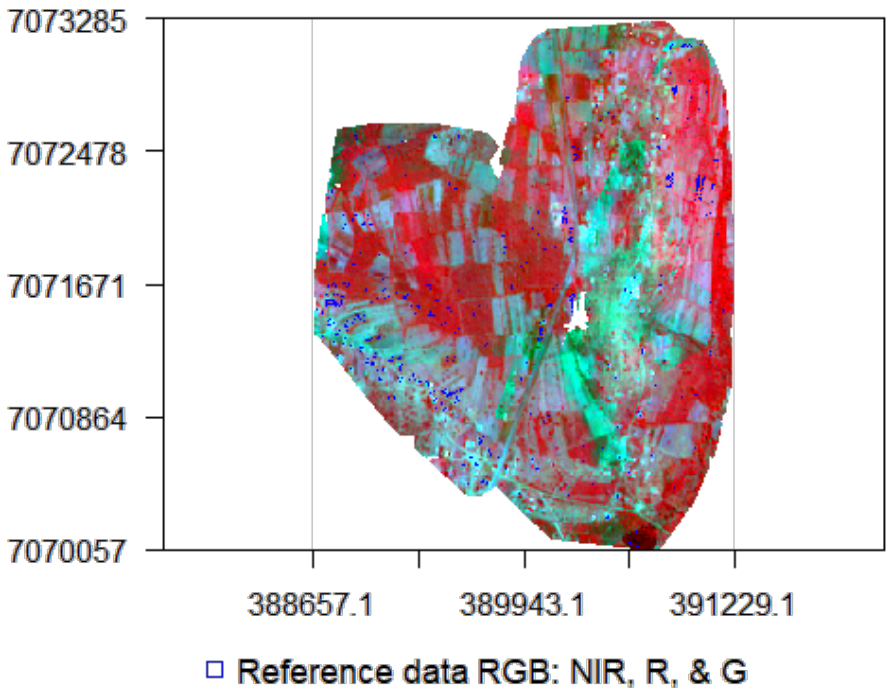

Figure 17: The PCA-based fusion image from UAV and S2 images over Mpolonjeni pilot site. The image is overlaid with training sites collected for crop mapping.

6.2 Crop Mapping and Yield modeling

The increasing world's population coupled with climate change has steadily increased demand for food. Consequently, countries have been faced with the challenge ensuring food security to their citizens. To meet this mandate governments require agricultural production information to aid resource allocation and sustainable farming practices so as to attain improved food security for the developing world. Information on the spatial distribution of crops is therefore an important step towards sustainable agricultural production. It is important to know where crops are before the estimation the yield in a given region. Ground mapping approaches like surveying are expensive and time intensive. Remote sensing offers an effective and efficient platform for mapping due to improved temporal and spatial resolutions. This capability provides a reliable system with near-term potential to provide stakeholders with timely information on crop distribution, status, and predicted yield.

An operational cropland mapping and yield estimation is an efficient and less expensive collection of reference data to train and validate mapping procedures [28]. With the traditional methods of collecting ground truth data being cost and time intensive, UAVs have become a reliable alternative that offer a faster and more accurate alternative for collecting such data. The advantage of using UAVs is not only in its cost-effectiveness but also in the ability to repeat ground surveys across a growing season. Another advantage of using drones is the ability to collect training data that is area based rather than point based which improves mapping accuracy. It is possible to extract an entire plot of farmed land using a very high resolution imagery from drones while that would not be possible

when relying on point data. A combination of the two methods would provide optimal results.

6.2.1 Collection of Training Sites

Exploiting the synergy between UAV and satellite data is essential for understanding the dynamics of the Earth's surfaces [29]. For instance, UAV can quickly acquire data with high spatial resolution, short revisit period and minimal atmospheric effects compared to space-borne systems [27]. UAVs have also been used to aid collection of ground reference data for image classification [30, 28]. To aid in selection of training sites, field points collected using drones in the four pilot sites were used and additional sites collected based on visual image interpretation from S2 data to supplement UAV data. S2 data are available freely with a revisit period of at least 5 days worldwide through the COPERNICUS Earth observation project. This process was done using ArcGIS and QGIS software which are commercial and open source geographical information data management tools, respectively. While selection of pure pixels is highly encouraged to reduce issues of mixed pixels and mixed classification, the classification algorithm adopted required a minimum of 400 pixels as training sites for any land use class. This presented a challenge for a site like Mpolonjeni in which, due to it being a low production zone, acquiring pure pixels for maize required many polygons to be digitized. This called for generalization of the maize farms driven by the fact that the fusion of drone imagery with satellite imagery reduces the native spatial resolution of the UAV imagery.

6.2.2 Image Classification

The availability of S2 and UAV data at a low cost has spurred development of machine-learning models for mapping and yield prediction [31, 32]. In this case study two different classification algorithms or schemes were used:

i. Random Forests (RF) [33]
ii. Conventional Maximum Likelihood Classification (MLC)

The crop mapping pilot used WingtraOne images acquired between 1-14 Apr 2021. Five drone flight missions from Mpolonjeni were mosaicked or merged to form one image over the entire site with a 1 m spatial resolution. A corresponding S2 image was also downloaded and clipped or resized to match the extent of the UAV merged image (Figure 18). Training sites covering major land cover classes in the pilot site (built, grassland, maize, sorghum, sweet potato. trees, water bodies and cassava) were collected during the field work to collect drone imagery as well as during the analysis to create a representative sample for each of the classes. Pixel values representing the spectral reflectance of each land cover class were extracted using the training sites (Figure 17).

Overall, the contribution of PCA-based fused image from multi-spectral Sentinel 2 and UAV is clearly illustrated by slighly better results as shown in **??**. RF gives a better accuracy for crops classes and grasslands for the fused image ((RF_PCA) compared to other classes as well as accuracy scores for un-fused UAV and S2 images. Generally, RF also performs better compared to MLC but MLC has equally good results for all the classes. It is important to note that accuracy scores are dependent on the quality of training and validation sites. It is incredibly vital to ensure that training sites are as representative of the diversity of land cover available in a location as possible and that digitization of these training sites is done carefully in order to minimize contamination of classes. All diligence

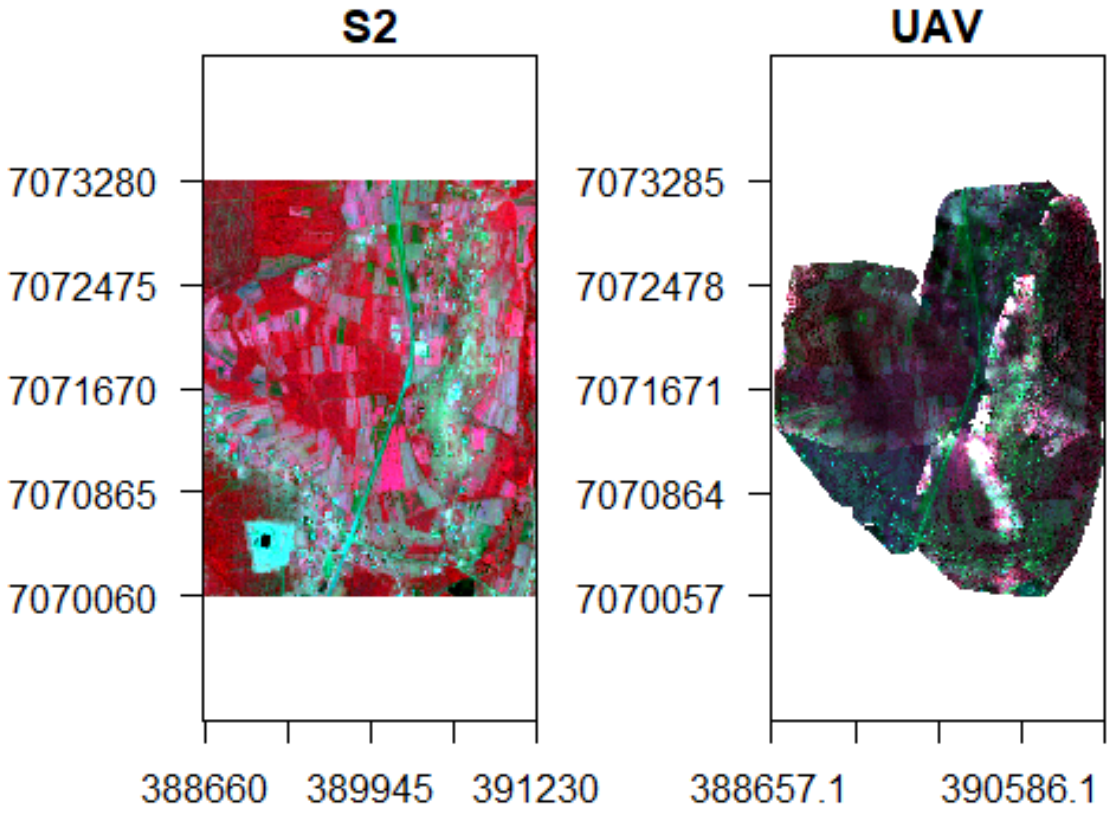

Figure 18: UAV & S2 false colour composite images for Mpolonjeni site.

should be taken to ensure that pure pixels (i.e. each training site includes only pixels for one class and not a mix of two or more classes). The output maps from the classification schemes for the different images are shown in Table 6.

These results show the potential of using UAVs in Eswatini to map cropped areas every season. To demonstrate that this kind of mapping can be scaled up across the whole country, a test mapping was done using S2 imagery across the country. This is was possible because S2 images are available for the entire country whereas UAV imagery is typically only available over smaller areas. The advantage that this test possesses is the ability to use UAV images acquired over the four pilot sites (Gege, Sidzakeni, Sigangeni and Mpolonjeni) to generate training sites and then complement them with additional sites generated using S2 images and visual image interpretation (Figure 19. The same process used in the pilot crop mapping detailed in the previous section was replicated for this test. However, due to difficulties in discriminating between crop types using visual assessment due to the lower resolution of the S2 imagery, landcover types were generalized into cropland, forestland, grassland, water body, other land and sugarcane. These are the dominant land cover types in Eswatini. This generalization also allows the achievement of higher classification accuracy where training data may be contaminated.

The MLC classification attained the best overall accuracy of 80% compared to RF method which attained only 45%. In both classifications, cropland only managed a best score of 58% using the MLC method (Table 8). It is believed that these classification results would significantly improve if UAVs were used exclusively to collect classification

Image Type	RF	MLC
UAV multi-spectral image	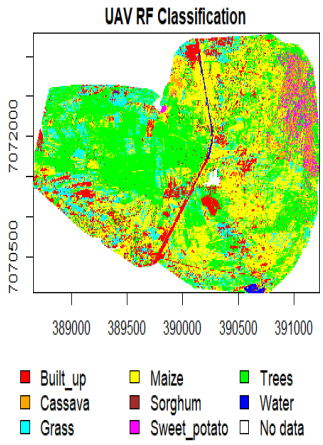	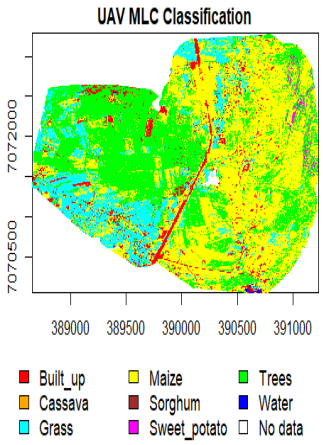
Sentinel-2 multispectral image	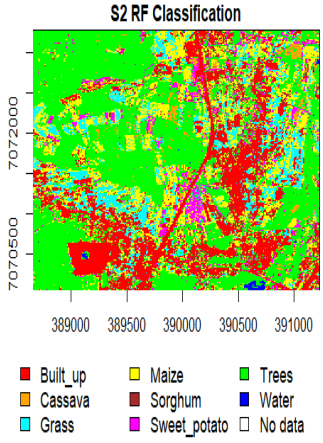	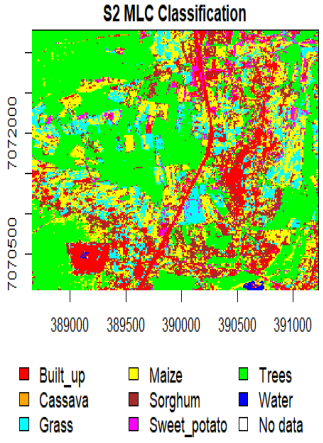
PCA-fused multi-spectral image	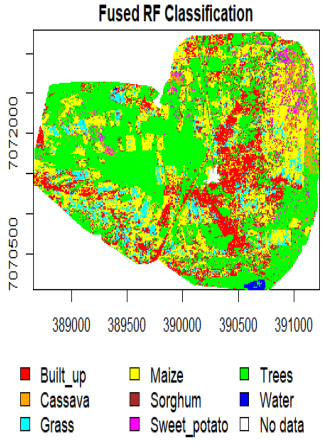	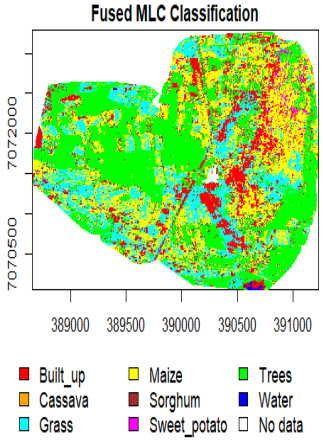

Table 6: Land cover classification results for Mpolonjeni pilot site.

training data and that samples were well distributed across the country. This is a clear limitation of how much precision can be attained when low-medium resolution imagery like S2 is used to collect training data. In future interventions, it is recommended that representative land cover samples are collected using UAVs during the growing season for the purpose of mapping cropped areas.

Table 7: Accuracy scores for RF and MLC classifications based on fused PCA image, UAV, and Sentinel-2.

Land cover class	RF_PCA	RF_UAV	RF_S2	MLC_PCA	MLC_UAV	MLC_S2
Built up	97.3%	98.9%	93.8%	92.1%	97.3%	89.3%
Cassava	98.7%	97.5%	88.9%	96.3%	100.0%	100.0%
Grassland	90.8%	88.7%	75.6%	67.9%	77.8%	51.1%
Maize	95.1%	95.0%	79.0%	84.6%	88.4%	63.7%
Sorghum	97.4%	95.4%	82.4%	92.3%	90.3%	42.9%
Sweet Potato	100.0%	99.8%	87.5%	99.4%	99.6%	90.3%
Trees/Forest	98.0%	98.4%	94.9%	95.0%	96.8%	90.7%
Waerbody	100.0%	100.0%	100.0%	99.1%	98.2%	100.0%

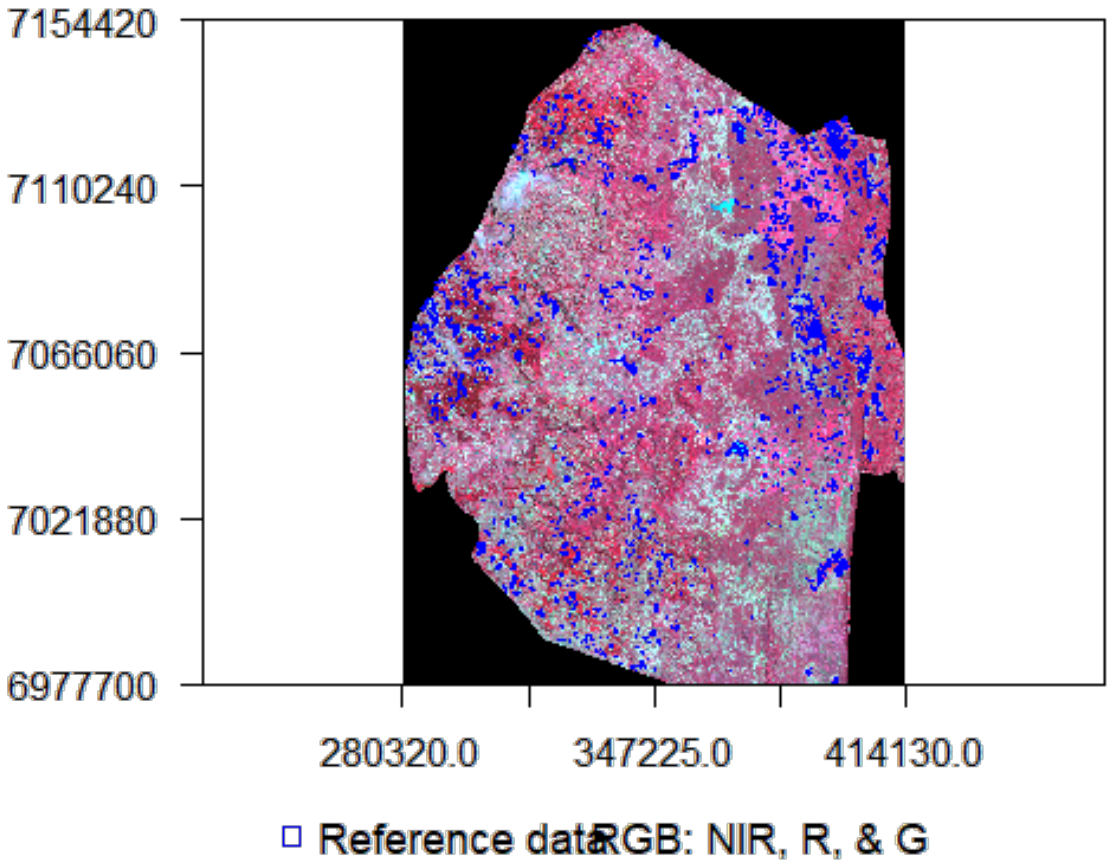

Figure 19: Training sites overlaid on a wall-to-wall S2 image over Eswatini.

Table 8: Classification accuracy scores by land cover type. A wall-to-wall Sentinel-2 imagery covering the entire country was used to map land cover. Overall accuracy scores were 80% and 45% for MLC and RF, respectively.

Land cover type	MLC_S2	RF_S2
Cropland	58.3%	26.4%
Forestland	93.4%	78.4%
Grassland	59.2%	30.4%
Open water	100%	67.9%
Otherland	88.8%	29.8%
Sugarcane	81%	33.4%

6.2.3 Yield Prediction

Crop yield modeling was piloted on maize production in 2020. Five predictor variables from MODIS vegetation indices products were used: Normalized Vegetation Index (NDVI), Enhanced Vegetation Index (EVI), Fraction of Photosynthetically Active Radiation (FPAR), Leaf Area Index (LAI) and Gross Primary Product (GPP). To predict end of season maize yield at a national level, reported yield data was collected from FAOSTAT for the period 2000 to 2019 (Figure 20). MODIS vegetation indices were downloaded for the months of January to March 2020 when crop growth is robust. These indices were then spatially (national) and temporally (3 months) aggregated using mean statistics. Z-score standardization was applied to the indices in order to capture long-term deviations of an index from the average. The standardized indices (Figure 21) were then used as input variables for training and validating three models: RF, Support Vector Machine (SVM) and Linear regression models (LM).

Model validations showed that the RF model had the best results (i.e. lowest MAPE and RMSE). This model was thus used to predict 2020 maize yield. Results showed that the country would have attained a yield of **92,500 MT**. This was a 6% overestimation error compared to the reported yield for that year which was 82,000 MT. Generally, it can be argued that the model gave a good prediction with a relatively small error. However, it should also be noted that the best and most robust model should explore more indicator variables known to affect crop yields such as soil moisture, temperature etc. It is also recommended that more ground data is used to train the models, and more effort should be made to gather yield data dis-aggregated at province level in order to increase the variability, and to allow a more precise prediction.

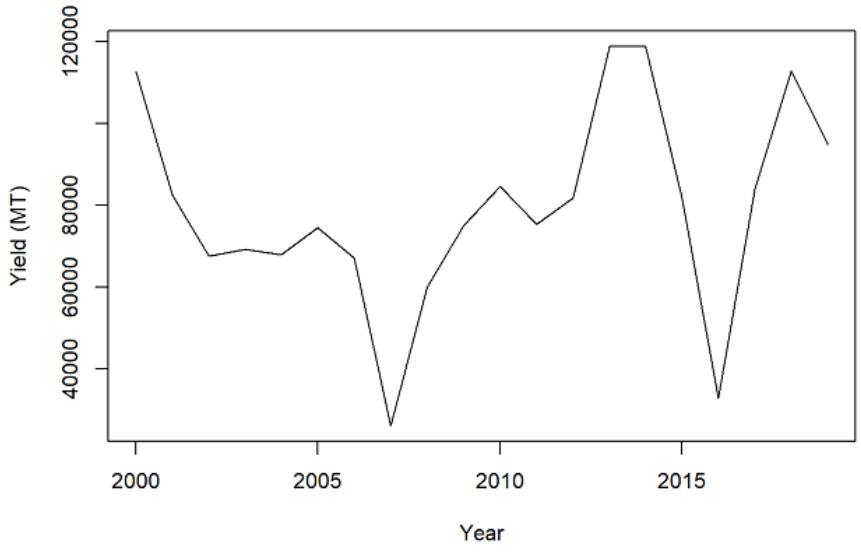

Figure 20: A timeseries plot of reported historical maize yield at the national level in metric tonnes (MT) for 2000-2019.

This case study demonstrates that it is possible to use machine learning models to statistically predict end-of-season yields with sufficient lead time for planning. In this case, a scenario could have been built such that the predict yield could have been part of a decision making process to determine whether that year was expected to attain below

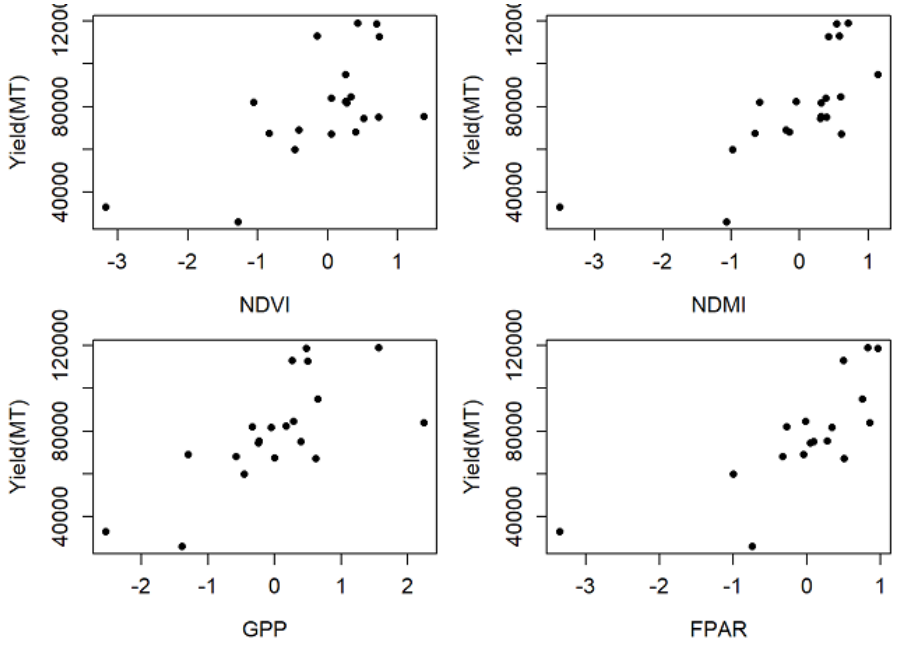

Figure 21: A plot showing the relationship between standardized reported maize yield and satellite metrics.

average, average or above average yields. Such decisions based on quantitative data and transparent scientific methods make it possible for food security agencies to determine specific actions related to agricultural production management including timing and the quantity of imports and exports.

6.3 Climate Analysis

6.3.1 Climate Baseline

Over 70% of the population in Eswatini relies on livelihoods that rely on rain-fed agriculture. Out of this, 75% are smallholder farmers. Impacts from climate change and variability has worsened the vulnerability of this group of the population. These impacts have largely been associated with recurrent droughts, partly due to the location of the country in a generally dry geography but also due to an increasingly uncertain rainfall and increasing aridity [34]. According to data from the World Bank Group's Climate Change Knowledge Portal (`https://climateknowledgeportal.worldbank.org/country/eswatini/climate-data-projections`) the country receives an annual rainfall of between 500 mm in the southern lowland to 1,500 mm in the northern Highveld. The main rainy season tends to occur between October to April with much of the rainfall received in November to February, overlapping with the typically hottest period annually. Temperature on the other hand has ranged between 15°C and 23.4°C. According to data from the Climate Research Unit (CRU), the average annual rainfall and temperature across the entire country for the period 1901-2020 is 810.5 mm and 20.1°C, respectively (Figure 23 and 24).

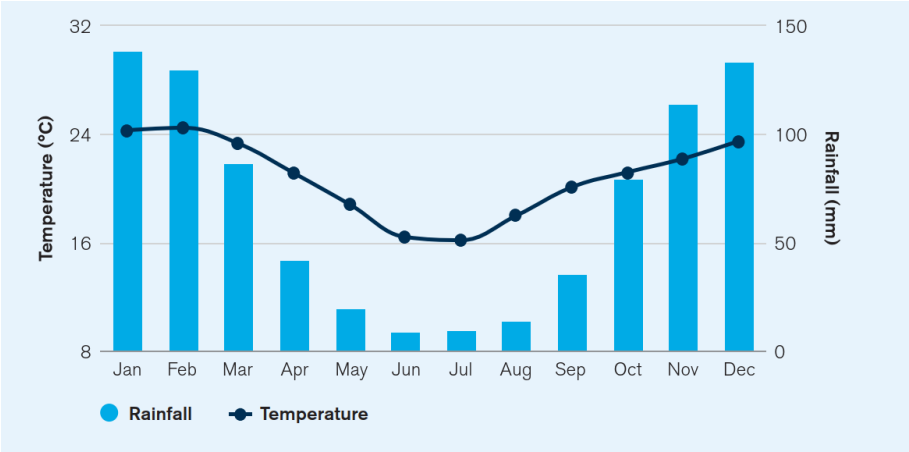

Figure 22: Average monthly rainfall and temperature for Eswatini between 1991-2020. Source: World Bank Climate Change Knowledge Portal.

Key Trends

Rainfall in Eswatini is considerably variable from year to year. This has led to periods of flash flooding during wet extremes and droughts during dry extremes. Drought is particularly a recurrent hazard due to the country's semi-arid climate. Rainfall trends from CRU point to a slight decrease in the number of rainy days, which poses an implication on the intensity of rainfall events and dry spell duration. Apart from changes in total annual rainfall, there have been observed changes to intra-seasonal characteristics including changes to onset, duration, intensity and frequency of rainfall events. According to trends in Figure 23, the rainfall pattern indicates a general increase in inter-annual variability.

Monthly mean temperatures from 1901 and 2020 show patterns of consistent warming over the country (Figure 24). This is consistent with other studies that have found daily maximum and minimum temperatures to be on the rise, with the latter having a more rapid increase compared to the former [35]. The period since 1990s has been warmer than earlier decades with the past two decades experiencing an increased frequency of very hot

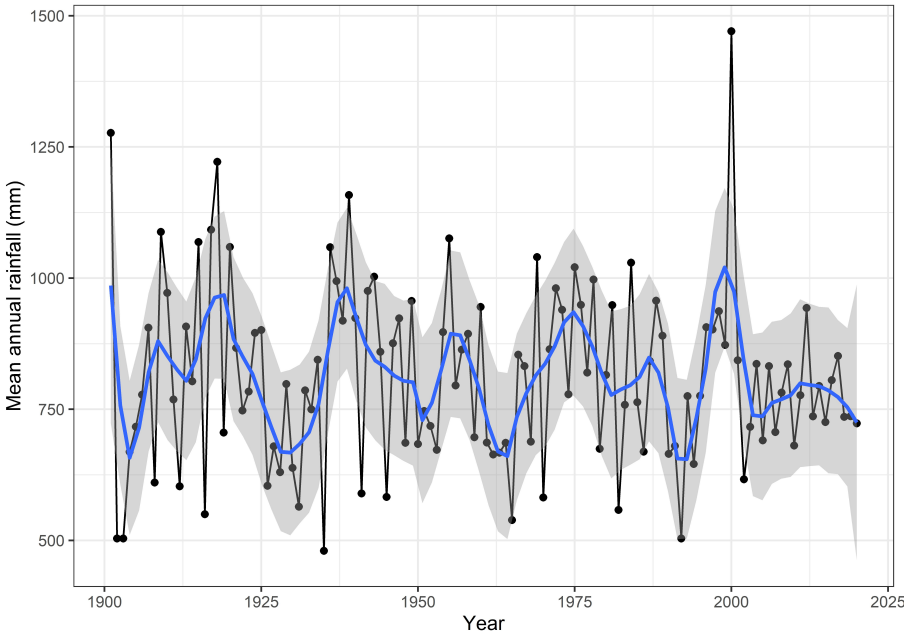

Figure 23: Annual mean rainfall averaged over Eswatini for the period 1901-2020. Data source: World Bank Climate Change Knowledge Portal.

days, often exceeding 34°C. In general, the number of cold nights have decreased whilst hot nights frequency has increased.

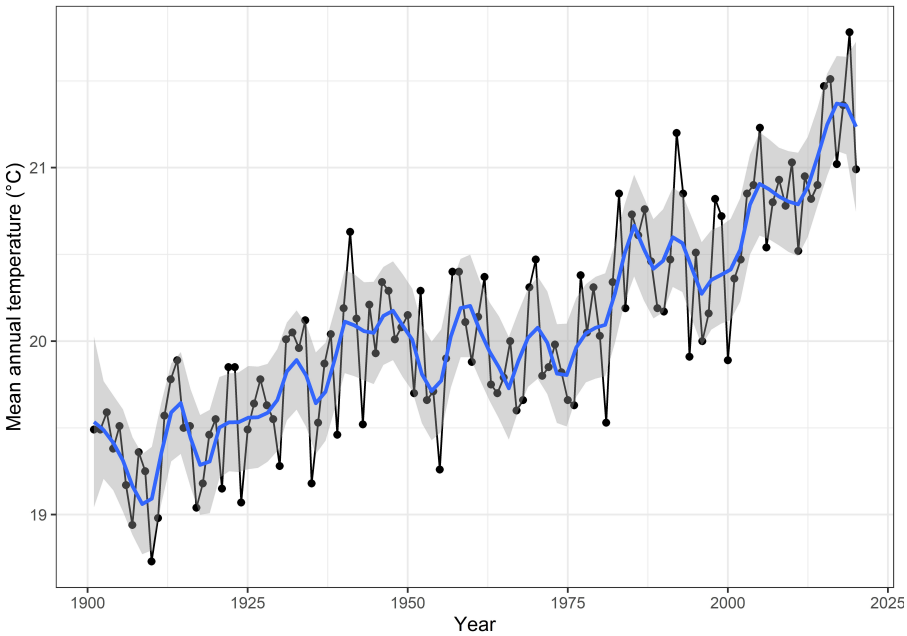

Figure 24: Annual mean temperature averaged over Eswatini for the period 1901-2020. Data source: World Bank Climate Change Knowledge Portal.

6.3.2 Climate Future

Rainfall and temperature projections in this case study are derived from an ensemble of 32 Global Climate Models (GCMs) that are part of the Coupled Model Inter-comparison Project Phase5 (CMIP5), and used for the Fifth Assessment Report (AR5) of the Intergovernmental Panel on Climate Change. Four Representative Concentration Pathways defined by their total radiative forcing (i.e. cumulative measure of GHG emissions from all sources) were considered. These are RCPs 2.6 (low), 4.5 (medium), 6.0 (medium-high) and 8.5 (high).

Precipitation projections for Eswatini are highly variable, with a high degree of uncertainty in rainfall projections. However, available projections suggest increased aridity and a higher occurrence in the number and frequency of dry spells over the summer season, October to February. Decreases in frost days are expected for the Highveld region. Changes in rainfall patterns are expected and this will alter streamflow and downstream catchment intakes. Runoff changes range from -17.4% to 26.6%; -31.2% to 18.1%; -40.3% to 27.7%; and -40.8% to 34.9% in the Komati, Mbuluzi, Usutu and Ngwavuma catchments, respectively. The median of the runoff change is negative for the majority of months in three catchments (Usutu, Mbuluzi and Ngwavuma) excluding the Komati catchment.

Increases in precipitation are expected through the 2030s, with increasingly significant decrease expected throughout the rest of the century, under the high emissions scenario, RCP8.5. Given the projected increasing trend of temperatures and slight decreases in variable rainfall, Eswatini's agricultural and water sectors are projected to be the most impacted and most at risk. Likewise, the probability of drought for much of Southern African sub-region. Figure 25 shows the projected trends for nationally aggregated annual precipitation for the different emission scenarios through the end of the century. Projections indicate a slight increase across each emission scenario. Water routing and storage and other management options, are often very different if the precipitation input comes as many weak or a series of heavy rainfall events.

Minimum and maximum temperatures are projected to increase through the 2090s and temperature is expected to rise by as much as 1.9°C by the 2050s, under an RCP8.5 scenario. Hot Days are expected to rise by as many as 24.4 days by the 2050s. Temperature is expected to increase year-round, with peaks felt in the hottest period of October to December, under RCP8.5. Projections also indicate a decrease in cold days and nights, which is expected to have harmful impacts on Eswatini's agriculture and livestock productivity. Across all emission scenarios, temperature increase for Eswatini are projected throughout the end of the century. As seen in the graph below, under a high-emission scenario, average temperatures are expected to increase rapidly by mid-century (Figure 26). An increase is also expected for the change in the number of summer days (Tmax >25°C), and the change in number of days across the seasonal cycle is also expected. Increases in the number of days over 25°C, calculated at national scale aggregation, are expected to remain largely the same. However, some areas, such as the Highveld are expected to experience greater changes in temperature increases. Increased heat and extreme heat conditions will result in significant implications for human and animal health, agriculture, and ecosystems [35].

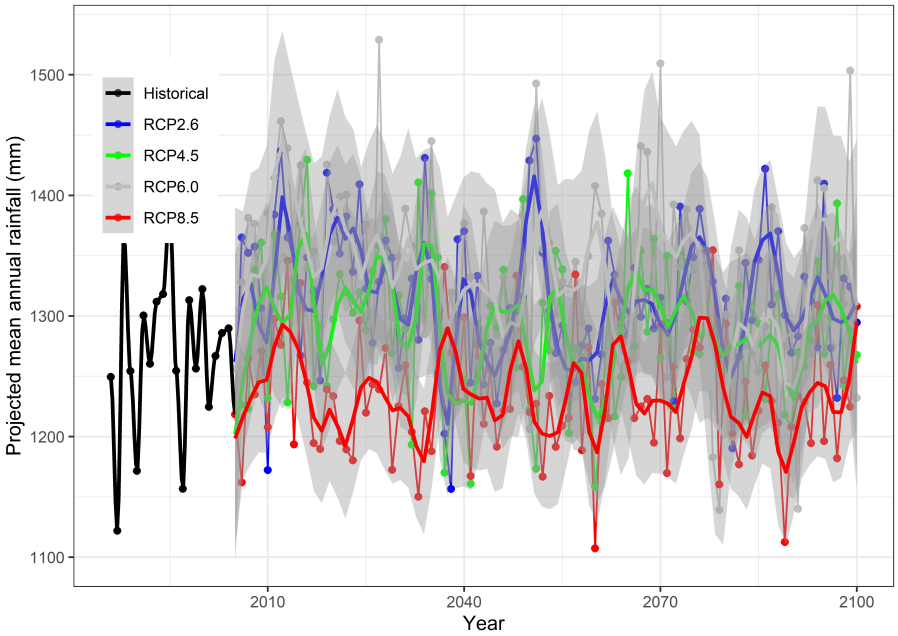

Figure 25: Projected annual mean rainfall from 32 CMIP5 climate models averaged over Eswatini for the period 2006-2100 for four Representative Concentration Pathways (RCPs). The reference period (historical) is from 1986-2005. Data source: World Bank Climate Change Knowledge Portal.

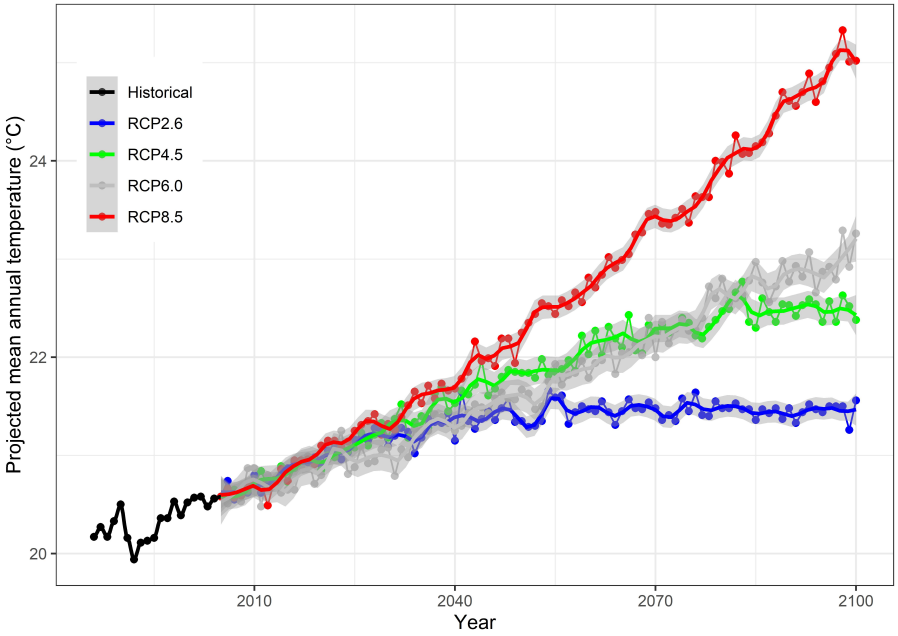

Figure 26: Projected annual mean temperature from 32 CMIP5 climate models averaged over Eswatini for the period 2006-2100 for four Representative Concentration Pathways (RCPs). The reference period (historical) is from 1986-2005. Data source: World Bank Climate Change Knowledge Portal.

6.4 Early Warning Tools

Climate related disasters such as droughts and floods have become a common phenomenon across much of the southern African region. A number of early warning systems have been established to provide actionable information to mitigate the impact of these disasters on

people, their livelihoods and property. Some of the available systems over Africa, including Eswatini are well documented in this recent paper by Nakalembe et al. [1]. Data are at the centre of most of these early warning systems. The growth of earth observation data has seen a proliferation of methods and systems that can leverage big data from satellites and ground observations, and coupled them with knowledge from other traditional sources such as farmers. The outcome of such complementary systems that leverage various sources of information has been improved preparedness before catastrophes occur.

To add to these systems, the humanitarian community is actively developing risk mitigation mechanisms such as crop and livestock insurance, forecast-based financing and early warning early action protocols, all of which to some part rely on data from satellites and ground observations. Due to the rain-fed reliance of agriculture, the mainstay of economies of most developing countries in the sub-Saharan Africa, monitoring hydro-meteorological conditions (rainfall, temperature, soil moisture, vegetation condition etc.) and providing early warning information through forecasts is imperative to any outcomes aimed at reducing the impacts of hydro-meteorological disasters.

Several early warning systems are available covering Eswatini. These include the Early Warning eXplorer (EWX) which is primarily dedicated to providing earth observations (EO) data focused on droughts and floods and the GEO Global Agricultural Monitoring (GEOCLAM) initiative that is focused on crop conditions and food security. The two systems are described in more detail below and examples of their use in Eswatini is also provided.

6.4.1 Early Warning eXplorer

The Early Warning eXplorer or simply EWX is a web-based single-page application for exploration of geo-spatial data mainly related to agricultural drought monitoring providing early warning information. The EWX provides easy and routine access to critical EO with the primary goal of enhancing their application for disaster mitigation and supporting long-term resilience. These EO are best suited to monitor meteorological and agricultural drought conditions, and examine long-term changes and trends [1, 36]. This portal was developed by the Climate Hazards Centre at the University of California- St. Barbara and a customized version of the portal is now available at RCMRD.

The EWX allows users to access maps and time-series graphs, aggregated over pre-defined polygons. The EWX allows for quick access to maps of climate and vegetation (Figure 27). Typically, maps of all the datasets are available as absolute values, additive anomaly, and standardized anomaly (additive anomaly divided by standard deviations). While maps provided by EWX allow for a quick overview of drought conditions at a regional scale, for in-depth, targeted, local-scale analysis, the EWX also provides spatially aggregated time-series graphs of EO. Like the maps, time-series graphs are of absolute value, additive anomaly, and standardized anomaly [1, 36].

The EWX can be used to access and download EO in a form that is compatible with widely used open-source GIS tools such as QGIS, and programming languages such as Python, to support further analyses. Data accessible in EWX include a rainfall climatology from blended satellite and *in-situ* observations known as the Climate Hazards InfraRed Precipitation with Stations (CHIRPS), CHIRPS-GEFS (a bias-corrected and downscaled version of NCEP Global Ensemble Forecast System precipitation forecasts made to be spatially compatible with various CHIRPS products), MODIS Land Surface Temperature and NDVI. The RCMRD version of the EWX portal can be accessed through this link:

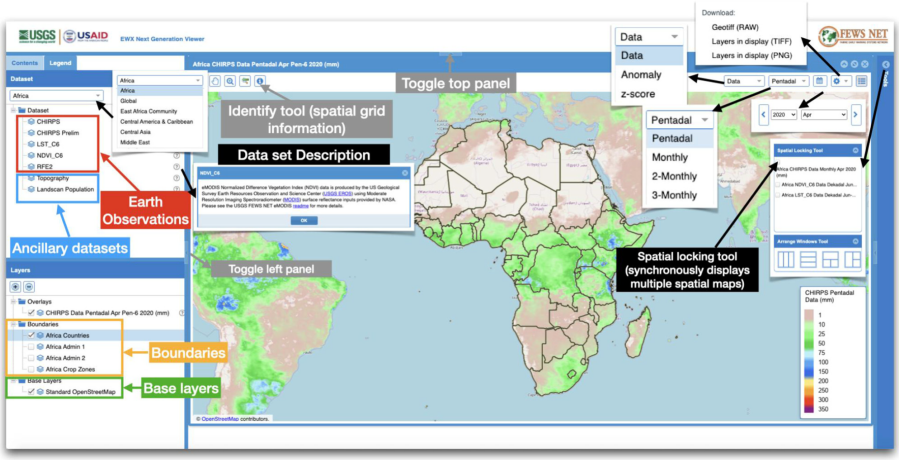

Figure 27: A snapshot of the EWX portal showing key tools to navigate the data and visualization components [36].

https://data.rcmrd.org/ewx-viewer/.

The example in Figure 28 shows how the EWX could have been used to track the 2015 - 2016 drought in Eswatini using a 3-months Standard Precipitation Index (SPI) or Z-score; a standardized index based on rainfall anomaly. SPI is tracked from the month of October 2015 at the beginning of the main rainy season to the end of the season, May 2016. According to the Rapid Assessment Report of 2016, the country's 2015/16 rainfall fell below the average by over 50 % due to El Nino Southern Oscillation effect over Southern Africa that resulted in dry conditions. The worst hit regions were Tinkundla, Madlngampisi, Lomahasha and Somntongo. Using the EWX and CHIRPS gridded satellite-station rainfall data, the SPI showed that the worst months were between October and January when much of the rainfall is received over most parts of the country.

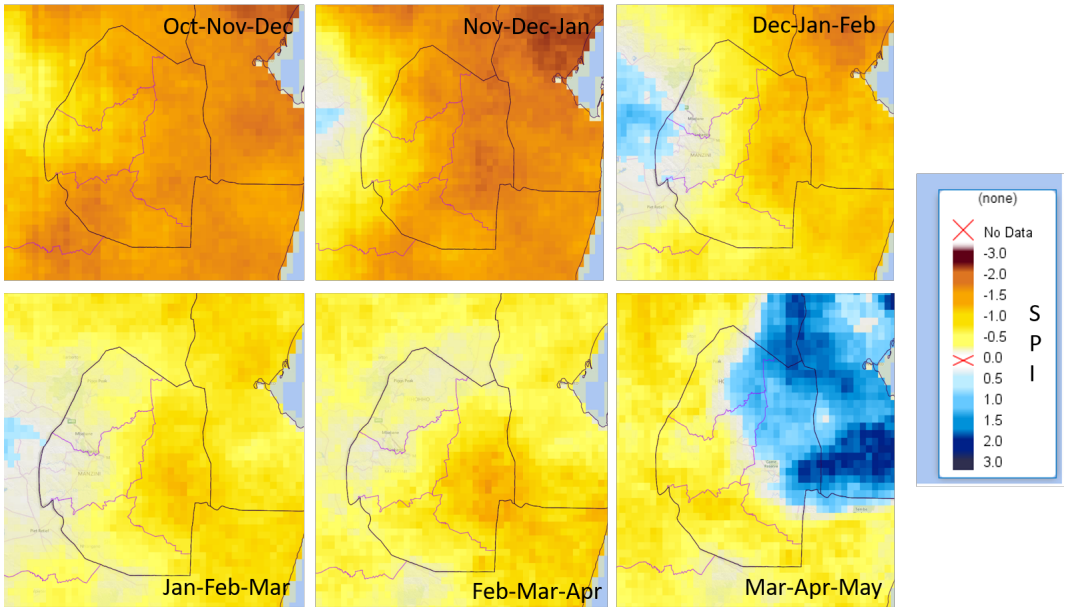

Figure 28: Time-sequence maps of 3-months Standardized Precipitation Index (SPI) tracking the 2015/2016 drought over Eswatini. Drought conditions are shown by values below zero while wet conditions are shown by values above zero.

6.4.2 GEOGLAM

The Group on Earth Observations Global Agricultural Monitoring Initiative (GEOGLAM) is an effort focused on promoting and improving agricultural monitoring by leveraging information from various sources, including earth observations. The initiatives aims to produce information on the current state of agricultural land cover and land use. It has identified several EO-based products for operational monitoring, including cropland masks, soil moisture, rainfall, temperature, run-off and evapotranspiration. An integral component of this initiative is the Crop Monitor. Several national and regional crop monitors have been established e.g. in Kenya, Tanzania, Rwanda, Ethiopia, Zambia and Uganda, including a regional crop monitor for East Africa [1, 37].

In many 'countries at risk', agrometeorological and remote sensing information is often the first and even the sole source of information on crop conditions, allowing rapid and large-scale assessment of potential weather-related impacts on agricultural production. EO data sets are often used to identify anomalies that can be associated with potential agricultural impacts and are used together to provide a robust basis for convergence of evidence of agricultural conditions, which is especially useful when field reports are unavailable. Additionally, EO data sets are operationally being used in many counties to make pre-harvest production forecasts and in assessing the impact of drought (GEOGLAM 2021). Complementary to the Crop Monitor is the Agricultural Monitoring Information System (AMIS).

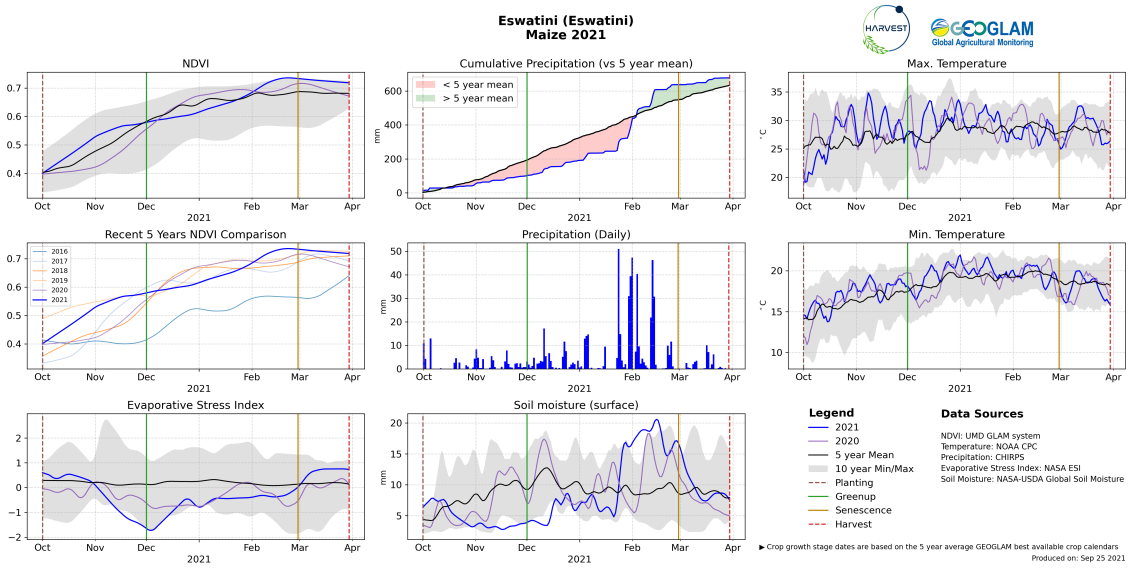

Figure 29: A snapshot of the GEOGLAM Crop Monitor Explorer showing trends in key EO products relevant to crop condition monitoring aggregated over Eswatini for the maize crop in 2021. The tool can be accessed via: `https://cropmonitor.org/index.php/eodatatools/cmet/`.

6.4.3 Integrated Phase Classification Food Security Outlooks

The Integrated Food Security Phase Classification (IPC) is an innovative multi-partner initiative for improving food security and nutrition analysis and decision-making. By using the IPC classification and analytical approach, Governments, UN Agencies, NGOs, civil society and other relevant actors, work together to determine the severity and magnitude of acute and chronic food insecurity, and acute malnutrition situations in a country, according to internationally-recognised scientific standards.

The main goal of the IPC is to provide decision-makers with a rigorous, evidence- and consensus-based analysis of food insecurity and acute malnutrition situations, to inform emergency responses as well as medium- and long-term policy and programming. The IPC Acute Food Insecurity (IPC AFI) classification provides strategically relevant information to decision makers that focuses on short-term objectives to prevent, mitigate or decrease severe food insecurity that threatens lives or livelihoods. In particular, the IPC Acute Food Insecurity classification provides:

i Differentiation between different levels of severity of acute food insecurity, classifying units of analysis in five distinct phases: (1) Minimal/None, (2) Stressed, (3) Crisis, (4) Emergency, (5) Catastrophe/Famine. Each of these phases has important and distinct implications for where and how best to intervene, and therefore influences priority response objectives;

ii A snapshot of the current severity of acute food insecurity situations as well as a projection of future conditions. This information over two time periods provides stakeholders with an early warning statement for proactive decision-making;

iii A food insecurity situation analysis that combines international standards - including food consumption levels, livelihoods changes, nutritional status, and mortality - and triangulates them with several contributing factors (food availability, access, utilization and stability, and vulnerability and hazards) analyzed within local contexts; and

iv Identification of key drivers of acute food insecurity.

The IPC Acute Food Insecurity classification is conducted according to the four functions of the IPC, including: 1) consensus building, 2) methodical evaluation, review and convergence of all evidence available against global thresholds, 3) strategic communication for action, and 4) quality assurance.

The current IPC outlook for Eswatini and a projection to March 2022 is shown in Figure 30. Key results from the outlooks as provided by the IPC are summarized below:

R Nearly 262,000 people (22% of the analysed population) in Eswatini are experiencing high levels of acute food insecurity (IPC Phase 3 or above) between June and September 2021 and require urgent humanitarian assistance. Of these, 240,000 people are experiencing Crisis food acute insecurity (IPC Phase 3) and 22, 000 Emergency acute food insecurity (IPC Phase 4). An additional 342,000 people (29%) are Stressed (IPC Phase 2). The situation has slightly deteriorated when compared to 2019/20 when the food insecure population in IPC Phase 3 or above was 205,000. During the projected period, which corresponds with the lean season, the number of people expected to experience Crisis or worse acute food insecurity is expected to increase by an estimated 5% from the current levels of 262,000 to around 317,000. The likely impact of the COVID-19 pandemic, high commodity prices and poor performance of the agricultural season will greatly influence this increase.

Urban livelihood zones have also shown increased levels of acute food insecurity. The Peri-urban and Lubombo Plateau had the highest proportion (45%) of households classified in Crisis or worse (IPC Phase 3 or above). The Livestock Cattle and Maize (the largest livelihood zone in terms of area covered and population) has over 90,000 people (40%) in IPC Phase 3 or above requiring urgent assistance. The deterioration is attributed to the impact of COVID-19 pandemic households in the urban and peri-urban areas. Most urban areas were classified in Crisis (IPC Phase 3) or worse, averaging above 20% in these conditions, with Lubombo reaching 35% and Shiselweni Urban 25%. Limited livelihood opportunities, high food prices and the impact of the COVID-19 pandemic are the key drivers of acute food insecurity in the urban areas.

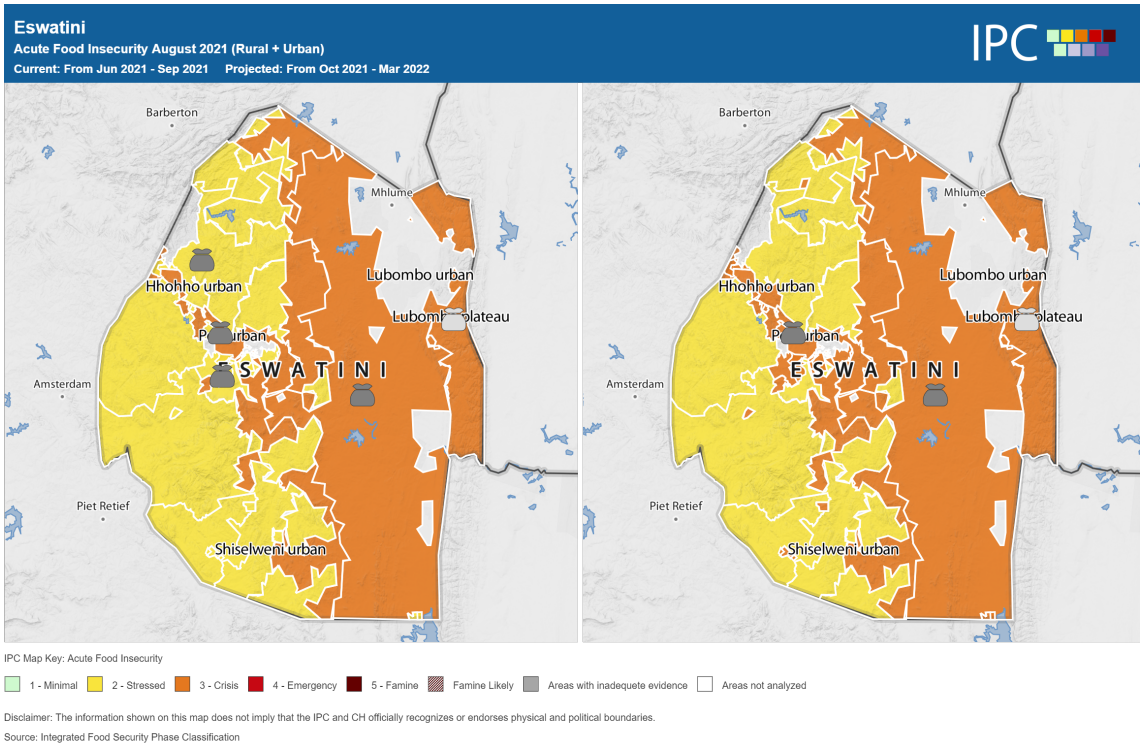

Figure 30: A snapshot of a food security outlook for Eswatini for July - September 2021 (left) and a projection for October 2021 - March 2022 (right). The tool can be accessed via: `http://www.ipcinfo.org/ipc-country-analysis/details-map/en/c/1155121/`.

Box 3

Stakeholders in Eswatini can use the early warning systems described in this section (EWX, GEOGLAM Crop Monitor exploring tool and the IPC Food Security outlooks) to monitor the progress of a growing season by leveraging the diversity of EO data, capabilities and stakeholder engagements provided by these systems. Beyond the basic access via these systems, as shown with EWX, it is also possible to download the data underlying the visual graphics and carry out further analysis. For instance, data analysts with skills and knowledge on the use of GIS mapping tools can generate more insights from the raw data, and can overlay other types of data (e.g. cropland masks) to provide more context. It is recommended that country stakeholders led by NDMA, the Department of Meteorology and the Ministry of Agriculture form a joint team that can build skills necessary to use of these tools in order to provide the monitoring service to the government and other stakeholders working in the agricultural sector.

6.5 Gender and Agriculture in Eswatini

The government of the Kingdom of Eswatini recognizes gender inequality as an impediment to sustainable national development and has backed its constitutional guarantees of equality with a number of statutes, policies, and strategies. These include its 2004 ratification of the United Nations Convention on the Elimination of All Forms of Discrimination against Women (CEDAW), its National Gender Policy (2010), and its 2018 Sexual Offences and Domestic Violence Bill. These enabling mechanisms have provided an opportunity to make progress toward gender equality in Eswatini.

Eswatini women need to be specifically targeted due to the following reasons:

i. Women make up 53% of the population in a country with 63% of the population living in poverty; therefore solving their problems is solving the problems of the majority.
ii. Statistics support that women are amongst the most vulnerable in the country and it is the vulnerable groups which experience an intensification of challenges under additional vulnerability to the environment. The Eswatini Household Income and Expenditure Survey 2009/10 reported female-headed households as having higher poverty incidence at 67% when compared to their male counterparts at 59%.There increased vulnerability is connected to the fact that women have fewer resources and therefore low adaptive capacities.
iii. Eswatini women generally have lower economic status than men as the 2013-2014 Draft Labor Force Survey indicates that male earnings are 67% higher than those of women. Additionally, the survey indicates female labour participation rate at only 45% and women participation in the labour force is lower in all the regions as well as across rural and urban areas.
iv. Women have unique expertise and experience on climate adaptation which they pass on to their children e.g. skills on how to manage water collection and how to collect firewood which are a vital household asset during drought.
v. Adaptive interventions need to bear in mind the cultural norms; unequal distribution of roles, resources and power. This builds the case for strategies which need to mark the appropriate target. The same economic and societal roles that make women more vulnerable to the effects of climate change are also the same key challenges which mark women as key actors for driving sustainable development. Therefore National Disaster Management Agency needs to pay particular attention to women, their needs, and their unique experience of vulnerability in instances of disasters.

Gender equality

Eswatini has one of the highest HIV prevalence rates in the world, at 27 per cent among the adult population. Young girls and women aged 15-24 years bear the brunt of the epidemic, with an HIV incidence of 1.8% among females, ranking five times more than incidence among male counterparts. Gender-based violence is prevalent, with 1 in 3 women experiencing some form of sexual violence by age 18 years and 48 per cent in their lifetime, arising from negative social norms and discriminatory practices within customary laws. Furthermore, patriarchy, early marriage and limited engagement with men and boys, weak multi-sectoral coordination, and inconsistent enforcement of legislation and policy implementation continue to constrain efforts to achieve gender equality and end gender based violence. When compared with 2019 levels, the Royal Eswatini Police Service report for April and May 2020 indicated a 15 per cent increase in the cases of gender-based

violence during the lockdown period instituted to control the coronavirus pandemic.

For CEDAW, the indicators of equality are not the policies, laws and institutions that have been created to provide women with opportunities, but what these policies, laws and institutions have achieved in terms of women having the same opportunities as men in all spheres of life including agricultural livelihoods. For example while the Eswatini Constitution provides for equality before the law and non-discrimination, it does not prevent discrimination on the grounds of sex and gender identity. Gender stereotypes and expectations relegate women to second-class citizens and are major barriers to their participation in public decision-making processes and electoral systems.

Further to the above, under Eswatini law and custom, Eswatini Nation Land is distributed for a nominal fee at the discretion of the chief, solely to married men or male sons upon an allegiance ceremony, or khonta, that includes the payment of cattle. Single men and women are not supposed to be allocated any Eswatini Nation Land; in recent years, however, chiefs have also been known to allocate Eswatini Nation Land to single men for cash further disenfranchising women who have less access to opportunities for wage labour.

Such discriminatory practices have resulted into harsh consequences. Women are denied an adequate standard of living because without access to land, they cannot build a home or grow food for themselves and their family; women's health and lives are endangered because they must attach themselves to and stay with abusive or HIV positive men in order to access the land they need to survive; women have no security of occupation on Eswatini Nation Land and may be evicted arbitrarily and with no compensation; and women who are evicted from Eswatini Nation Land are torn apart from their children because men retain custodial rights over the children. Because nearly seventy percent of the population lives on Eswatini Nation Land, the exclusion of women from land allocation has discriminatory negative effects on a big section of the population and needs to be corrected.

In addition, under the common law marital power, and the Marriage Act of 1964 a married woman cannot conclude contracts without her husband's permission, she cannot represent herself in civil suits, and she cannot administer property. This restriction on the right to conclude contracts included restrictions on the ability to access bank loans, mortgages, and financial credit generally. Common law marital power therefore relegated married women to the legal status of minors under the guardianship of their husbands. In a situation where a woman is deserted by her husband the marital power could not allow her to sell any asset they jointly owned, including what she had purchased with her own money because they are registered in her husband's name.

Regional Gender issues relevant to Eswatini

Agriculture in Africa depends heavily on manual labour, supplied by farmers' households, families and communities. Yet women farmers face many difficulties in mobilizing extra help to work on their farms, and these challenges begin in the home. On average, female farmers tend to live in smaller households with fewer men, possibly due to widowhood, migration or divorce. When the male laborers are hired they generate lower returns for female farmers relative to male farmers. Female farmers also face challenges in hiring effective outside labour because they may not be able to afford to pay as much as men for effective farm workers; that cultural norms may mean that these labourers work harder for a male supervisor; and/or that women's time constraints (due to their household roles)

may affect their ability to supervise their farm labourers. Indeed, women typically assume a larger role in child-care and household responsibilities than men, which is likely to restrict their ability to work on their own farms or manage their labourers. Men, meanwhile, tend to have greater control over how to allocate family labour, including that of younger household members. For these reasons, having a larger proportion of children in the household (relative to adults) reduces women's productivity more than men's. types of labour challenges, evidence on policies aiming to help women overcome these barriers is rare.

Gender-disaggregated data remain sparse, which hinders problem identification and trends analysis with respect to women's empowerment in agriculture. For example, Techno serve's Coffee Initiative in East Africa began collecting data at the individual – instead of the household – level in order to more accurately track training attendance and coffee tree ownership by gender. This was one of multiple measures that may have contributed to increasing female participation in the programme from 6% to 42%. Female researchers remain underrepresented at most African research agencies. In Eswatini it was observed that there was a gender imbalance among professional staff at agricultural research agencies e.g. during the period 2011-2016. There was a gradual decline among of female professionals from 41% to 28% with the reverse among the males who had an increase from 59% to 72% Gender balance among professional staff at agricultural research agencies is important, given that women researchers and professors offer different insights and perspectives that can help agricultural research and training more effectively address the unique and pressing challenges of female farmers. Women researchers serve as important role models to students and they are better suited to represent female farmers in their communication with political decision makers. This means that women have less influence in policy- and decision making processes, potentially creating a bias in decision making and priority-setting.

Findings from previous research in the region highlighting the gender gap in agriculture has focused exclusively on women's access to key inputs, such as fertilizer, agricultural information and farm labour, concluding that if women had better access, they would be equally productive. This research also revealed that, even when women have access to the same amount of inputs as men, equal access does not achieve the same effect in terms of agricultural productivity. This novel insight points to broader norms, market failures or institutional constraints that alter the effectiveness of these resources for women. There is evidence that women benefit less than men, in terms of increased agricultural productivity from extension advice that their households receive, suggesting that current agricultural extension programmes may be better attuned to the needs of male farmers. These crucial new findings will empower governments and development organizations to better tailor policies and programmes to those issues and constraints that are most critical to the livelihoods of women farmers in their countries.

The Eswatini Rural Women Assembly highlighted some of the challenges that rural women farmers were experiencing as a result of COVID-19 and the attendant regulations and restrictions. These challenges were:

i. Many of them were stuck with their produce because of limited movements, especially in the Shiselweni region where they farm sweet potatoes and sell in Manzini.
ii. The Eswatini Rural Women Assembly also reported that some of the women in the country sell their produce at the bus stations in the main cities but were unable to do so as a result of the lockdown.
iii. Some also feared COVID-19 infection as they did not have personal protective equipment to protect themselves, and therefore decided not to venture out to sell at

their usual points. Under normal circumstances, some of the women distribute and sell their produce on credit and collect their money at the end of the month when urban workers receive their monthly salaries.

iv. The initial lockdown in Eswatini came towards the end of the month in March 2020 and many of the women were unable to travel to the urban areas to collect their money. The Eswatini Rural Women Assembly reported that this impacted the women's household incomes, leading to domestic violence as family members, especially men demanded food, which the women were unable to provide. The impact of the lockdown in this case therefore went beyond loss of income for the rural women farmers, but also had secondary effects in the form of domestic violence.

Opportunities and Best Practices

Increasing women's access to and control over assets has been shown to have positive effects on important human development outcomes including household food security, child nutrition and education, and women's own well-being and status within the home and community. According to FAO, 50% to 75% of farm labour time is spent on weeding by hand, with 90 percent of this being done by women. With the introduction of Climate smart agriculture women have enough time to look after other family responsibilities. Most importantly, they report having time to rest and none of their children is forced to abscond from school because of farming. Climate smart agriculture was introduced as a pilot in two Eswatini Regional Administrative Areas; Ngwempisi and Ntfonjeni. This programme is relatively new although it is gaining momentum among farmers. This technology follows research by the Climate-Smart Market Oriented Agriculture Project (CSMA) where it was discovered that women have too many household chores yet they still have to spend many hours for days on end in the field. Women farmers are able to use simple digital apps like WhatsApp to communicate to NAM Board extension officers to give them updates on crops by taking pictures of the crops, and if diseased, they can help with a diagnosis and a possible resolution.

Rapid prototyping and testing should help ensure that D4Ag solutions are responsive to women's needs. Many of the most active players in D4Ag have applied this to various elements of their businesses targeting women. For example, MyAgro recognized that women farmers typically have smaller land plots and less liquidity than men, and began selling inputs in smaller batches for crops that women typically grow. Due to social norms and COVID-19 related restrictions many women across the continent are largely confined to their homes. Digital tools like advisory services and market linkage can allow them to access products and services despite this restriction. In doing so, these tools have the potential to increase women's ability to organize and work collectively – one of the most significant drivers of women's empowerment.

MyAgro's wider work stands out as an exemplar of how to build a strong base of women users. MyAgro is a mobile layaway programme in Mali and Senegal that equips farmers to buy seeds, fertiliser and training packages. In a short period, it has demonstrated impressive impact by spurring 50–100% increases in harvest yields and €108–334 additional income per farmer. It has also managed to build a user base that is 60% women. MyAgro attributes this achievement to a number of factors:

i. It involves women in its design phases, particularly for products used in the types of farming dominated by women (e.g., peanut farming, or farming on plots smaller than three hectares);
ii. It offers smaller seed and fertilizer packets and mobile layaway options, which benefit

women, who are more likely to be cash poor;

iii. It disseminates information and products through women-dominated village savings and loan associations (VSLAs);
iv. It develops village-level distribution centers to work around women's mobility constraints;
v. It focuses explicitly on recruiting female field agents; and
vi. Perhaps most importantly, it also tracks the impact of these efforts by collecting and analyzing gender-disaggregated data.

Successes elsewhere in Africa introducing digital technologies and promoting women participation can significantly improve gender related outcomes in Eswatini.

Eswatini supportive laws

The 2005 Constitution of Eswatini provides for equal access to land for women and men alike. Sub-section 212 (3) states that a citizen of Eswatini, without regard of gender, shall all have equal access to land for domestic purposes. The Deeds Registry Act No. 37 of 1968 and the Deeds Registry (Amendment) Act, 2012 promote equal access to land for women and men alike, guaranteeing the right to land ownership across gender. It also ensures that property is fairly distributed between all parties at the dissolution of a marriage or the death of a spouse. The High Court of Eswatini ruled on 23 February 2010 that some married women will be allowed to register property in their own name. Gender activists greeted the ruling as a small victory but continued advancement of positive progress towards women emancipation would result in positive outcomes for this groups of society and the general society wellbeing. Women need better access to land, as well as the confidence and security that their land investments will benefit themselves and their families. For these reasons, policies aimed at strengthening women's land rights should be considered and currently Eswatini has institutions that support women in cases of access to land for productive use. These include: Land Management Board , Commission on Human Rights and Public Administration, Women and Law in Southern Africa - Eswatini and the JPR Department – Council of Eswatini Churches.

Recommendations for gender considerations

The following recommendations are made based on this gender analysis:

1. Sensitization of the general public most especially the monarchy and chiefs on the harmful cultural gender norms, attitudes, discriminatory laws and behavior.
2. Mainstreaming gender in their climate change policy is very important because climate is not gender neutral.
3. To address the gender gap in D4Ag, the entire sector needs to make women a priority. This will require mainstreaming gender in D4Ag initiatives by building gender concerns into donor programming and enterprise solution design. It will also require advocacy to ensure that gender becomes a funding priority. Industry players can take steps to make it easier to work with women – starting with more inclusive data and solution design. A recent World Bank and International Food Policy Research Institute (IFPRI) study found that female extension agents are more likely to serve female farmers than are male agents (the ratio of women to men was 1.30 for female agents and 0.53 for male agents).
4. Enhance the effectiveness of farmers' organizations by institutionalizing training that recognizes the differential needs and challenges of women and men farmers and that includes farm visits, farmer-to-farmer exchanges, and visits to research

institutions. Training provision should be flexible, taking into account rural women's time constraints, especially for the mothers of small children, and the social dynamics that affect women's participation (e.g. mobility, care giving responsibilities). Farmers' organizations need to make provisions and ensure budgets for daycare facilities that enable women to participate in training to strengthen their livelihoods and overall well-being, as well as building their skills and confidence in assuming greater leadership roles within their organizations.

5. Build the knowledge base on women's participation in various community activities, to establish a more comprehensive and detailed picture of the extent of women's participation and to identify ways of eliminating constraints; Develop action plans that highlight practical barriers to women's participation in community activities and suggest ways of eliminating these barriers; develop and implement programmes for increasing community sensitivity to women's participation issues; develop and implement policies and programmes that support rural women's active participation in producers' organizations and cooperatives, because membership, leadership or management of such organizations brings enhanced status and a greater voice in the community and society in general.
6. Implement measures (including through land laws, family and marriage laws, and inheritance and housing laws) that ensure rural women's full access to and control over land and other resources, including through ownership, co-ownership, inheritance and succession.
7. Consider enacting national laws and policies that guarantee women's right to land, including after divorce and separation, and their rights to inheritance in both customary and statutory systems.Direct access to Eswatini Nation Land gives the growing number of female household's access to low cost land on which they can build a home and raise food for their family.
8. To secure equality in the allocation of Eswatini Nation Land for women and to uphold respect for the authority of local chiefs, a village land board, including the chief, should be established to oversee the allocation process in each Eswatini chiefdom. In order for the Board to be more representative of the community, the Board should be comprised of at least half women and can include the chief and representatives from the chief's inner council.
9. In order to ensure that women have full rights to their personal property, Eswatini land should consider abolishing the marital power. Many countries around the world and in Africa have already done away with the marital power, requiring that spouses have equal rights to use property and that both are consulted before any action is taken with respect to property.

6.6 Conclusions

This activity has developed a framework that can serve as a guide for stakeholders in Eswatini to use in monitoring agricultural performance in the country using UAVs and satellite remote sensing technologies. The introduction of agricultural technologies that use UAVs and satellite remote sensing needs to consider several factors before their implementation. On one hand, data collection will require the right combination of skills, knowledge, equipment and software. Other other hand,information generation and dissemination needs to put into consideration who the target audience is as different audience may require different forms of data packaging. The timing of such information is also key as different decisions are needed to be made at different levels at different times. It

is also imperative to consider the impact of new digital technologies on outcomes of interest and to ensure that such technologies do not disadvantage sections of the population who may not have a conducive type of environment for their introduction due to various social, economical, cultural, natural and technological factors.

Capacity building is also an integral part of a successful program. UAV technologies are relatively new compared to satellite remote sensing. Both technologies however require skills and knowledge about data acquisition, analysis and information dissemination. A drone pilot license is also needed in order to qualify to fly such instruments in any country. Along with an enabling regulatory environment, stakeholders in Eswatini need to build their Big data management skills. It is recommended that these skills be primarily built around the use of GIS and Remote Sensing in natural resources management, climate risk assessments as well as gender analysis. Further, a comprehensive technology readiness assessment is recommended to evaluate strengths, weaknesses and opportunities that can facilitate or impede an operational agricultural monitoring program that uses UAVs and satellite remote sensing.

7. Appendices

7.1 Data fusion, land cover mapping and crop yield modeling using R statistical tool

Introduction

The increasing world's population coupled with climate change has steadily increased demand for food. Consequently, countries have been faced with the challenge ensuring food security to their citizens. To meet this mandate, governments require agricultural production information to aid resource allocation and sustainable farming practices so as to attain improved food security for the developing world. Information on spatial distribution of crops is therefore an important step towards sustainable agricultural production. We need to know where the crops are before we estimate the yield in a given region. Ground mapping approaches like surveying are expensive and time intensive. Remote sensing offers an effective and efficient platform for mapping thanks to improved temporal and spatial resolutions. This capability provides a reliable system with near-term potential to provide stakeholders with timely information on crop distribution, status, and predicted yield. The advent of light Unmanned Aerial Vehicles has also pushed the frontiers of data acquisition and phenomena monitoring.

Exploiting the synergy between UAV and satellite data is essential for understanding the dynamics of the Earth's surface (Künzer, Dech, & Wagner, 2015). For instance, UAV can quickly acquire data with high spatial resolution, short revisit period and minimal atmospheric effects compared to spaceborn systems (Zhao et al., 2019). UAV have also been used to aid collection of ground reference data for image classification (Beach, Lapidus, Hegarty-Craver, O'Neil, & Dorota, 2020; Kattenborn, Lopatin, Förster, Braun, & Fassnacht, 2019). In this action, UAVs were used to collect training data with ground expert knowledge. In addition, we supplement UAV spectral information using Sentinel~2 (S2) optical through image fusion experiment for crop mapping. S2 data is available freely with a revisit period of at least 5 days worldwide through the COPERNICUS Earth observation project. The availability of such data at a low cost has spurred development of machine-learning models for mapping and yield prediction (Chlingaryan, Sukkarieh, & Whelan, 2018; Kamilaris & Prenafeta-Boldú, 2018). In this case study we use two different classification algorithms:

1. Random Forests (RF) (Breiman, 2001), and
2. the conventional Maximum Likelihood Classification (MLC).

Image Fusion

Introduction

This tutorial seeks to illustrate how image fusion can be conducted. We use an Unmanned Aerial Vehicle (UAV) and Sentinel 2 optical image acquired within the same area and period. **Data fusion** is a formal framework in which are expressed means and tools for the alliance of data originating from different sources. It aims at obtaining information of greater quality; the exact definition of "greater quality" will depend upon the application (Ranchin and Wald, 2010).

The principal motivation for image fusion is to improve the quality of the information contained in the output image in a process known as synergy. A study of existing image fusion techniques and applications shows that image fusion can provide us with an output image with an improved quality. In this case, the benefits of image fusion include:

1. Extended range of operation.
2. Extended spatial and temporal coverage.
3. Reduced uncertainty.
4. Increased reliability.
5. Robust system performance.
6. Compact representation of information.

Data preparation

Load libraries, declare variables and data paths.

```
rm(list=ls(all=TRUE))    #Clears R memory

unlink(".RData")

if (!require("pacman")) install.packages("pacman"); library(pacman) #package manager( loads required pa
ckages/libraries in list as below if not installed they will be installed

p_load(raster, terra)


options(warn=1)

cat("Set variables and start processing\n")

## Set variables and start processing

Root       <- 'D:/JKUAT/RESEARCH_Projects/Eswatini/Data/'

Path_out    <- paste0(Root,"Output/")
```

Load UAV and Sentinel 2 optical images.

```
path <- list.files(paste0(Root,'S2/interim/'),pattern = (".tif$"), recursive = TRUE, full.names = TRUE)

path

## [1] "D:/JKUAT/RESEARCH_Projects/Eswatini/Data/S2/interim/RT_T36JUR_20210418T073611_B0
2.tif"

## [2] "D:/JKUAT/RESEARCH_Projects/Eswatini/Data/S2/interim/RT_T36JUR_20210418T073611_B0
3.tif"

## [3] "D:/JKUAT/RESEARCH_Projects/Eswatini/Data/S2/interim/RT_T36JUR_20210418T073611_B0
4.tif"

## [4] "D:/JKUAT/RESEARCH_Projects/Eswatini/Data/S2/interim/RT_T36JUR_20210418T073611_B0
8.tif"

s <- rast(path)

s

## class       : SpatRaster

## dimensions  : 10980, 10980, 4  (nrow, ncol, nlyr)

## resolution  : 10, 10  (x, y)

## extent      : 3e+05, 409800, 6990220, 7100020  (xmin, xmax, ymin, ymax)

## coord. ref. : +proj=utm +zone=36 +south +datum=WGS84 +units=m +no_defs

## sources     : RT_T36JUR_20210418T073611_B02.tif
```

```
##              RT_T36JUR_20210418T073611_B03.tif
##              RT_T36JUR_20210418T073611_B04.tif
##              ... and 1 more source(s)
## names       : RT_T36J~611_B02, RT_T36J~611_B03, RT_T36J~611_B04, RT_T36J~611_B08
```

```
path <- list.files(paste0(Root,'WingtraOne/'),pattern = (".tif$"), full.names = TRUE)
#reorder the bands to macth those in S2
paths <- path
paths[3] <- path[4]
paths[4] <- path[3]
paths
```

```
## [1] "D:/JKUAT/RESEARCH_Projects/Eswatini/Data/WingtraOne/mpolonjeni_05042021m3f1_transparent_reflectance_blue.tif"
## [2] "D:/JKUAT/RESEARCH_Projects/Eswatini/Data/WingtraOne/mpolonjeni_05042021m3f1_transparent_reflectance_green.tif"
## [3] "D:/JKUAT/RESEARCH_Projects/Eswatini/Data/WingtraOne/mpolonjeni_05042021m3f1_transparent_reflectance_red.tif"
## [4] "D:/JKUAT/RESEARCH_Projects/Eswatini/Data/WingtraOne/mpolonjeni_05042021m3f1_transparent_reflectance_nir.tif"
```

```
v <- rast(paths)
v
```

```
## class       : SpatRaster
## dimensions  : 12981, 6363, 4  (nrow, ncol, nlyr)
## resolution  : 0.12059, 0.12059  (x, y)
## extent      : 390445, 391212.3, 7070171, 7071736  (xmin, xmax, ymin, ymax)
## coord. ref. : +proj=utm +zone=36 +south +datum=WGS84 +units=m +no_defs
## sources     : mpolonjeni_05042021m3f1_transparent_reflectance_blue.tif
##               mpolonjeni_05042021m3f1_transparent_reflectance_green.tif
##               mpolonjeni_05042021m3f1_transparent_reflectance_red.tif
##               ... and 1 more source(s)
## names       : mpolonj~ce_blue, mpolonj~e_green, mpolonj~nce_red, mpolonj~nce_nir
```

Now check image properties and assign meaningful names to its bands.

```
#Resolution
```

```
res(s)
## [1] 10 10
#Extents
ext(s)
## SpatExtent : 3e+05, 409800, 6990220, 7100020 (xmin, xmax, ymin, ymax)
#image dimensions
dim(s)
## [1] 10980 10980     4
#Number of bands
nlyr(s)
## [1] 4
names(s) <- c("b", "g","r", "nir")
s
## class       : SpatRaster
## dimensions  : 10980, 10980, 4  (nrow, ncol, nlyr)
## resolution  : 10, 10  (x, y)
## extent      : 3e+05, 409800, 6990220, 7100020  (xmin, xmax, ymin, ymax)
## coord. ref. : +proj=utm +zone=36 +south +datum=WGS84 +units=m +no_defs
## sources     : RT_T36JUR_20210418T073611_B02.tif
##               RT_T36JUR_20210418T073611_B03.tif
##               RT_T36JUR_20210418T073611_B04.tif
##               ... and 1 more source(s)
## names       : b, g, r, nir
res(v)
## [1] 0.12059 0.12059
ext(v)
## SpatExtent : 390445.0352, 391212.34937, 7070171.12052, 7071736.49931 (xmin, xmax, ymin, ymax)
dim(v)
## [1] 12981  6363     4
names(v) <- c("b", "g","r", "nir")
v
```

```
## class       : SpatRaster
## dimensions  : 12981, 6363, 4  (nrow, ncol, nlyr)
## resolution  : 0.12059, 0.12059  (x, y)
## extent      : 390445, 391212.3, 7070171, 7071736  (xmin, xmax, ymin, ymax)
## coord. ref. : +proj=utm +zone=36 +south +datum=WGS84 +units=m +no_defs
## sources     : mpolonjeni_05042021m3f1_transparent_reflectance_blue.tif
##               mpolonjeni_05042021m3f1_transparent_reflectance_green.tif
##               mpolonjeni_05042021m3f1_transparent_reflectance_red.tif
##               ... and 1 more source(s)
## names       : b, g, r, nir
```

Crop/clip Sentinel 2 image to UAV image extents.

```
s <- crop(s, ext(v), snap="near")
```

Display the images side by side.

```
x11()
par(mfrow = c(1, 2)) #c(bottom, left, top, right)
plotRGB(s, r="nir", g="r", b="g", stretch="lin", axes=T, mar = c(4, 5, 1.4, 0.2), main="S2", cex.axis=0.5)
box()
plotRGB(v, r="nir", g="r", b="g", stretch="lin", axes=T, mar = c(4, 5, 1.4, 0.2), main="UAV", cex.axis=0
.5)
box()
```

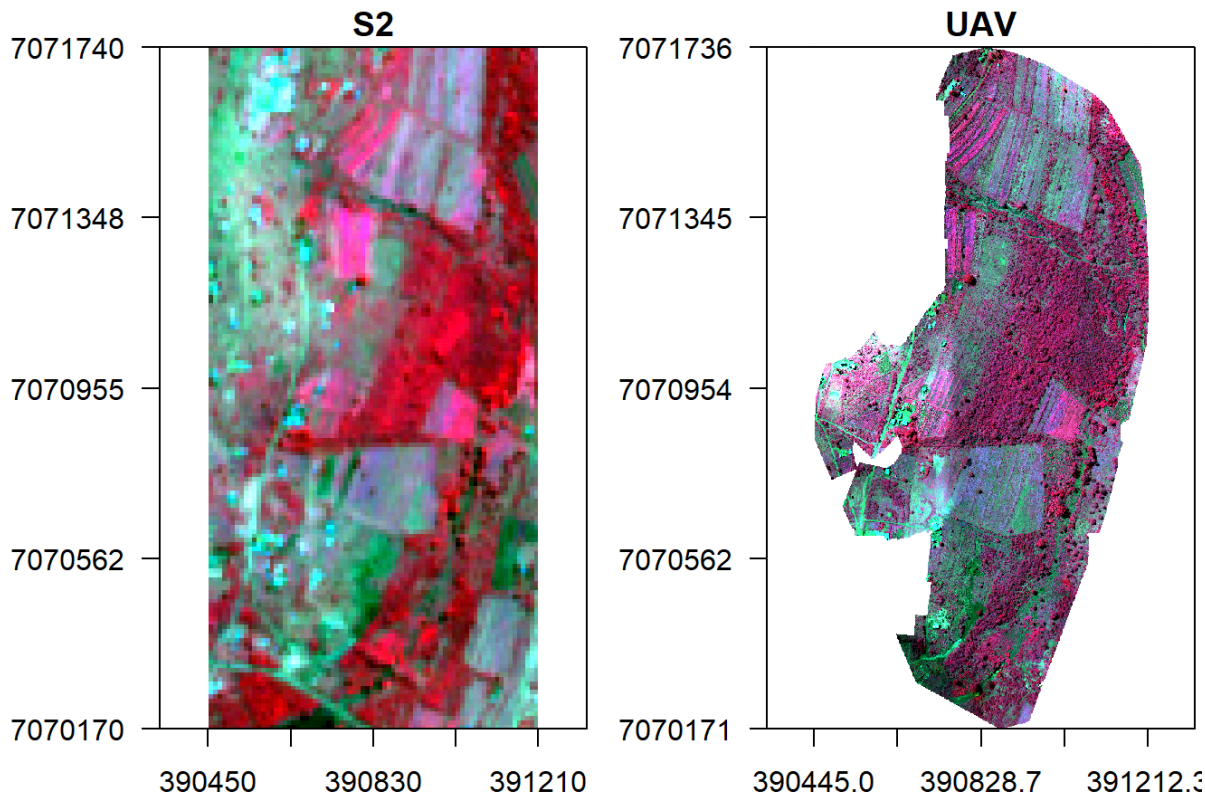

First let us conduct a spectral fusion of S2 and UAV images. To do this we have to resample UAV image to S2 extents and another to one to 1 m.

```
v_r <- resample(v, s, method='bilinear')
ext(v_r) == ext(s)
## [1] TRUE
temp <-rast(nrow=1570,ncol=760,ext(s)) #empty object to upscale UAV to 1 m resolution
res(temp)
## [1] 1 1
v1 <- resample(v, temp, method='bilinear')
res(v1)
## [1] 1 1
```

Pixel fusion

The following sections consider fusion techniques which rely on simple pixel based operations on input image values. The assumption is that the input images are spatially and temporally aligned, semantically equivalent and radiometrically calibrated. Therefore, let us fuse the two images by multiplication and display it against the original ones.

```
#Fuse by multiplication
f1 <- s * v_r
f1
## class       : SpatRaster
## dimensions  : 157, 76, 4  (nrow, ncol, nlyr)
## resolution  : 10, 10  (x, y)
## extent      : 390450, 391210, 7070170, 7071740  (xmin, xmax, ymin, ymax)
## coord. ref. : +proj=utm +zone=36 +south +datum=WGS84 +units=m +no_defs
## source      : memory
## names       :          b,          g,          r,        nir
## min values  : 0.0002068561, 0.0005442272, 0.0003042399, 0.0094109712
## max values  :  0.01279990,  0.01698387,  0.02435488,  0.18333833
#Display fused image alongside original UAV
x11()
par(mfrow = c(1, 3),mar = c(4, 5, 1.4, 0.2))
plotRGB(v, r="nir", g="r", b="g", stretch="lin", axes=T, mar = c(4, 5, 1.4, 0.2), main="UAV", cex.axis=0
.7)
box()
plotRGB(s, r="nir", g="r", b="g", stretch="lin", axes=T, mar = c(4, 5, 1.4, 0.2), main="S2", cex.axis=0.7)
box()
plotRGB(f1, r="nir", g="r", b="g", stretch="lin", axes=T, mar = c(4, 5, 1.4, 0.2), main="Fused_multi", ce
x.axis=0.7)
box()
```

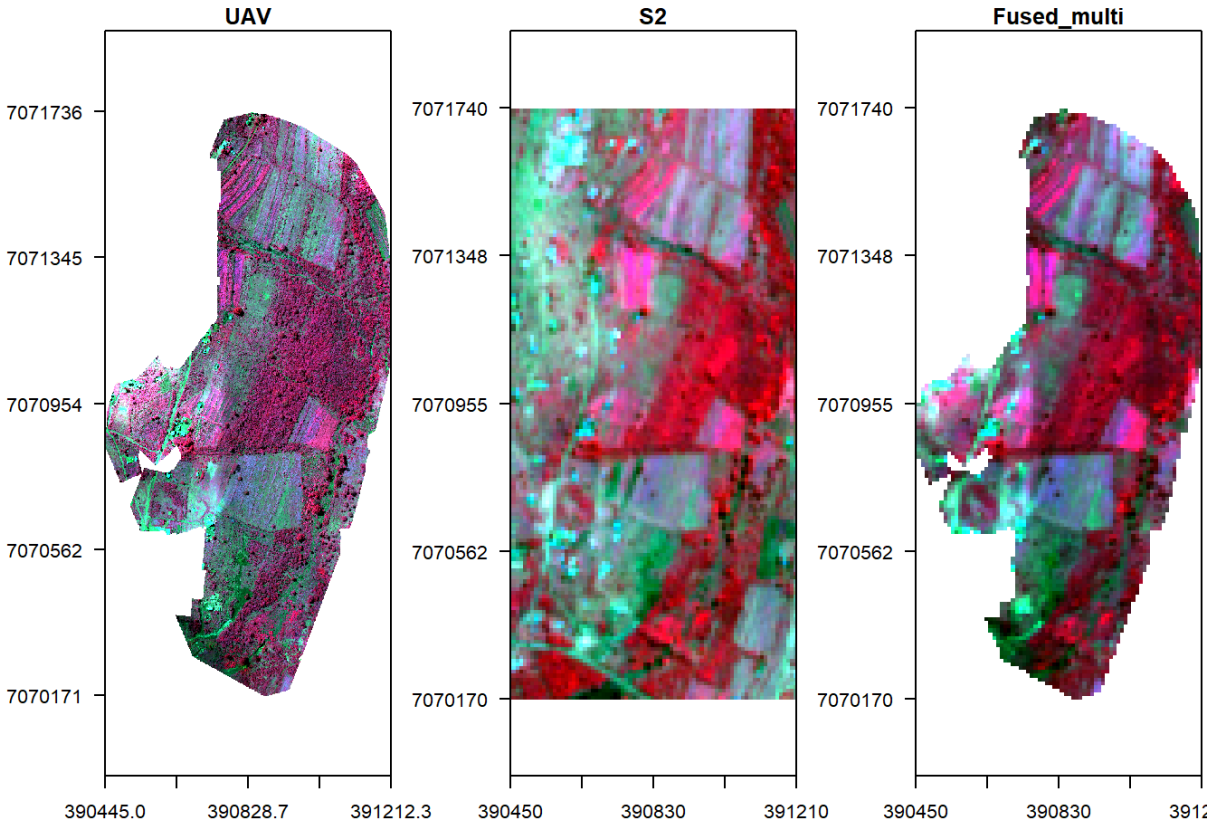

What about mean fusion (i.e. taking the mean of each pixel's reflectance in both UAV and S2)?

```
#Fuse by multiplication
f2 <- mean(s, v_r)
f2
```

```
## class       : SpatRaster
## dimensions  : 157, 76, 4  (nrow, ncol, nlyr)
## resolution  : 10, 10  (x, y)
## extent      : 390450, 391210, 7070170, 7071740  (xmin, xmax, ymin, ymax)
## coord. ref. : +proj=utm +zone=36 +south +datum=WGS84 +units=m +no_defs
## source      : memory
## names       :         b,         g,         r,       nir
## min values  : 0.01532078, 0.02351120, 0.01861056, 0.09712517
## max values  :  0.1225800,  0.1548688,  0.1717744,  0.4470450
```

```
#Display fused image alongside original UAV
```

```
x11()
par(mfrow = c(2, 2), mar = c(4, 5, 1.4, 0.2))
plotRGB(v, r="nir", g="r", b="g", stretch="lin",  main="UAV", axes=T, mar = c(4, 5, 1.4, 0.2))
box()
plotRGB(s, r="nir", g="r", b="g", stretch="lin", main="S2", axes=T, mar = c(4, 5, 1.4, 0.2))
box()
plotRGB(f1, r="nir", g="r", b="g", stretch="lin", main="Fused_mult", axes=T, mar = c(4, 5, 1.4, 0.2))
box()
plotRGB(f2, r="nir", g="r", b="g", stretch="lin", main="Fused_mean", axes=T, mar = c(4, 5, 1.4, 0.2))
box()
```

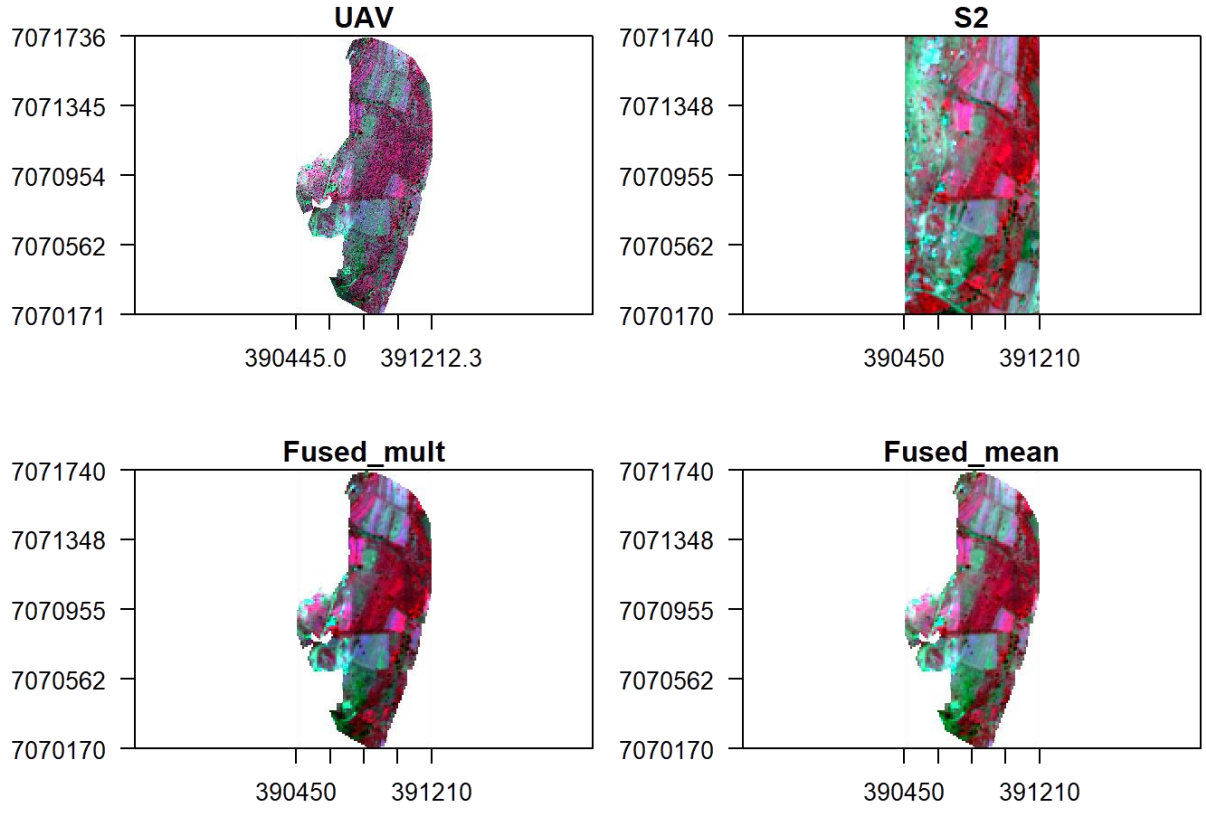

Let us finally follow the fusion approach in Zou et al (2018).

```
f3 = (s/v_r)*v_r
x11()
par(mfrow = c(2, 3), mar = c(4, 5, 1.4, 0.2))
```

```
plotRGB(v, r="nir", g="r", b="g", stretch="lin",  main="UAV", axes=T, mar = c(4, 5, 1.4, 0.2))
box()
plotRGB(s, r="nir", g="r", b="g", stretch="lin", main="S2", axes=T, mar = c(4, 5, 1.4, 0.2))
box()
plotRGB(f1, r="nir", g="r", b="g", stretch="lin", main="Fused_mult", axes=T, mar = c(4, 5, 1.4, 0.2))
box()
plotRGB(f2, r="nir", g="r", b="g", stretch="lin", main="Fused_mean", axes=T, mar = c(4, 5, 1.4, 0.2))
box()
plotRGB(f3, r="nir", g="r", b="g", stretch="lin", main="Zhou etal", axes=T, mar = c(4, 5, 1.4, 0.2))
box()
```

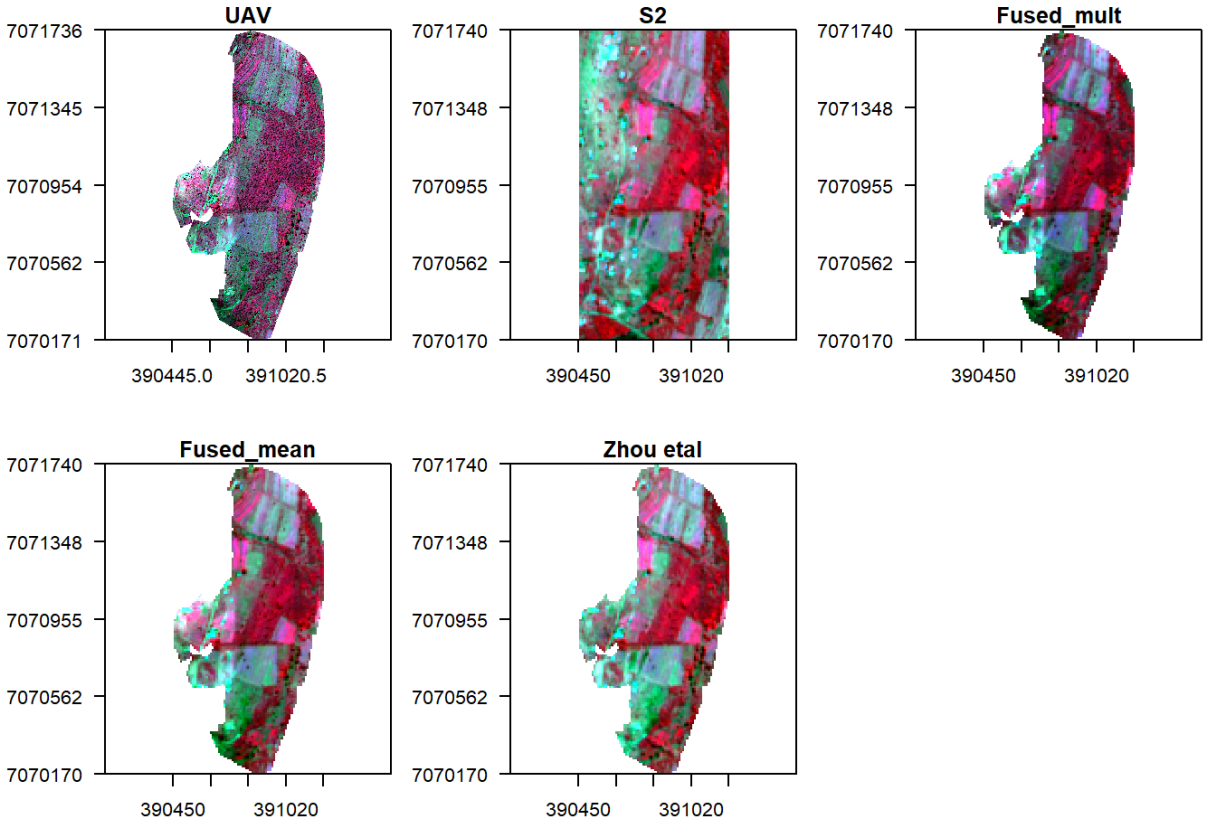

There seem to be some linear relationship between UAV and Sentinel 2 surface reflectance. However it is evident that reflectance values from UAV are higher compared to those in Sentinel 2. So what now?

Feature based fusion

In *feature fusion* we fuse together the features Fk,k∈1,2,…,KFk,k∈1,2,…,K. These features can be vegetation indices like Normalized Difference Index (NDVI) or feature maps that have been made semantically equivalent by transforming them into probabilistic p(m,n)p(m,n), or likelihood, maps.

Let us start with NDVI (NDVI=NIR−RedNIR+RedNDVI=NIR−RedNIR+Red. First compute NDVI for both UAV and S2.

```
n_v <- (subset(v_r,"nir")-subset(v_r,"r"))/(subset(v_r,"nir")+subset(v_r,"r"))
n_s <- (subset(s,"nir")-subset(s,"r"))/(subset(s,"nir")+subset(s,"r"))
```

How can we fuse the NDVI index? Let us take an average of the two.

```
nf <- mean(n_v, n_s)
x11()
par(mfrow = c(2, 2), mar = c(5, 5, 1.4, 0.2))#c(bottom, left, top, right)
plot(n_v, main="UAV NDVI")
plot(n_s, main="S2 NDVI")
plot(nf, main="Fused NDVI")
```

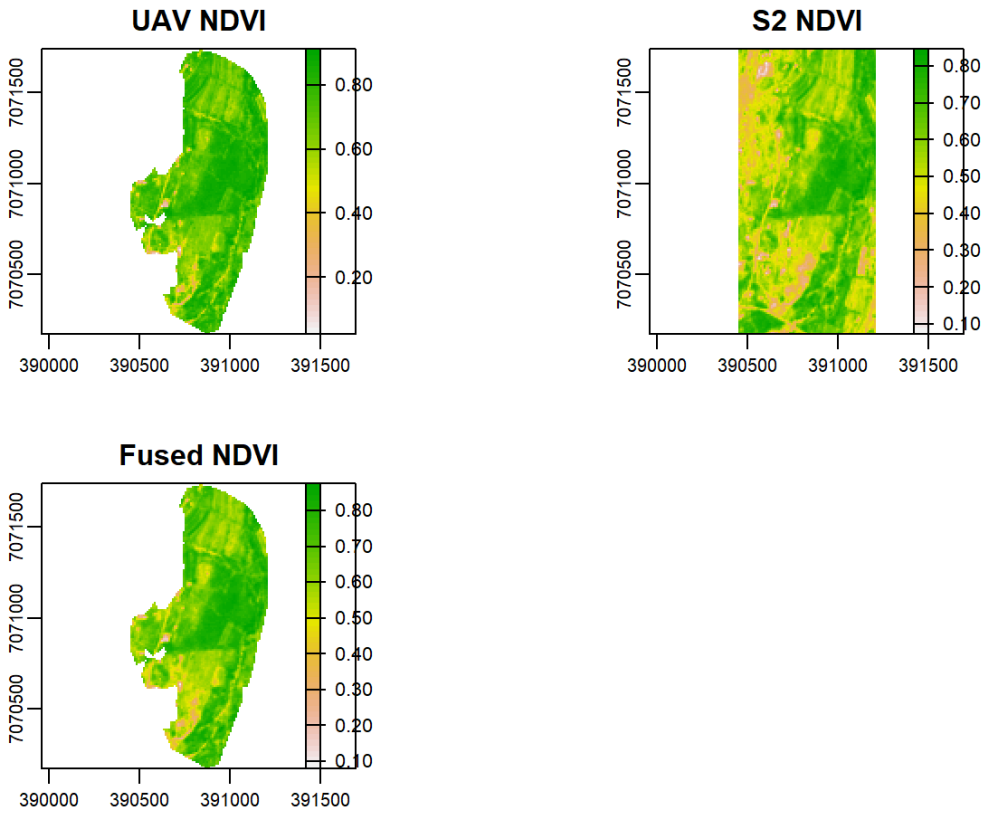

Is there any difference between S2, UAV, and the fused NDVI images as shown above?

Previously we upsampled the UAV image in order to conduct fusion. While this reduces spectral variability it destroys spatial resolution. Therefore, in this section we will first donwsample the Satellite image to match UAV spatial resolution and then proceed to conduct image fusion. This way, we will improve both spatial and spectral information of Sentinel 2 image and spectral information for UAV.

Modelling reflectance

1. Can we improve the resolution of S2 using UAV?
2. Can we predict UAV reflectance in places not imaged by the drones?

Let's check the relationship between the two.

```
x11()

par(mfrow = c(2, 2), mar = c(4, 5, 1.4, 0.2))

plot(as.vector(subset(s,'b')),as.vector(subset(v_r,'b')), xlab='S2', ylab='W1 UAV', main="Blue band",pch=16,cex=0.75, col='blue')

plot(as.vector(subset(s,'g')),as.vector(subset(v_r,'g')), xlab='S2', ylab='W1 UAV', main="Green band",pch=16,cex=0.75, col='green')

plot(as.vector(subset(s,'r')),as.vector(subset(v_r,'r')), xlab='S2', ylab='W1 UAV', main="Red band",pch=16,cex=0.75, col='red')

plot(as.vector(subset(s,'nir')),as.vector(subset(v_r,'nir')), xlab='S2', ylab='W1 UAV', main="NIR band",pch=16,cex=0.75)
```

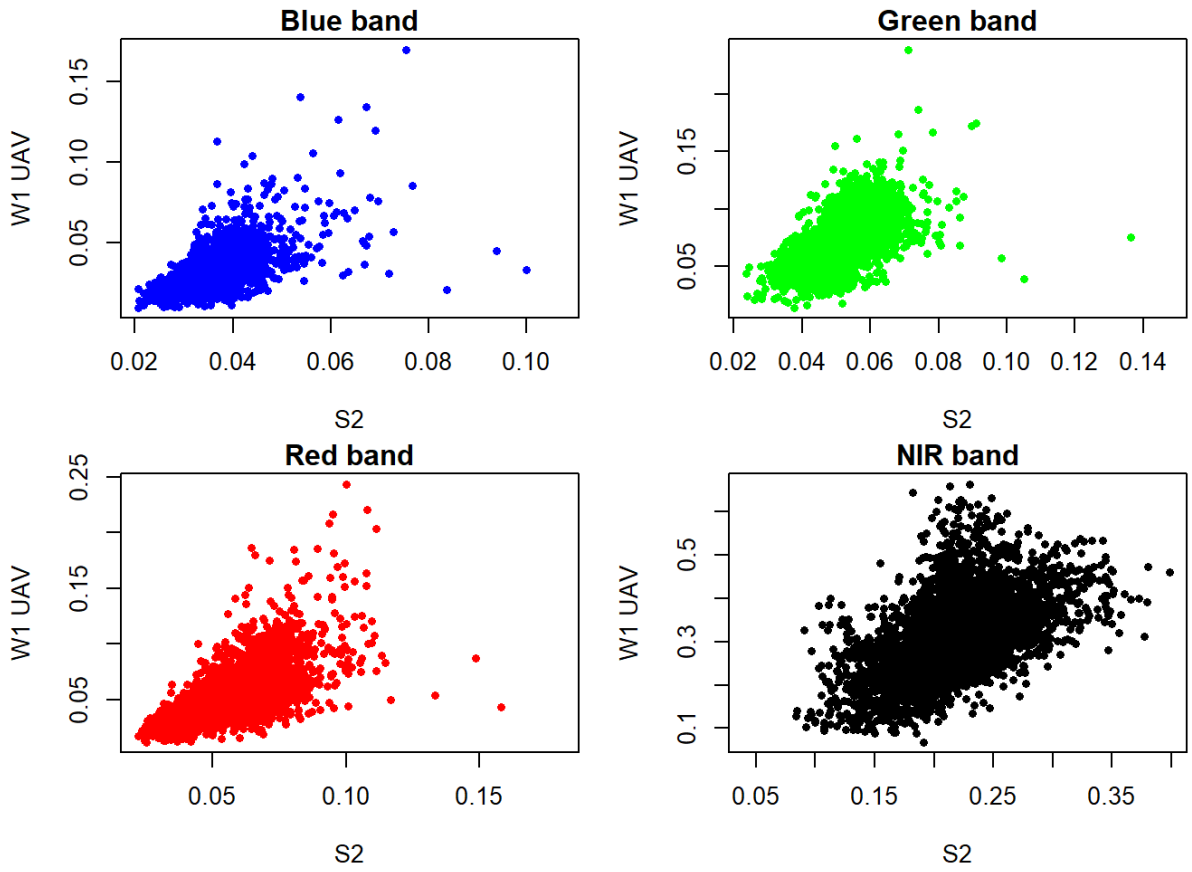

Lets create sample points from S2 (10 m resolution) and upscaled UAV (10 m resolution) and use them to create a model that we can predict S2 reflectance based on UAV 1 m resolution. Essentially what we are doing here is to create a model that can predict S2 reflectance at a resolution of 1 m.

```
set.seed(530)

x11()

points <- spatSample(v_r, 900, "random", as.points=T, na.rm=T, values=F)

plotRGB(v_r, r="nir", g="r", b="g", stretch="lin",  main="UAV+sampling points", axes=T, mar = c(4, 5, 1.4, 0.2))

plot(points,add=T)
```

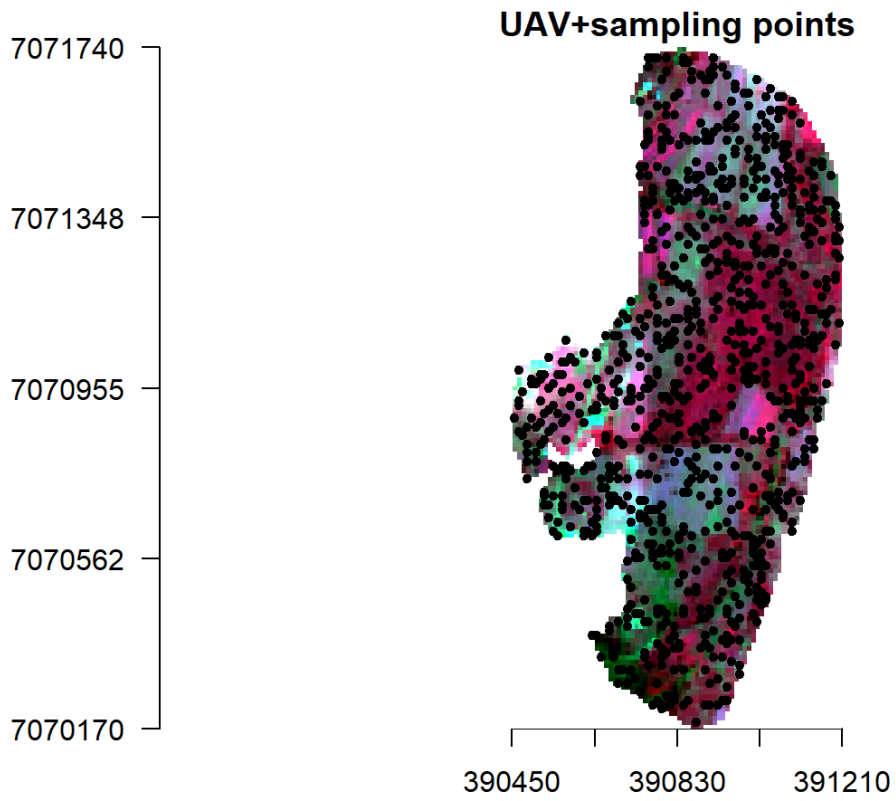

Now extract reflectance values from the two images.

```
s2_p <- extract(s, points, drop=F)
head(s2_p)
##   ID         b         g         r    nir
## 1  1 0.03010000 0.04340000 0.04370000 0.2039
## 2  2 0.02669999 0.04040000 0.03190000 0.2555
## 3  3 0.02600000 0.03800000 0.02760000 0.2727
## 4  4 0.02719999 0.03929999 0.03590000 0.1978
## 5  5 0.04079999 0.06200000 0.06999999 0.2210
## 6  6 0.04020000 0.05670000 0.06260000 0.2209
vr_p <- extract(v_r, points, drop=F)
head(vr_p)
##   ID         b         g         r       nir
## 1  1 0.02557389 0.05894550 0.03758506 0.3497387
```

```
## 2  2 0.01882389 0.05033908 0.02247731 0.3220550
## 3  3 0.01982662 0.05362828 0.02300457 0.3844531
## 4  4 0.02047731 0.05194858 0.02767093 0.3193594
## 5  5 0.04172961 0.09754695 0.07302261 0.4105712
## 6  6 0.03550068 0.07566584 0.05827252 0.2950630
```

Create a model.

```
data <- data.frame(S2=s2_p[,-1], UAV=vr_p[,-1])
head(data)
##         S2.b      S2.g      S2.r S2.nir     UAV.b     UAV.g     UAV.r
## 1 0.03010000 0.04340000 0.04370000 0.2039 0.02557389 0.05894550 0.03758506
## 2 0.02669999 0.04040000 0.03190000 0.2555 0.01882389 0.05033908 0.02247731
## 3 0.02600000 0.03800000 0.02760000 0.2727 0.01982662 0.05362828 0.02300457
## 4 0.02719999 0.03929999 0.03590000 0.1978 0.02047731 0.05194858 0.02767093
## 5 0.04079999 0.06200000 0.06999999 0.2210 0.04172961 0.09754695 0.07302261
## 6 0.04020000 0.05670000 0.06260000 0.2209 0.03550068 0.07566584 0.05827252
##     UAV.nir
## 1 0.3497387
## 2 0.3220550
## 3 0.3844531
## 4 0.3193594
## 5 0.4105712
## 6 0.2950630
# Plot the data
plot(S2.b~UAV.b, data=data, pch=16)
# Create a linear regression model
l.model <- lm(S2.b~UAV.b, data=data)
# Add the fitted line
abline(l.model, col="red")
```

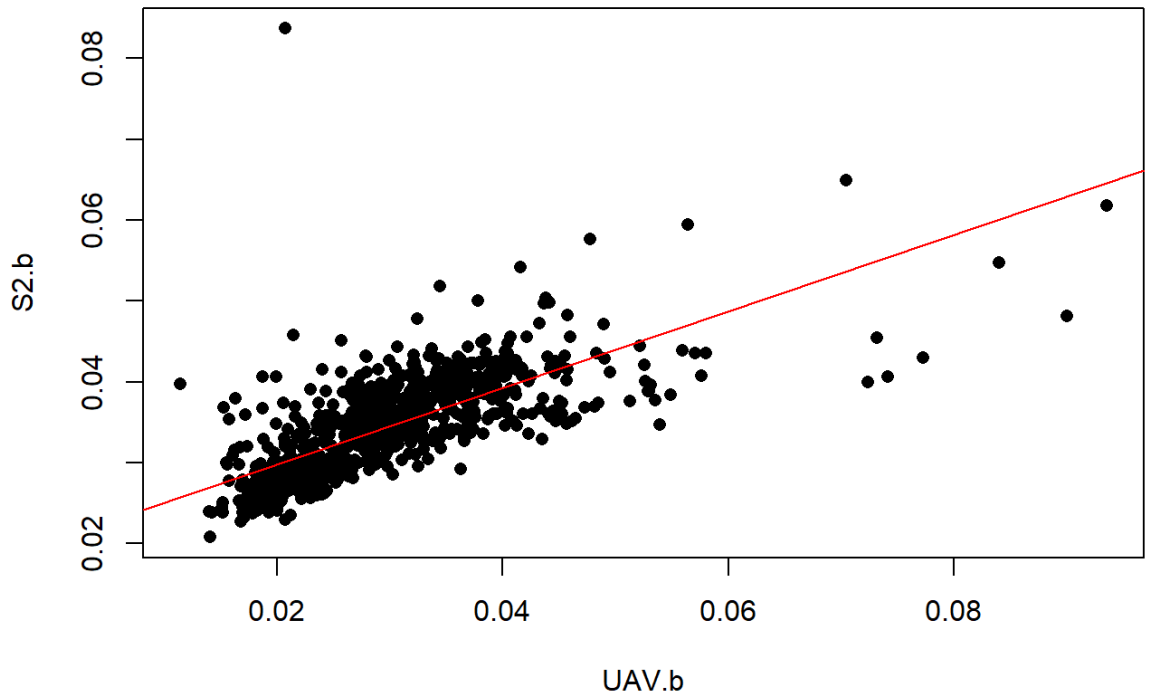

Looks like the relation within the blue band is not linear. Let's try a non-linear SVM model.

```
#SVM
library(e1071)
svm.model <- svm(S2.b~UAV.b, data=data)
svm.pred <- predict(svm.model, data)
#SVM
library(randomForest)
rfmod <- randomForest(S2.b~UAV.b, data=data)
rf.pred <- predict(rfmod, data)
x11()
plot(S2.b~UAV.b,data, pch=16)
points(data$S2.b, svm.pred, col = "blue", pch=4)
points(data$S2.b, rf.pred, col = "red", pch=4)
legend("topright",c("Data","SVM","RF"), pch= c(16, 4, 4),col=c("black", "blue","red"))
```

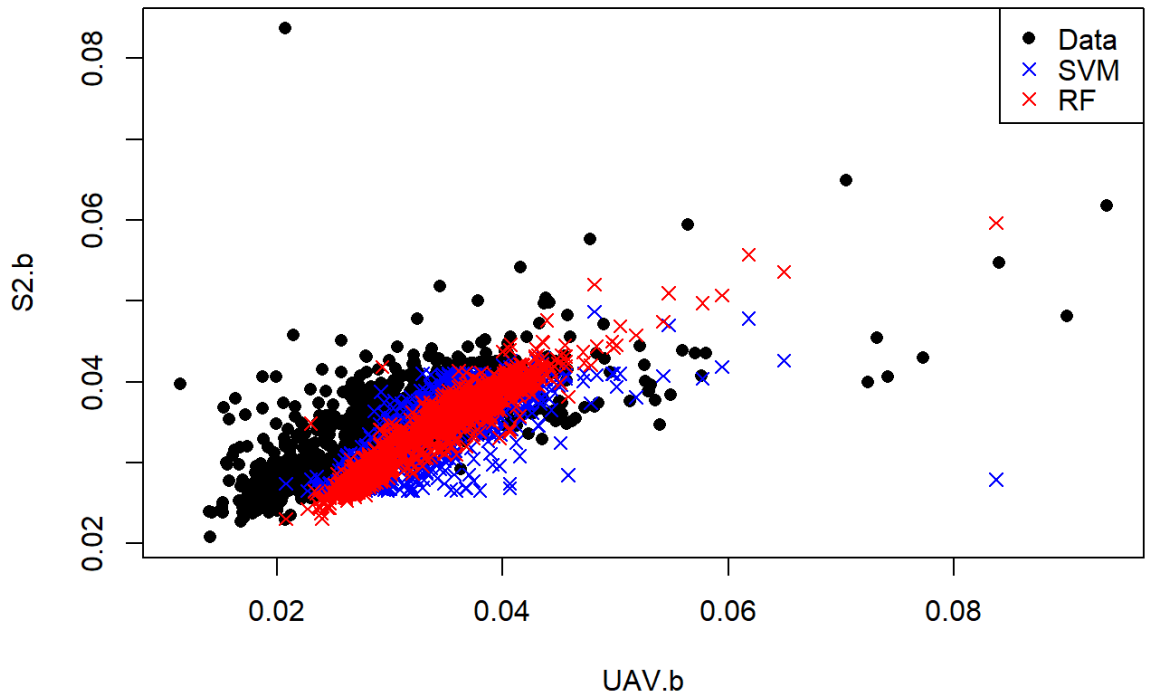

Predicting Sentinel 2 reflectance

SVM and RF models have better characterized the relationship between S2 and UAV blue bands. Let predict high resolution S2 band from existing UAV.

```
UAV <- v1[['b']]
names(UAV) <-'UAV.b'
s2h.b <- predict(UAV, rfmod, na.rm=T)


s2h.svm <- predict(UAV, svm.model, na.rm=T)


x11()
par(mfrow = c(1, 2), mar = c(4, 5, 1.4, 0.2))
plot(s2h.svm,  main="svm S2 1m Blue band")
plot(s2h.b, main="RF S2 1m Blue band")
```

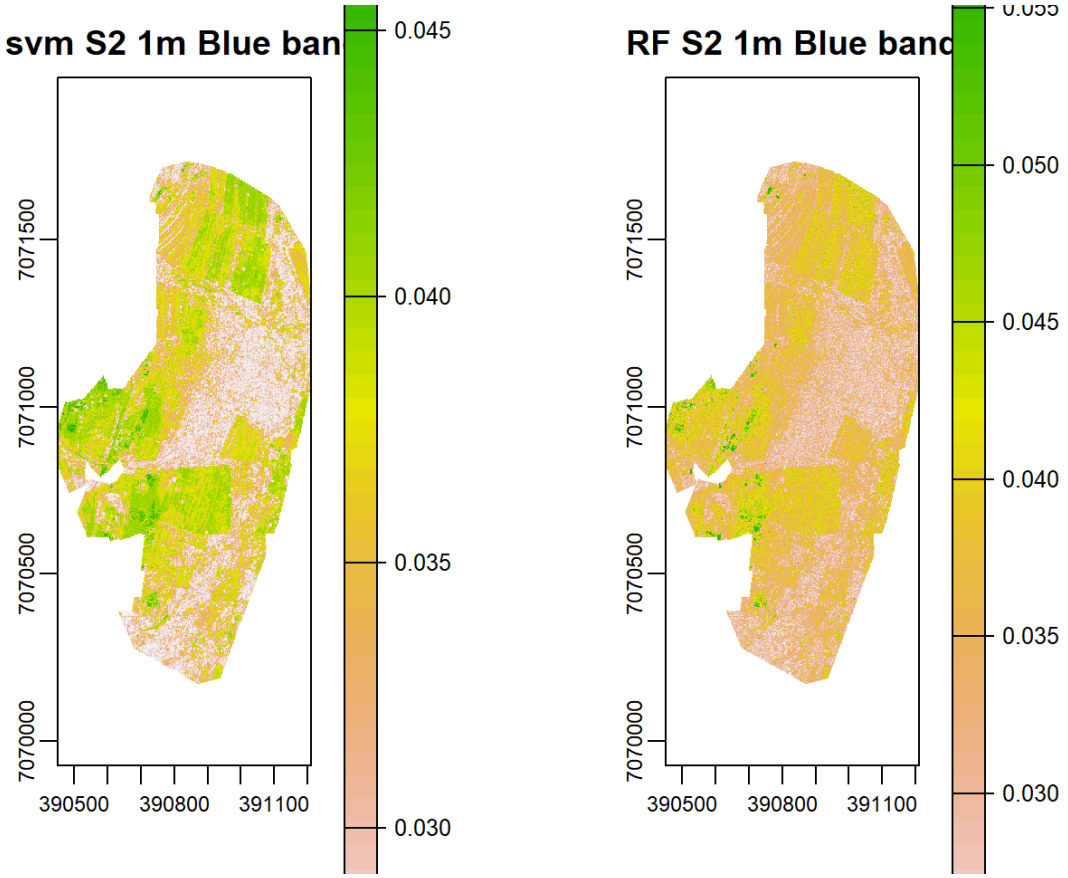


```
# #parallel processing in raster
# UAv <- raster(UAV)
# library(snow)
# startTime <- Sys.time()
# cat("Start time", format(startTime),"\n")
# beginCluster()
#  r4 <- predict(UAV, rfmod,na.rm=T)
# endCluster()
# timeDiff <- Sys.time() - startTime
# cat("\n Processing time", format(timeDiff), "\n")
```

Validation

But how do we know if this predictions are accurate? We can plot predicted vs actual and also compute RMSE and Mean Absolute Percentage Error (MAPE) using training data. MAPE is given as:

```
MAPE <- function (y_pred, y_true){
```

```
  MAPE <- mean(abs((y_true - y_pred)/y_true))
  return(MAPE*100)
}
```

and RMSE,

```
rmse <- function(error){
 sqrt(mean(error^2))
}
```

So lets compute MAPE and RMSE for both methods.

```
svm.rmse <- rmse(svm.pred-data$S2.b)
svm.rmse
## [1] 0.003996155
rf.rmse <- rmse(rf.pred-data$S2.b)
rf.rmse
## [1] 0.002186289
svm.mape <- MAPE(svm.pred, data$S2.b)
svm.mape
## [1] 7.315199
rf.mape <- MAPE(rf.pred, data$S2.b)
rf.mape
## [1] 4.358044
```

From the validations Random Forest gives better prediction than Support Vector machines because it has low MAPE and RMSE error. In that case we can adopt the high resolution S2 image predicted/simulated by RF and fuse it with UAV image at 1 m resolution. Note that we only predict the blue band, we can model and predict the other bands and then fuse them.

```
#Green band
rfmod <- randomForest(S2.g~UAV.g, data=data)
UAV=subset(v1,'g')
names(UAV) <-'UAV.g'
s2h.g <- predict(UAV, rfmod, na.rm=T)
#red band
```

```
rfmod <- randomForest(S2.r~UAV.r, data=data)
UAV=subset(v1,'r')
names(UAV) <-'UAV.r'
s2h.r <- predict(UAV, rfmod, na.rm=T)
#NIR band
rfmod <- randomForest(S2.nir~UAV.nir, data=data)
UAV=subset(v1,'nir')
names(UAV) <-'UAV.nir'
s2h.nir <- predict(UAV, rfmod, na.rm=T)

#Stack them
s2h <- stack(x=c(s2h.b,s2h.g,s2h.r,s2h.nir))
names(s2h) <- c("b", "g","r", "nir")
s2h
```

```
## class      : RasterStack
## dimensions : 1570, 760, 1193200, 4  (nrow, ncol, ncell, nlayers)
## resolution : 1, 1  (x, y)
## extent     : 390450, 391210, 7070170, 7071740  (xmin, xmax, ymin, ymax)
## crs        : NA
## names      :         b,         g,         r,       nir
## min values : 0.02305458, 0.03414621, 0.02679058, 0.12475280
## max values : 0.06060897, 0.08070807, 0.10184987, 0.30137640
```

However, the predicted reflectance ranges in all bands except NIR are very low. Why could this be so? Now lets create a high resolution fused image using Zhou's approach.

Fusion

```
s2h.fused <- (rast(s2h)/v1)*v1
s2h.fused
```

```
## class      : SpatRaster
## dimensions  : 1570, 760, 4  (nrow, ncol, nlyr)
## resolution  : 1, 1  (x, y)
## extent      : 390450, 391210, 7070170, 7071740  (xmin, xmax, ymin, ymax)
```

```
## coord. ref. :
## source      : memory
## names       :        b,        g,        r,      nir
## min values  : 0.02305458, 0.03414621, 0.02679058, 0.12475280
## max values  : 0.06060897, 0.08070807, 0.10184987, 0.30137640
```

```
x11()
par(mfrow = c(1, 2), mar = c(4, 5, 1.4, 0.2))
plotRGB(s2h.fused, r="nir", g="r", b="g", stretch="lin",  main="UAV+S2 high res", axes=T, mar = c(4, 5, 1.4, 0.2))
box()
plotRGB(v, r="nir", g="r", b="g", stretch="lin", main="UAV", axes=T, mar = c(4, 5, 1.4, 0.2))
box()
```

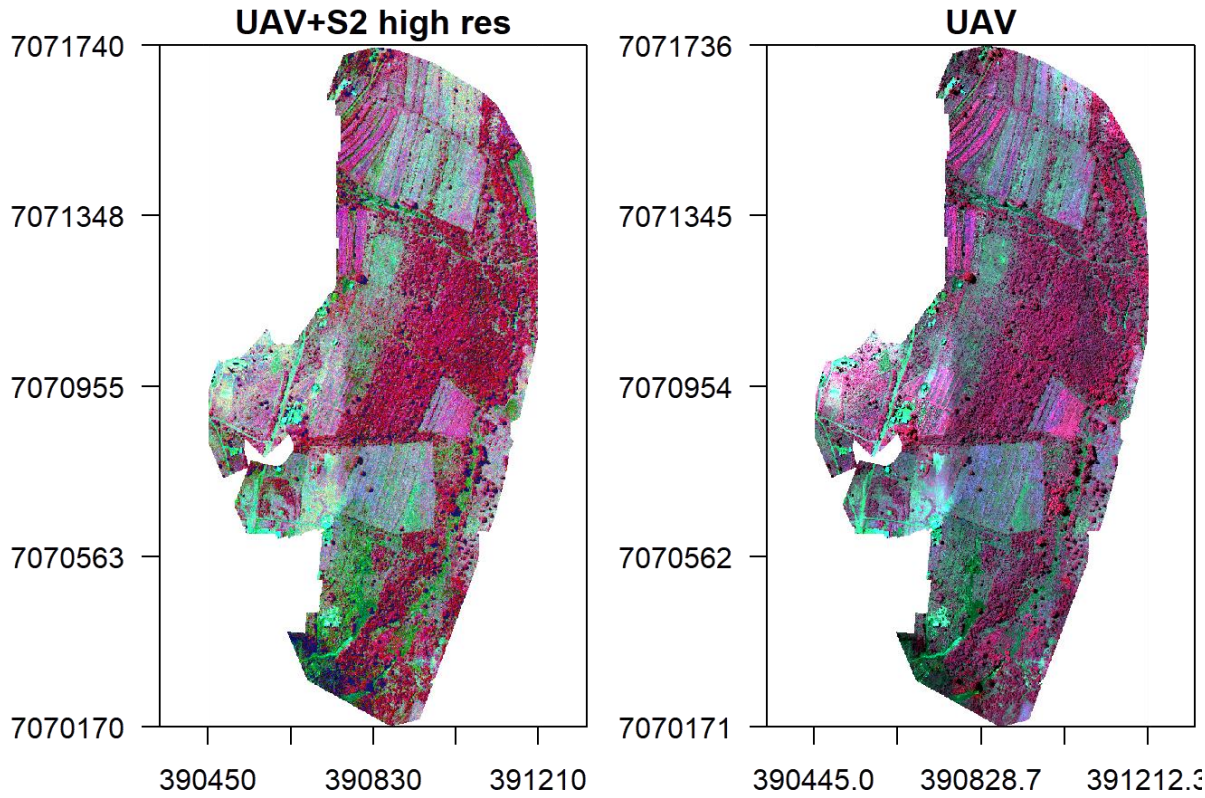

The other option would be use S2 to predict UAV in areas not covered by the drone and then fuse it with S2. However this approach would require consideration of similar land-cover. For instance, we can not train the model in an area with different land-cover say cropland and predict in another area with say Forest. Food for thought.

But let's step back a little, could sampling from land-cover categories have improved prediction of high resolution S2 done previously with RF? To test this, let us perform a K-means classification and sample from its land-cover map.

```
image <- v_r
image[is.na(image)] <- 0
nclass <- 4
system.time(
E <- kmeans(as.data.frame(image, na.rm=F), nclass, iter.max = 100, nstart = 9)
)
##    user  system elapsed
##    0.07    0.00    0.08
k.map <- image[[1]]
values(k.map) <- E$cluster
k.map[is.na(v_r[[1]])] <- NA
plot(k.map)
```

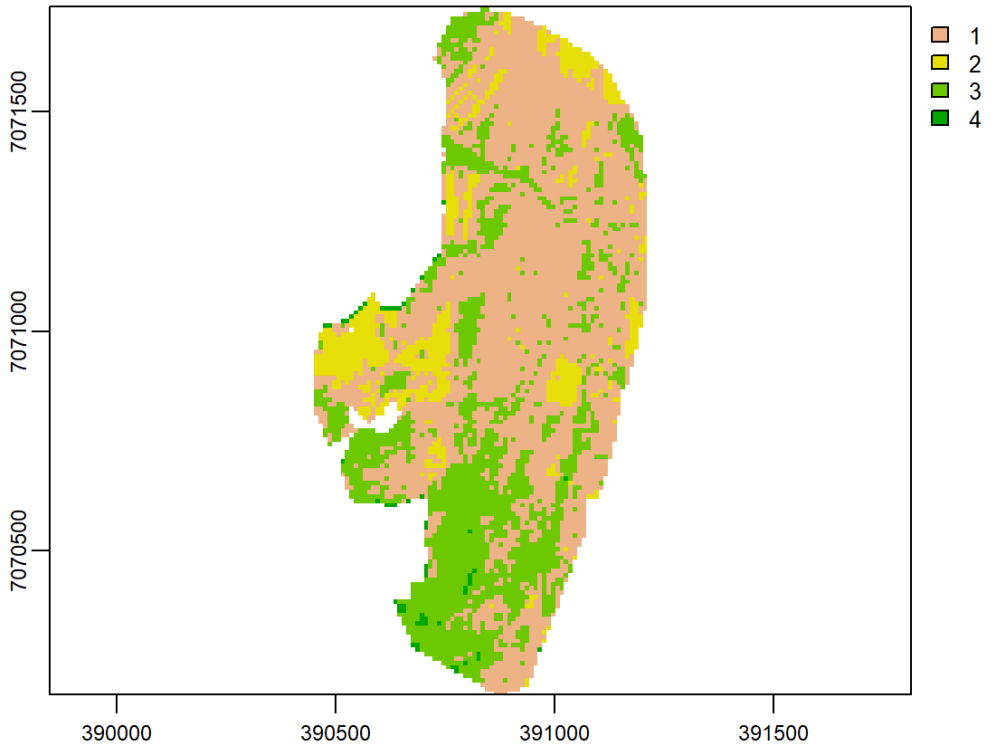

Sample points using stratified random sampling based on the K-means land-cover map.

```
set.seed(530)
points <- spatSample(k.map, 900, "stratified", as.points=T, na.rm=T, values=F)
x11()
plot(k.map,  main="K-means +sampling points", axes=T, mar = c(4, 5, 1.4, 0.2), col=topo.colors(max(values(k.map),na.rm=T)))
plot(points,add=T)
```

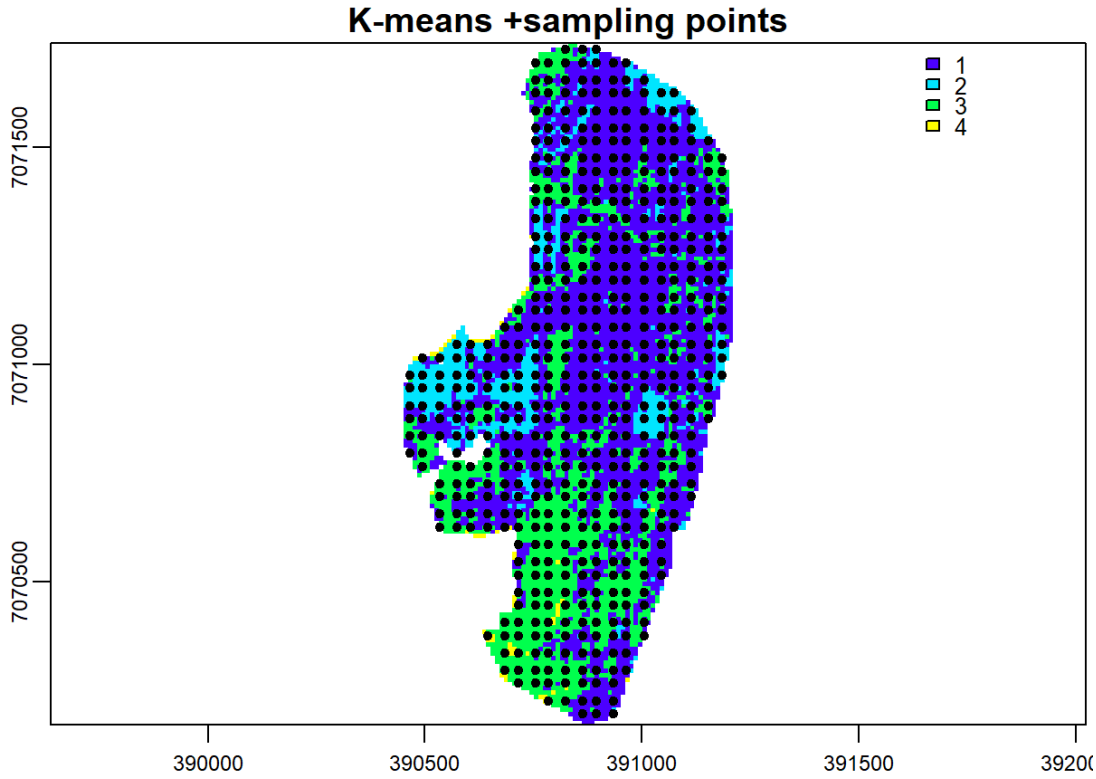

Use the stratified randomly sample points to train and predict simulated high resolution S2.

```
s2_p <- extract(s, points, drop=F)
head(s2_p)
##   ID         b         g         r    nir
## 1  1 0.04770000 0.05939999 0.07750000 0.1492
## 2  2 0.03960000 0.05549999 0.07099999 0.2073
## 3  3 0.03320000 0.04880000 0.05010000 0.2258
```

```
## 4  4 0.03379999 0.04790000 0.06040000 0.1966
## 5  5 0.04420000 0.06200000 0.07959999 0.2172
## 6  6 0.04070000 0.05980000 0.06649999 0.2101
vr_p <- extract(v_r, points, drop=F)
head(vr_p)
##   ID         b         g         r       nir
## 1  1 0.05413008 0.09205989 0.11132049 0.2734993
## 2  2 0.04446261 0.10010008 0.08397383 0.4695161
## 3  3 0.03073439 0.07668109 0.05490024 0.4001549
## 4  4 0.02435945 0.06213900 0.04357978 0.3155672
## 5  5 0.03281799 0.06734130 0.06080524 0.2811245
## 6  6 0.03464006 0.07732372 0.05422943 0.3122228
data <- data.frame(S2=s2_p[,-1], UAV=vr_p[,-1])
rfmod <- randomForest(S2.b~UAV.b, data=data)
rf.pred <- predict(rfmod, data)
```

Lets evaluate if stratified random sampling improved RF accuracy.

```
rf.rmse <- rmse(rf.pred-data$S2.b)
rf.rmse
## [1] 0.00193131
rf.mape <- MAPE(rf.pred, data$S2.b)
rf.mape
## [1] 4.36695
```

We can see that RMSE has improved by a small margin compared to the case of random sampling. MAPE more or less remained constant. Thus there is a chance that sampling over different land-cover improves prediction.

As an assignment now predict S2 high resolution using a RF model trained on stratified random samples from K-means classifier.

Crop Mapping

Materials and methods

This section describes data used for the pilot study. Methods use to implement the study are also presented side by side with code and results.

Study site and data

The pilot study covers four sites namely: Gege, Mpolonjeni, Sidzakeni, and Sigangeni. We used S2 and Wingtra one (WI) UAV images acquired between 1st–14th April 2021 over the four sites in Eswatini. Table 1 shows their central and bandwidth wavelengths in nanometres (nm).

Table 1: Central and bandwith wavelengths (in nm) of Wingtra one UAV and Sentinel 1.

	Wingtra one		Sentinel 2	
Bands	Central	Bandwidth	Central	Bandwidth
Blue	475	32	492	66
Green	560	27	560	36
Red	668	14	665	31
NIR	842	57	833	106

Data preparation

In this section we load necessary R libraries and conduct any image pre-processing required such as clipping, renaming bands e.t.c. We use Mpolonjeni site as an example. So first load necessary R libraries, declare variables and data paths.

```
rm(list=ls(all=TRUE))                                    #Clears R memory
unlink(".RData")
if (!require("pacman")) install.packages("pacman"); library(pacman)
p_load(raster, terra, randomForest, RStoolbox, tictoc)
options(warn=1)
cat("Set variables and start processing\n")

## Set variables and start processing

Root <- 'D:/JKUAT/RESEARCH_Projects/Eswatini/Data/'
Path_out <- paste0(Root,"Output/")
```

Load Mpolonjeni UAV images for mission 1–5 and Sentinel 2. We will mosaic the UAV images to one image at 1 m spatial resolution and save to disk later. Once this is done we skip this process every other time we run the script.

```
#Sentinel 2
path <- list.files(paste0(Root,'S2/interim/'),pattern = (".tif$"), recursive = TRUE, full.names = TRUE)
s <- rast(path)
names(s) <- c("b", "g","r", "nir")
s

## class : SpatRaster
## dimensions : 10980, 10980, 4 (nrow, ncol, nlyr)
## resolution : 10, 10 (x, y)
## extent : 3e+05, 409800, 6990220, 7100020 (xmin, xmax, ymin, ymax)
## coord. ref. : +proj=utm +zone=36 +south +datum=WGS84 +units=m +no_defs
## sources : RT_T36JUR_20210418T073611_B02.tif
## RT_T36JUR_20210418T073611_B03.tif
## RT_T36JUR_20210418T073611_B04.tif
```

```
##                                                    ...    and    1    more    source(s)
## names       : b, g, r, nir

#UAV
mosaicname                    <-                    paste0(Path_out,'Mpolonjeni_W1_Mosaic.tif')
if(!file.exists(mosaicname)){
folders                <-                list.dirs(paste0(Root,'WingtraOne/Mpolonjeni'),recursive=TRUE)[-1]
folders
for                    (i                    in                    1:length(folders))                    {
 path                <-                list.files(folders[i],                pattern                =                (".tif$"))
 #        Remove        all        before        and        up        to        "reflectance_"        in        gsub
 path                                <-                                path[order(gsub(".*reflectance_","",path))][-4]
 #reorder            the            bands            to            match            those            in            S2
 paths                                                <-                                                path
 paths[3]                                                <-                                                path[4]
 paths[4]                                                <-                                                path[3]
 temp                                    <-                                                rast(paste0(folders[i],"/",paths))
 names(temp)                <-                c("b",                "g",                "r",                "nir")
 assign(paste0("v",                                                i),                                                temp)
}
}else{
 v                                        <-                                                rast(mosaicname)
}
```

We now have all the image missions loaded from corresponding sub-folders, stacked, and dynamically allocated variables i.e. v1,v2, ...,v5. Resample all the images to 1 m spatial resolution using bilinear approach and mosaic them.

```
if(!file.exists(mosaicname)){
 temp                        <-                        aggregate(v1[[1]],                        9)
 res(temp)                            <-                            c(1,                            1)
 v1                <-                resample(v1,                temp,                method='bilinear')
 temp                        <-                        aggregate(v2[[1]],                        9)
 res(temp)                            <-                            c(1,                            1)
 v2                <-                resample(v2,                temp,                method='bilinear')
 temp                        <-                        aggregate(v3[[1]],                        9)
 res(temp)                            <-                            c(1,                            1)
 v3                <-                resample(v3,                temp,                method='bilinear')
 temp                        <-                        aggregate(v4[[1]],                        9)
 res(temp)                            <-                            c(1,                            1)
 v4                <-                resample(v4,                temp,                method='bilinear')
 temp                        <-                        aggregate(v5[[1]],                        9)
 res(temp)                            <-                            c(1,                            1)
 v5                <-                resample(v5,                temp,                method='bilinear')
}
```

Let's now mosaic the scenes to form one image. We will use median to average out the overlaps. Median is preferred because it has been shown to be robust to outliers compared to the mean.

```
if(!file.exists(mosaicname)){
 v        <-        mosaic(v1,        v2,        v3,        v4,        v5,        fun="median")
}
```

Save the mosaic to disk.

```
mosaicname <- paste0(Path_out,'Mpolonjeni_W1_Mosaic.tif')
if(!file.exists(mosaicname)){
  writeRaster(v, mosaicname)
}
```

Crop/clip Sentinel 2 image to UAV image extents.

```
s <- crop(s, ext(v), snap="near")
```

Figure 1 shows UAV and S2 false colour composite of Mpolonjeni site.

```
#x11()
par(mfrow = c(1, 2)) #c(bottom, left, top, right)
plotRGB(s, r="nir", g="r", b="g", stretch="lin", axes=T, mar = c(4, 5, 1.4, 0.2), main="S2", cex.axis=0.5)
box()
plotRGB(v, r="nir", g="r", b="g", stretch="lin", axes=T, mar = c(4, 5, 1.4, 0.2), main="UAV", cex.axis=0
.5)
box()
```

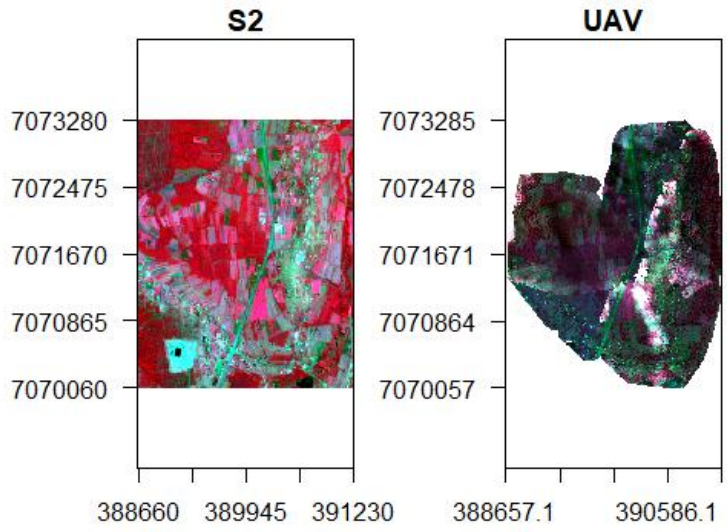

Figure 1: UAV & S2 false colour composite images (RGB: NIR, R, B).

Spectral image fusion

- Principal Component Analysis (PCA) or Gram-Schmidt fusion

The PCA fusion follows the following steps as noted in (Metwalli, Nasr, Farag Allah, & El-Rabaie, 2009; Zhao et al., 2019):

(a) The panchromatic band is computed by taking the mean of UAV RGB bands following (Jenerowicz, Siok, Woroszkiewicz, & Orych, 2017; Yilmaz & Gungor, 2015), i.e.,: pan $= \frac{R+G+B}{3}$.

```
pan <- (subset(v,'b')+subset(v,'g')+subset(v,'r'))/3
names(pan) <- 'pan'
```

b) The S2 multi-spectral image bands are transformed by the principal component transformation.

c) The first principal component of the multi-spectral image is replaced by the histogram matched panchromatic imagery (this is taken care by the option norm=FALSE and pc = 1 in the function panSharpen' inRStoolbox`). The new merged multi-spectral imagery is obtained by computing inverse of principal component transformation.

```
tic('PCA Fusion')
 pca <- panSharpen(brick(s), raster(pan), r, g, b, pc = 1, method = "pca", norm = FALSE)
toc()

## PCA Fusion: 51.38 sec elapsed

names(pca) <- c("b", "g", "r", "nir")
```

Having obtained the PCA fused image, we proceed to crop classification in the next section.

Crop classification

Load train data.

```
#ref <- vect(paste0(Root,'Vector/Training_Sites_Mpolonjeni.shp'), "polygons")
ref <- shapefile(paste0(Root,'Vector/Training_Sites_Mpolonjeni.shp'))
ref <- spTransform(ref, crs(v))
```

Sample points from the polygons (using stratified random sampling). Statified random sampling ensures that all classes are fairly represented in the training data.

```
set.seed(530)
samp <- spsample(ref, 4000, type='stratified')

## Warning in proj4string(obj): CRS object has comment, which is lost in output

# add the land cover class to the points
samp$class <- over(samp, ref)$Name
samp$code <- over(samp, ref)$code
knitr::kable(table(samp$class), align = 'l')
```

Var1	Freq
built_up	734
cassava	109
grass	132
maize	749
sorghum	235
sweet_potato	738
trees	918
waterbody	368

```
sum(table(samp$class))

## [1] 3983
```

Declare the class names and their number.

```
nClasses <- 8
Classes <- data.frame(classID=c(1:8),class=c('Built_up','Cassava', 'Grass', 'Maize', 'Sorghum', 'Sweet_potato','Trees','Water'))
```

Display training polygons over the fused image. To do this we will create a function to aid in legend display.

```
add_legend <- function(...) {
 opar <- par(fig=c(0, 1, 0, 1), oma=c(0, 0, 0, 0),
  mar=c(0, 0, 0, 0), new=TRUE)
 on.exit(par(opar))
 plot(0, 0, type='n', bty='n', xaxt='n', yaxt='n')
 legend(...)
}
```

Then display the training points over the image as shown in Figure 2.

```
x11()
par(mar = c(4, 5, 1.4, 0.2)) #c(bottom, left, top, right)
plotRGB(pca, r="nir", g="r", b="g", stretch="lin", axes = TRUE)
#points(samp, col="blue", cex=.5)
lines(ref, col="blue", lwd=1.5)
add_legend("bottom", legend=c("Reference data",'RGB: NIR, R, & G'),
pch=c(0,15), col=c("blue",NA), horiz=T, bty='n', cex=1.1)
box()
```

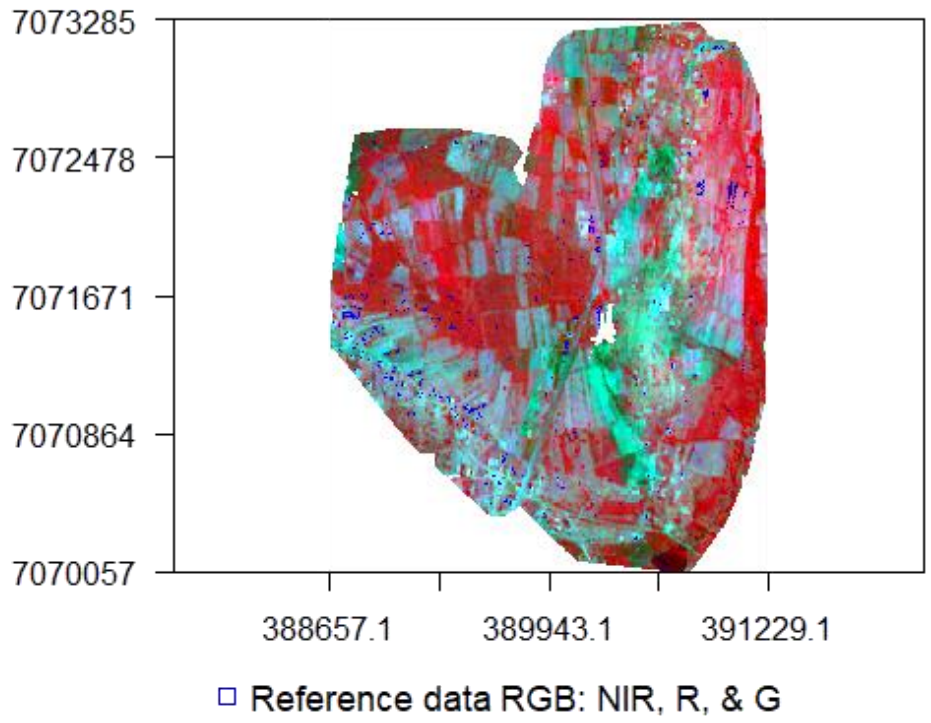

Figure 2: Ground reference polygons displayed over fused PCA image.

Extract pixels values overlaid by points and split them into training and validation points. These are used for model training and validation respectively. Note: that we use the same points to validate different models for consistent comparisons.

```
library(caTools)
#(NB: 0.4 means 40% for training and 60% for validation)
labels <- as.data.frame(samp[,1])
split <- sample.split(labels, SplitRatio = 0.4)
#validation data
valid <- subset(samp, split == FALSE)
#PCA
train.pca <- subset(samp, split == TRUE)
train.pca <- extract(pca, train.pca, cellnumbers=F, df=T, sp=T)
knitr::kable(head(train.pca))
```

	class	code	b	g	r	nir
3	waterbody	8	0.0132108	0.0208158	-0.0149209	0.1893390
6	waterbody	8	0.0131452	0.0207851	-0.0151873	0.1904794
9	waterbody	8	0.0131382	0.0207818	-0.0152156	0.1906009
12	waterbody	8	0.0131882	0.0208052	-0.0150128	0.1897325
15	waterbody	8	0.0131970	0.0208093	-0.0149769	0.1895790
18	waterbody	8	0.0131970	0.0208093	-0.0149772	0.1895800

```
#UAV
train.v <- subset(samp, split == TRUE)
train.v <- extract(brick(v), train.v, cellnumbers=F, df=T, sp=T)
knitr::kable(head(train.v))
```

	class	code	b	g	r	nir
3	waterbody	8	0.0645692	0.0981981	0.1022022	0.0864920
6	waterbody	8	0.0642581	0.0969432	0.1003542	0.0865044
9	waterbody	8	0.0638511	0.0983707	0.0989428	0.0879992
12	waterbody	8	0.0644608	0.0987926	0.1003774	0.0853833
15	waterbody	8	0.0647740	0.0998590	0.0995177	0.0861715
18	waterbody	8	0.0640595	0.1001275	0.0999492	0.0849983

```
#S2
train.s <- subset(samp, split == TRUE)
train.s <- extract(brick(s), train.s, cellnumbers=F, df=T, sp=T)
knitr::kable(head(train.s))
```

	class	code	b	g	r	nir
3	waterbody	8	0.0228	0.0253	0.024	0.0227
6	waterbody	8	0.0228	0.0253	0.024	0.0227
9	waterbody	8	0.0228	0.0253	0.024	0.0227
12	waterbody	8	0.0228	0.0253	0.024	0.0227
15	waterbody	8	0.0228	0.0253	0.024	0.0227
18	waterbody	8	0.0228	0.0253	0.024	0.0227

Maximum Likelihood Classification

Classify the PCA fused image and compare the results to un-fused UAV and S2 images based on MLC algorithm based F1-score validation measure. The F1-score measure is expressed as: $F1 = 2\frac{\text{Prod}\times\text{User}}{\text{Prod}+\text{User}}$ where *Prod* and *User* corresponds to the producer and user accuracies respectively.

```
#Fused image classification
mlc.pca <- superClass(pca, train.pca[-2], responseCol = "class", model = "mlc")
val.pca <- validateMap(mlc.pca$map, valid[-2], responseCol="class", mode='classification', classMapping = mlc.pca$classMapping)
#UAV classification
mlc.uav <- superClass(brick(v), train.v[-2], responseCol = "class", model = "mlc", minDist = 1)
val.uav <- validateMap(mlc.uav$map, valid[-2], responseCol="class", mode='classification', classMapping = mlc.uav$classMapping)
#Sentinel 2 classification
mlc.s <- superClass(brick(s), train.s, responseCol = "class", model = "mlc", minDist = 1)
val.s <- validateMap(mlc.s$map, valid, responseCol="class", mode='classification', classMapping = mlc.s$classMapping)
```

The classified images need to be displayed at some point. Here we design a function to display classified images.

```
display <- function(map, method, nClasses){
  par(mar = c(7, 2, 1.6, 2)) #c(bottom, left, top, right)
  image(map, col=c("red", "orange", "cyan" , "yellow", "brown", "magenta", "green1","blue"), axes=T, ann=F)
  classes.Palette <- colorRampPalette(c("red", "orange", "cyan" , "yellow", "brown", "magenta", "green1","blue", "white"))
  add_legend("bottom", legend=c('Built_up','Cassava', 'Grass', 'Maize', 'Sorghum', 'Sweet_potato','Trees','Water', "No data"), fill=classes.Palette(nClasses+1), ncol=3, bty='n', cex=1.1, pt.bg = NA)
  title(paste0(method," Classification"))
}
```

Lets design a function for accuracy assessment.

```
accuracy <- function(val.test){
  assessment.storage <- val.test$performance
  #print(assessment.storage)
  list_of_datasets <- list("ConfusionMatrix" = as.matrix(assessment.storage$table),
                           "OverallAcc" = as.matrix(assessment.storage$overall),
                           "byClass" = as.matrix(assessment.storage$byClass))
  return(list_of_datasets)
}
```

Table 2 F1-score validation of MLC classified maps using PCA fused image, UAV, and S2 respectively. The results indicate that PCA fusion performs better than S2 and comparable to UAV classification.

```
#PCA
List.pca <- accuracy(val.pca)
#UAV
List.v <- accuracy(val.uav)
#S2
List.s <- accuracy(val.s)

f1 <- data.frame(MLC_PCA=round(List.pca$byClass['F1'],3),MLC_UAV=round(List.v$byClass['F1'],3)
,MLC_S2=round(List.s$byClass['F1'],3))
row.names(f1) <- gsub("Class: ","",row.names(f1))
knitr::kable(f1,align='l',caption = "F1-score measures for MLC based on fused PCA image, UAV and Sen
tinel 2.")
```

Table 2: F1-score measures for MLC based on fused PCA image, UAV and Sentinel 2.

	MLC_PCA	MLC_UAV	MLC_S2
built_up	0.921	0.973	0.893
cassava	0.963	1.000	1.000
grass	0.679	0.778	0.511
maize	0.846	0.884	0.637
sorghum	0.923	0.903	0.429
sweet_potato	0.994	0.996	0.903
trees	0.950	0.968	0.907
waterbody	0.991	0.982	1.000

Next we explore how RF classification compares to MLC.

Random Forest (RF)

In this section we use RF to classify the images (UAV, S2 and fused image) and compare its crop classification accuracy to that of MLC. First its important to evaluate training error and variable importance plots. We make these plots based on the PCA fused image as an example. From Figure 3, the training error reduces with increase in number of trees. We set the number of trees to 250 because it has been established that over 200 trees RF estimates are stable (Hastie, Tibshirani, & Friedman, 2011).

```
rf.pca <- randomForest(code~., data=na.omit(as.data.frame(train.pca[,-1]@data)), ntree = 250, importance
=T)
plot(rf.pca, main='RF Training Error')
```

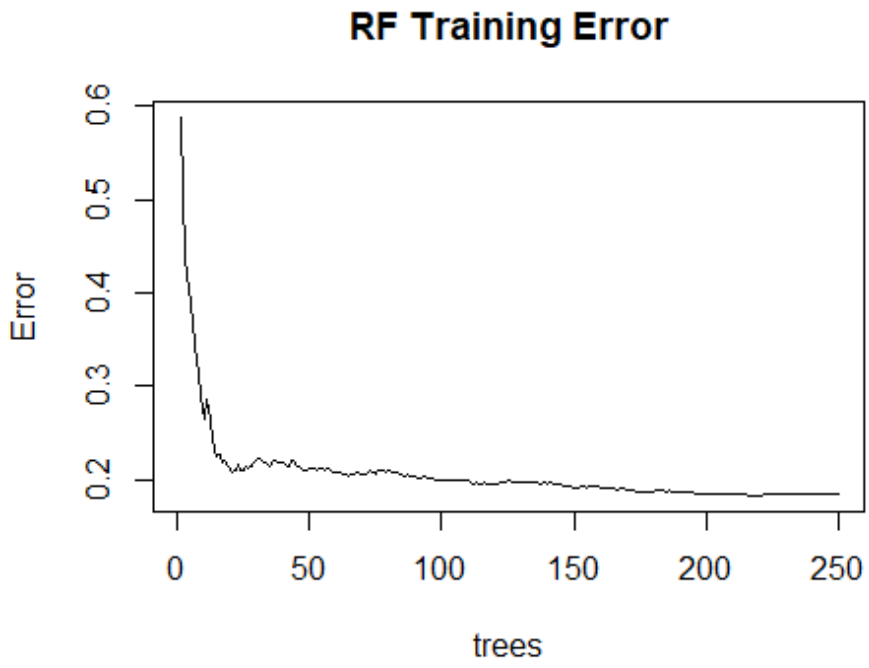

Figure 3: F Training Error w.r.t number of trees.

```
#knitr::kable(importance(rf.pca))
```

One way in which variable importance is estimated is using percentage increase in Mean Standard Error (MSE) (%IncMSE). In this case, the most important variable is one which has the highest increase in MSE when it is removed from the model training samples. Computation of variable importance based on %IncMSE is shown by Figure 4.

```
varImpPlot(rf.pca,sort=TRUE, n.var=min(dim(pca)[3], nrow(rf.pca$importance)), type = 1)
```

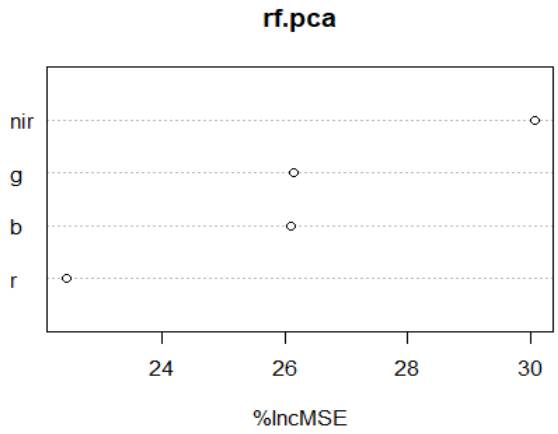

Figure 4: RF Variable importance based on mean decrease in MSE.

Mean Decrease Gini (IncNodePurity) plot is also used to measure RF variable importance as shown in Figure 5. It is a measure of variable importance based on the Gini impurity index (i.e. node purity) used for calculating the splits in trees. The higher the value of mean decrease accuracy or mean decrease gini score, the higher the importance of the variable to our model. However, IncNodePurity is biased and should only be used if the extra computation time of calculating %IncMSE is unacceptable.

```
varImpPlot(rf.pca,sort=TRUE, n.var=min(dim(pca)[3], nrow(rf.pca$importance)), type = 2)
```

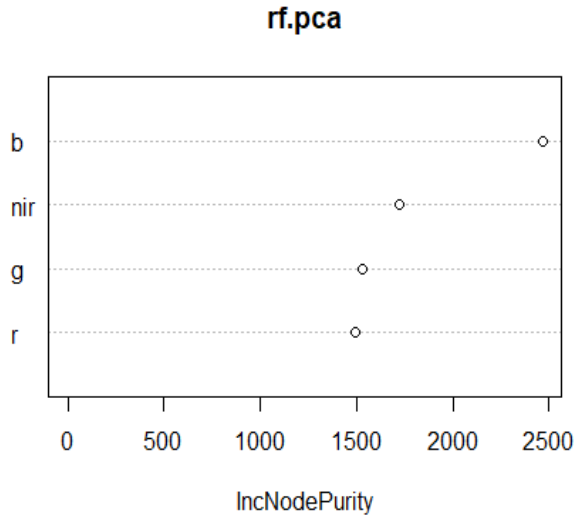

Figure 5: RF Variable importance based on mean decrease in Gini.

Now that we explored important variables we can decide to drop some during classification. However, in this case we use all the variables.

```
tic("RF classification of PCA fused image:")
rf.pca <- superClass(pca, train.pca, responseCol = "class", model = "rf")
val.rf.pca <- validateMap(rf.pca$map, valid, responseCol="class", mode='classification', classMapping = rf.pca$classMapping)
toc()

## RF classification of PCA fused image:: 109.1 sec elapsed

tic("RF classification of UAV image:")
rf.v <- superClass(brick(v), train.v, responseCol = "class", model = "rf")
val.rf.v <- validateMap(rf.v$map, valid, responseCol="class", mode='classification', classMapping = rf.v$classMapping)
toc()

## RF classification of UAV image:: 118.46 sec elapsed

tic("RF classification of S2 image:")
rf.s <- superClass(brick(s), train.s, responseCol = "class", model = "rf")
```

```
val.rf.s <- validateMap(rf.s$map, valid, responseCol="class", mode='classification',  classMapping = rf.s$
classMapping)
toc()

## RF classification of S2 image:: 2.96 sec elapsed
```

Results

We can now display all the classified images side by side. The fused images produced maps with well delineated crop parcels compared to the un-fused images (Figures 6 – 11). This illustrates the importance of data synergy. In addition, RF map is well delineated compared to MLC.

```
display(mlc.pca$map, "Fused MLC", nClasses)
```

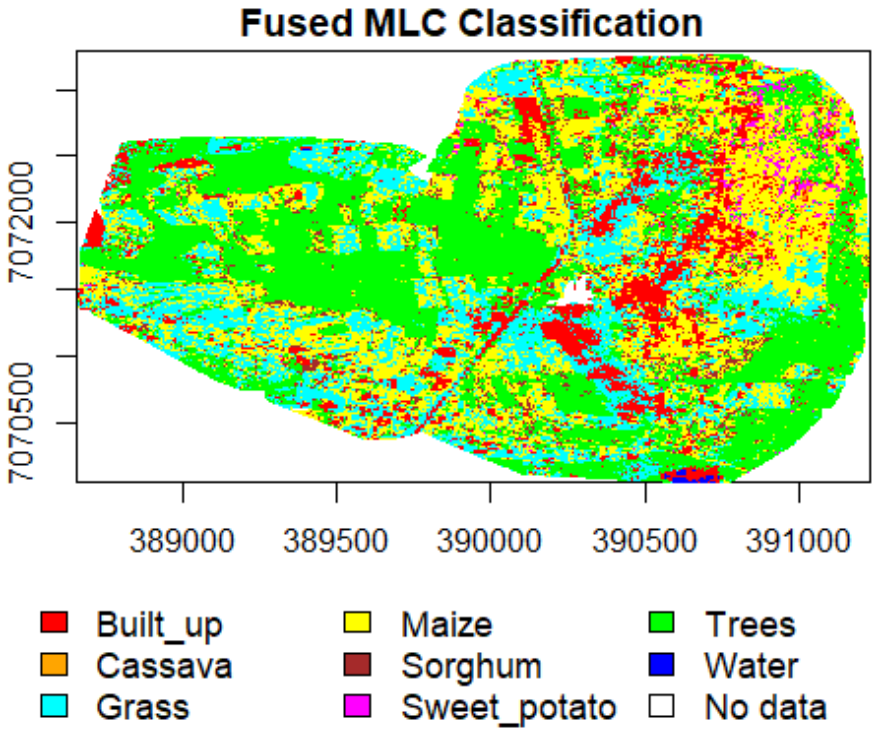

Figure 6: Crop distribution as mapped using MLC based fused image.

```
display(mlc.uav$map, "UAV MLC", nClasses)
```

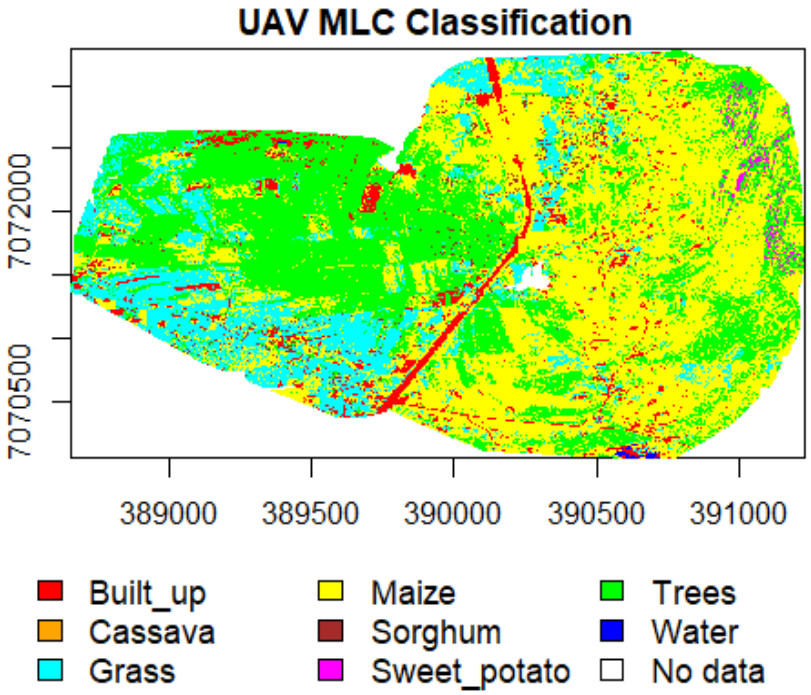

Figure 7: Crop distribution as mapped using MLC based UAV image.

```
display(mlc.s$map, "S2 MLC", nClasses)
```

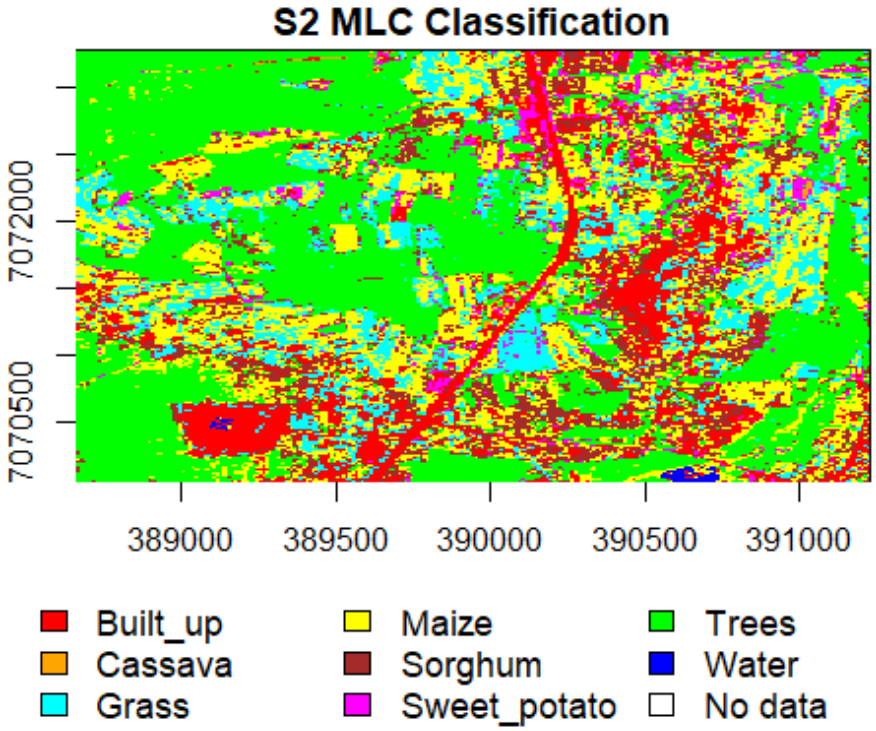

Figure 8: Crop distribution as mapped using MLC based S2 image.

```
display(rf.pca$map, "Fused RF", nClasses)
```

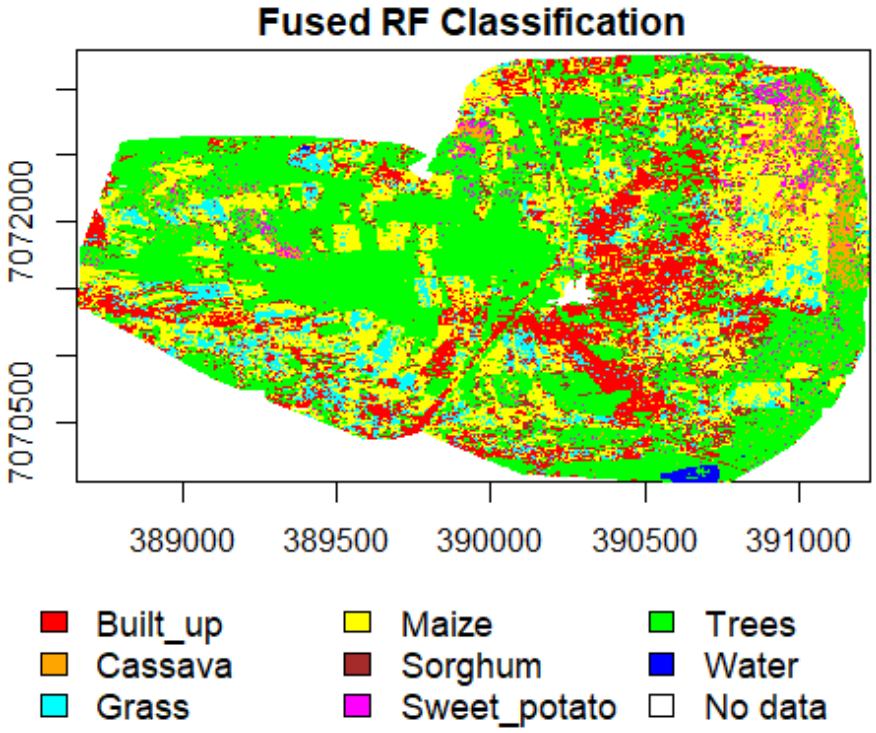

Figure 9: Crop distribution as mapped using RF based fused image.

```
display(rf.v$map, "UAV RF", nClasses)
```

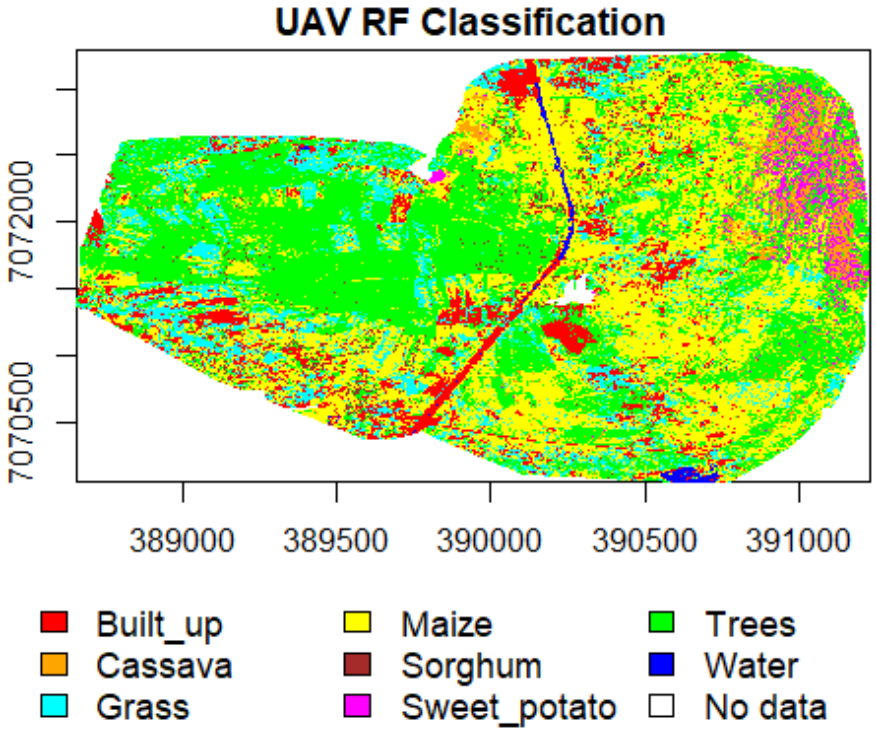

Figure 10: Crop distribution as mapped using RF based UAV image.

```
display(rf.s$map, "S2 RF", nClasses)
```

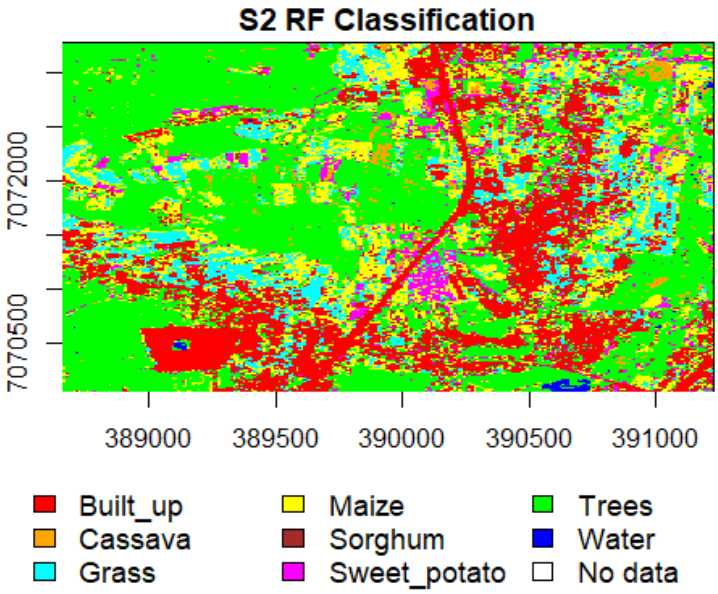

Figure 11: Crop distribution as mapped using RF based S2 image.

Finally, let us evaluate how RF and MLC classifications performed using fused PCA, UAV and S2 images. We use F1-score as shown in Table 3.

```
#PCA
List.rf.pca <- accuracy(val.rf.pca)
#UAV
List.rf.v <- accuracy(val.rf.v)
#S2
List.rf.s <- accuracy(val.rf.s)


f2 <- data.frame(RF_PCA=round(List.rf.pca$byClass[,'F1'],3),RF_UAV=round(List.rf.v$byClass[,'F1'],3)
,RF_S2=round(List.rf.s$byClass[,'F1'],3),MLC_PCA=round(List.pca$byClass[,'F1'],3),MLC_UAV=roun
d(List.v$byClass[,'F1'],3),MLC_S2=round(List.s$byClass[,'F1'],3))
row.names(f2) <- gsub("Class: ","",row.names(f1))
knitr::kable(f2,align='l',caption = "F1-score measures for RF and MLC classifications based on fused PCA
image, UAV and Sentinel 2.")
```

Table 3: F1-score measures for RF and MLC classifications based on fused PCA image, UAV and Sentinel 2.

	RF_PCA	RF_UAV	RF_S2	MLC_PCA	MLC_UAV	MLC_S2
built_up	0.973	0.989	0.938	0.921	0.973	0.893
cassava	0.987	0.975	0.889	0.963	1.000	1.000
grass	0.908	0.887	0.756	0.679	0.778	0.511
maize	0.951	0.950	0.790	0.846	0.884	0.637
sorghum	0.974	0.954	0.824	0.923	0.903	0.429
sweet_potato	1.000	0.998	0.875	0.994	0.996	0.903
trees	0.980	0.984	0.949	0.950	0.968	0.907
waterbody	1.000	1.000	1.000	0.991	0.982	1.000

The contribution of PCA based on PCAfusion of multi-spectral Sentinel 2 and UAV is clearly illustrated by RF as shown in Table 3. RF gives a better accuracy on the fused product compared to RF classification of un-fused images (UAV and S2). RF also performs better compared to MLC.

Eswatini wall-to-wall maize crop mapping

We are now going to upscale maize crop mapping in the entire Eswatini using a combination of training sites picked from UAVs in the 4 sites and from the sentinel 2 imageries across the entire country. S2 images were acquired on the 18th of April 2021.

```
# reading sentinel 2 mosaic with all images acquired on the 18th of April 2021

s.folder<- "E:/Osunga/Projects/2021/Eswatini_drone_agricultural_monitoring/analysis/sentinel2/eswatini/
outputs/"

s.raster <- "Eswatini_S2_mosaic_v2_clip_tif.tif"

 s.stack <- stack(paste0(s.folder,s.raster))
 names(s.stack) <- c("blue", "green","red", "nir")

 s.raster<-raster(paste0(s.folder,s.raster))
```

Plotting sentinel 2 imagery

As part of data exploration, we shall plot sentinel 2 imagery NearInfraRed Red Green (false color) and Red Green Blue (true color) composites side by side

```
par(mfrow = c(1, 2)) # 1 row, 2 columns
plotRGB(s.stack, r="nir", g="red", b="green", stretch="lin", axes=T, mar = c(4, 5, 1.4, 0.2), main="False color", cex.axis=0.5)
box()
plotRGB(s.stack, r="red", g="green", b="blue", stretch="lin", axes=T, mar = c(4, 5, 1.4, 0.2), main="True color", cex.axis=0.5)
box()
```

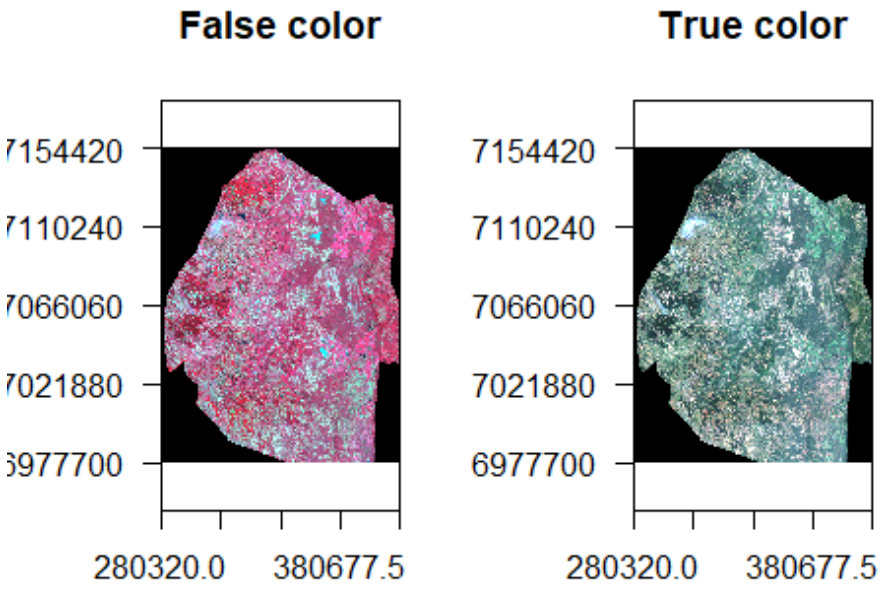

Loading training sites

Training sites were picked from UAVs in the 4 sites and from the sentinel 2 imageries across the entire country. Classes of interest included cropland, forestland, grassland, open water, otherland and sugarcane.

```
ref <- readOGR('E:/Osunga/Projects/2021/Eswatini_drone_agricultural_monitoring/analysis/training_sites/eswatini_training_sites_v1.shp')

## OGR data source with driver: ESRI Shapefile
## Source: "E:\Osunga\Projects\2021\Eswatini_drone_agricultural_monitoring\analysis\training_sites\eswatini_training_sites_v1.shp", layer: "eswatini_training_sites_v1"
## with 2012 features
## It has 1 fields

ref <- spTransform(ref, crs(s.raster))
```

Generating sample points from the training site polygons

Sample points were generated from the training site polygons using stratified random sampling. Stratified random sampling ensures that all classes are fairly represented in the training data.

```
set.seed(530)
samp <- spsample(ref, 4000, type='stratified')

# add the land cover class to the points
samp$class <- over(samp, ref)$lc
knitr::kable(table(samp$class), align = 'l')
```

Var1	Freq
cropland	541
forestland	837
grassland	723
open water	518
otherland	573
sugarcane	759

Creating legend to overlay training site polygons with s2 image

Display training polygons over the s2 image. To do this we will create a function to aid in legend display.

```
add_legend <- function(...) {
  opar <- par(fig=c(0, 1, 0, 1), oma=c(0, 0, 0, 0),
    mar=c(0, 0, 0, 0), new=TRUE)
  on.exit(par(opar))
  plot(0, 0, type='n', bty='n', xaxt='n', yaxt='n')
  legend(...)
}
```

Overlaying training site polygons with s2 image

As part of data exploration, we are going to display the training points over the s2 imagery as shown below

```
x11()
par(mar = c(4, 5, 1.4, 0.2)) #c(bottom, left, top, right)
plotRGB(s.stack, r="nir", g="red", b="green", stretch="lin", axes = TRUE)

#points(samp, col="blue", cex=.5)
lines(ref, col="blue", lwd=1.5)

add_legend("bottom", legend=c("Reference data",'RGB: NIR, R, & G'),
pch=c(0,15), col=c("blue",NA), horiz=T, bty='n', cex=1.1)

box()
```

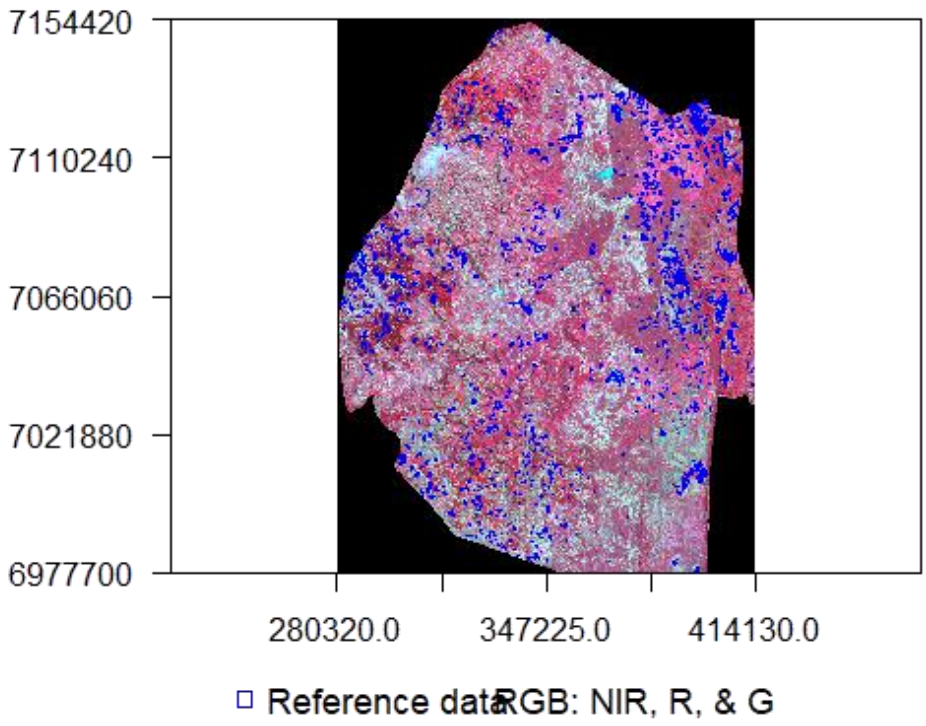

Extracting pixels values overlaid by points and split them into training and validation points

Extract pixels values overlaid by points and split them into training and validation points. These will be used for model training and validation respectively. Note that we use the same points to validate different models for consistent comparisons.

```
#(NB: 0.4 means 40% for training and 60% for validation)
labels <- as.data.frame(samp[,1])
split <- sample.split(labels, SplitRatio = 0.4)
#validation data
valid <- subset(samp, split == FALSE)

train.s <- subset(samp, split == TRUE)
train.s <- extract(s.raster, train.s, cellnumbers=F, df=T, sp=T)
knitr::kable(head(train.s))
```

	class	Eswatini_S2_mosaic_v2_clip_tif
2	open water	0.0511
5	open water	0.0506
8	open water	0.0502
11	open water	0.0493
14	open water	0.0502
17	sugarcane	0.0361

Classification of sentinel 2 mosaic based on MLC and RF algorithms

Classifying sentinel 2 imagery based on random forest (RF) and maximum likelihood classification (MLC) algorithms

```
start <-Sys.time()

#Sentinel 2 classification

tic("MLC and RF classification of S2 image:")

# MLC
mlc.s <- superClass(brick(s.stack), train.s, responseCol = "class", model = "mlc", minDist = 1)
val.s <- validateMap(mlc.s$map, valid, responseCol="class", mode='classification', classMapping = mlc.s$classMapping)

# RF

rf.s <- superClass(brick(s.raster), train.s, responseCol = "class", model = "rf",ntree=300,allowParallel=T)

val.rf.s <- validateMap(rf.s$map, valid, responseCol="class", mode='classification', classMapping = rf.s$classMapping)

toc()

## MLC and RF classification of S2 image:: 6899.5 sec elapsed

end<- Sys.time()

end-start

## Time difference of 1.91653 hours
```

Evaluating how MLC and RF over s2 mosaic performed using F1-score

Let us evaluate how MLC and RF performed using F1-score

```
#S2
List.mlc.s <- accuracy(val.s)

f1 <- data.frame(MLC_S2=round(List.mlc.s$byClass[,'F1'],3))
row.names(f1) <- gsub("Class: ","",row.names(f1))
knitr::kable(f1,align='l',caption = "F1-score measures for MLC based on Sentinel 2.")
```

F1-score measures for MLC based on Sentinel 2.

	MLC_S2
cropland	0.583
forestland	0.934
grassland	0.592

open water	1.000
otherland	0.888
sugarcane	0.810

```
List.rf.s <- accuracy(val.rf.s)

f1 <- data.frame(RF_S2=round(List.rf.s$byClass[,'F1'],3))
row.names(f1) <- gsub("Class: ","",row.names(f1))
knitr::kable(f1,align='l',caption = "F1-score measures for RF based on Sentinel 2.")
```

F1-score measures for RF based on Sentinel 2.

	RF_S2
cropland	0.264
forestland	0.784
grassland	0.304
open water	0.679
otherland	0.298
sugarcane	0.334

Evaluating how MLC and RF performed using confusion matrix

Let us evaluate how MLC and RF performed using the confusion matrix

```
#S2

# MLC
knitr::kable(List.mlc.s$ConfusionMatrix,align='l')
```

	cropland	forestland	grassland	open water	otherland	sugarcane
cropland	208	1	135	0	2	22
forestland	1	520	7	0	0	24
grassland	100	19	273	0	28	24
open water	0	0	0	352	0	0
otherland	2	5	26	0	365	28
sugarcane	35	17	37	0	1	402

```
# RF
knitr::kable(List.rf.s$ConfusionMatrix,align='l')
```

	cropland	forestland	grassland	open water	otherland	sugarcane
cropland	110	45	113	13	58	148
forestland	26	445	30	43	19	10
grassland	74	28	149	24	98	128
open water	4	21	17	231	45	10
otherland	21	7	46	27	93	34

sugarcane	111	16	123	14	83	170

Evaluating how MLC and RF performed using overall accuracy

Let us evaluate how MLC and RF performed by overall accuracy

```
#S2

#                                                                    MLC
knitr::kable(data.frame(Type=List.mlc.s$OverallAcc[,1],align='l'))
```

	Type	align
Accuracy	0.8048595	l
Kappa	0.7645258	l
AccuracyLower	0.7891996	l
AccuracyUpper	0.8198388	l
AccuracyNull	0.2133637	l
AccuracyPValue	0.0000000	l
McnemarPValue	NaN	l

```
#                                                                    RF
knitr::kable(data.frame(Type=List.rf.s$OverallAcc[,1],align='l'))
```

	Type	align
Accuracy	0.4548216	l
Kappa	0.3414663	l
AccuracyLower	0.4356744	l
AccuracyUpper	0.4740692	l
AccuracyNull	0.2133637	l
AccuracyPValue	0.0000000	l
McnemarPValue	0.0000000	l

Crop Yield Modelling Framework

Background

This is an R Markdown document documenting development of maize crop yield prediction using remote sensing to allow accurate, reliable and timely estimations over Eswatini. Particularly, this information is necessary to ensure the adequacy of a nation's food supply as well as to aid policy makers and farmers. This crop yield model framework uses MODIS vegetation indices products such as NDVI, EVI, FPAR, LAI and GPP to estimate/predict maize yield for the year 2020 using yield results from 2000 to 2019 obtained from FAOSTAT. After applying the quality flags on the MODIS products to mask out pixels that are cloudy, faulty, have high aerosols, and with water. After applying the quality flags, the indices were spatially and temporally aggregated over the maize growing season. Two periods were tested from January to March and December to March (Start of flowering to start of senescence). Z-score standardization was

applied to the indices in order to capture long-term deviations of an index from the average. After index standardization, maize yield prediction was conducted. From the results, the yield model framework predicted **92500.98 T** for January to March season and **69685.49 T/Ha** for December to January season.

The next step for this work is downscale this process and predict maize yield at district level but this depends on the availability of yield data at that level.

Data and Methods

Install required packages, in this case, we will use “Luna” package.

```
if (!"luna" %in% installed.packages()){
  remotes::install_github("rspatial/luna")
}

library(luna)
prod <- getProducts("^MOD13Q1|^MYD13Q1|^MOD17A2|^MYD17A2")
knitr::kable(table(head(prod, n=3)), align = 'l')
```

provider	concept_id	short_name	version	Freq
LPDAAC_ECS	C107705237-LPDAAC_ECS	MOD13Q1	005	1
LPDAAC_ECS	C115315503-LPDAAC_ECS	MOD13Q1	005	0
LPDAAC_ECS	C117500873-LPDAAC_ECS	MOD13Q1	005	0
LPDAAC_ECS	C107705237-LPDAAC_ECS	MOD17A2	005	0
LPDAAC_ECS	C115315503-LPDAAC_ECS	MOD17A2	005	0
LPDAAC_ECS	C117500873-LPDAAC_ECS	MOD17A2	005	1
LPDAAC_ECS	C107705237-LPDAAC_ECS	MYD13Q1	005	0
LPDAAC_ECS	C115315503-LPDAAC_ECS	MYD13Q1	005	1
LPDAAC_ECS	C117500873-LPDAAC_ECS	MYD13Q1	005	0

Let’s get Eswatini country boundary and start data downloads. This line of code can be used to get the boundary of any country.

```
library(raster)

## Loading required package: sp

Es <- getData("GADM", country="SWZ", level=0)
plot(Es)
text(Es,Es$NAME_0)
```

It is important to define data parameters: product name, start and end date, and area of interest. In this section one can select the growing season for yield prediction according to the countrys' growing season. In this work two seasons were tested: January to March and December to January which define the Maize growing season in Eswatini.

```
start <- "2018-01-01"
end <- "2019-12-31"
```

Thereafter, extract existing data files for variables important to crop yield modelling type MOD13Q1 to download NDVI & EVI, MCD15A2H for FPAR & LAI and GPP.

```
product <- "MOD13Q1"
mf <- luna::getModis(product, start, end, aoi=Es, download = FALSE)
length(mf)

## [1] 70
```

MODIS vegetation indices data can be download from EarthData. To download MODIS data, define the path to save downloaded data, a user's name and password to access the data from data repository. Here, the login details are save as pwd.rds in the MODIS folder. Once all the necessary information is set, data is downloaded for the maize growing season months only.

```
pass <- readRDS(file = "pwd.rds")
modis_path <- "Yield/Raw/"
mstart <- "-01-01"
mend <- "-01-31"
for(y in 2000:2000){
 cat(y,"downloading..\t")
 start <- paste0(y,mstart)
 end <- paste0(y,mend)
 luna::getModis(product, start, end, aoi=Es, download=TRUE,
        path=modis_path, username=pass$username,
        password=pass$password)
}

## 2000 downloading..
## 2001 downloading..
```

MODIS Data Processing

After downloading MODIS data, it is necessary to apply quality mask to the desired image bands. The quality flags that come with the images indicate the conditions of each pixel with respect cloud, aerosol, water presence, and any other failures/errors. This section covers these aspects.

Load previously downloaded NDVI and EVI files and define scale factor their scale factor.

```
rm(list = ls(all=TRUE))
unlink(".RData")
sf <- 0.0001 #scalefactor
root <- 'MODIS/'
##n <- list.files(paste0(root,'raw'), pattern=glob2rx("*MOD13Q1*"),full.names=T)
n <- list.files("MODIS/", pattern=glob2rx("*MOD13Q1*"),full.names=T)
length(n)
```

```
## [1] 221
```

Some properties of loaded images can be explored as follows for example to List Layers names

```
Names(r)
```

```
##[1] "MODIS_Grid_16DAY_250m_500m_VI:\"250m 16 days NDVI\""
##[2] "MODIS_Grid_16DAY_250m_500m_VI:\"250m 16 days EVI\""
##[3] "MODIS_Grid_16DAY_250m_500m_VI:\"250m 16 days VI Quality\""
##[4] "MODIS_Grid_16DAY_250m_500m_VI:\"250m 16 days red reflectance\""
##[5] "MODIS_Grid_16DAY_250m_500m_VI:\"250m 16 days NIR reflectance\""
```

Plot selected images e.g., NDVI & EVI

```
rm(list = ls(all=TRUE))

unlink(".RData")

sf <- 0.0001 #scalefactor

root <- 'Yield/MODIS/'

##n <- list.files(paste0(root,'raw'), pattern=glob2rx("*MOD13Q1*"),full.names=T)

n <- list.files("Yield/MODIS", pattern=glob2rx("*MOD13Q1*"),full.names=T)

length(n)
```

```
sf <- 0.0001
par(mfrow=c(2,2),mar = c(4, 4, 1.4, 0.1)) #c(bottom, left, top, right)
temp <- r[[1]]
temp <- temp*sf
plot(temp, main='NDVI')
temp <- r[[2]]
temp <- temp*sf
plot(temp, main='EVI')
```

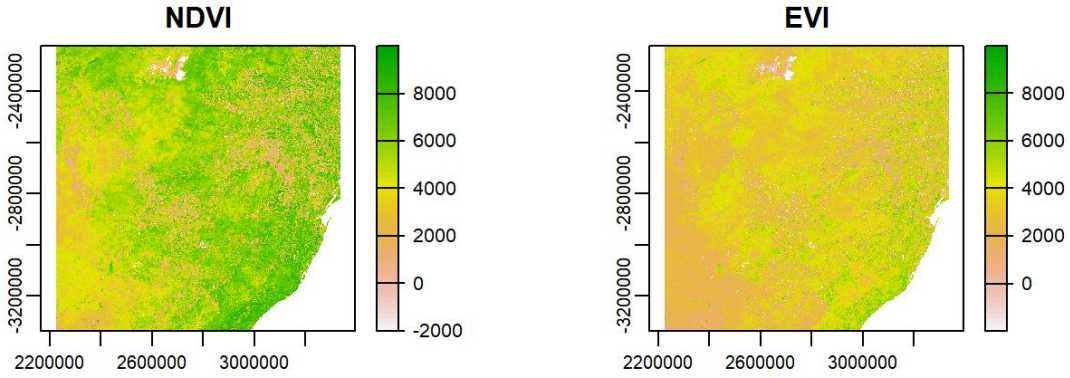

Applying Quality Flags to MODIS Vegetation Indices

Create quality flags

```
library(terra)

## terra version 1.3.4

r <- rast(n[1])

from <- c(1,2,6,11)
to <- c(2,5,7,13)
reject <- c("10,11", "1101,1110,1111", "11", "101,110,111")
qa_bits <- cbind(from, to, reject)
qa_bits
```

```
##      from to reject
## [1,] "1"  "2"  "10,11"
## [2,] "2"  "5"  "1101,1110,1111"
## [3,] "6"  "7"  "11"
## [4,] "11" "13" "101,110,111"
```

Plot quality flag map

```
library(luna)
qc <- r[[3]]
quality_mask <- modis_mask(qc, 16, qa_bits)
plot(quality_mask, main="Quality mask")
```

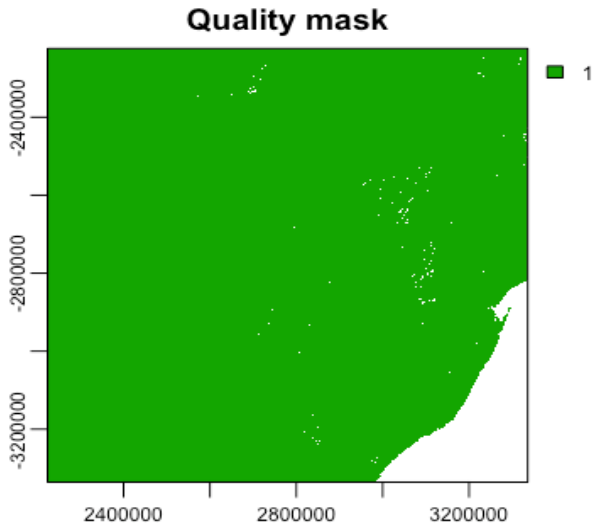

Test quality flag on NDVI and EVI images

```
temp                                    <-                                  r[[1]]*sf
rmask <- mask(temp, quality_mask)

sf                                      <-                                  0.0001
par(mfrow=c(2,2),mar    =    c(4,    4,    1.4,    0.1))    #c(bottom,    left,    top,    right)
temp                                     <-                                 r[[1]]
temp                                    <-                                  temp*sf
plot(temp,                                                                  main='NDVI')
temp                                     <-                                 r[[2]]
temp                                    <-                                  temp*sf
plot(temp, main='EVI')
```

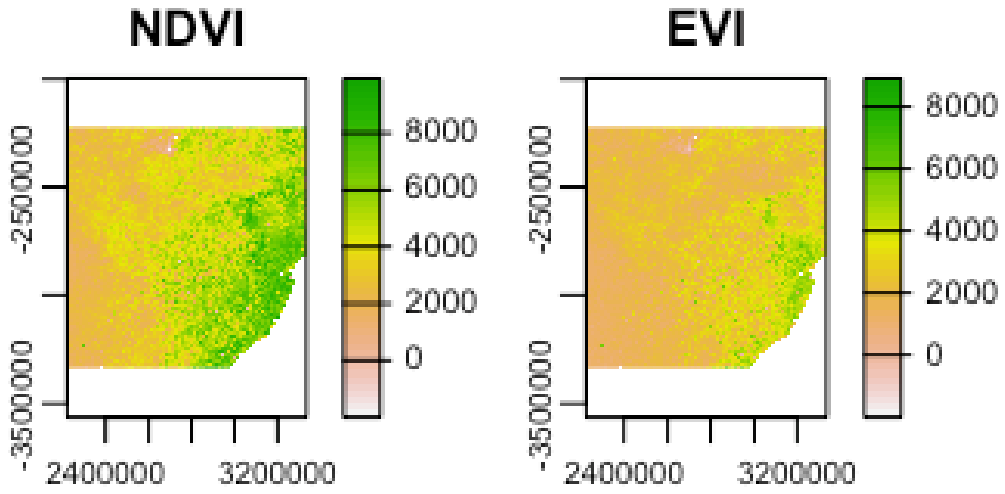

In this section, the quality assurance information available in the third band of **MOD13Q1** product is used to identify the bad pixels to remove in both NDVI and EVI images. The indices are then spatial aggregated over Eswatini boundary.

```
library(raster)

sz <- getData("GADM", country="SWZ", level=0)
#Change vector boundary coordinate reference system, so that it matches that of the MODIS data.
prj <- crs(rmask)
poly <- project(vect(sz),prj)
for(i in 1:length(n)){
 path <- paste0(root,'processed/')
 filename <- paste0(path,gsub(".hdf","",basename(n[i])),'.tif')
 if(!file.exists(filename)){
  r <- rast(n[i])
  qc <- r[[3]]
  quality_mask <- modis_mask(qc, 16, qa_bits)
  #NDVI
  temp <- r[[1]]*sf
  ndvi <- mask(temp, quality_mask)
  names(ndvi) <- "NDVI"
  #EVI
  temp <- r[[2]]*sf
  evi <- mask(temp, quality_mask)
  names(evi) <- "EVI"
  temp <- c(ndvi, evi)
  path <- paste0(root,'processed/')
  filename <- paste0(path,gsub(".hdf","",basename(n[i])),'.tif')
  #Crop to AOI
  out <- crop(temp, poly)
  writeRaster(out, filename, overwrite=TRUE)
 }
}
```

Gross Primary Productivity (GPP) and Fraction of Photosynthetically Active Radiation (FPAR)/ Leaf Area Index (LAI) (**MCD15A2H**) monthly can be computed as illustrated in the following process.

```
n <- list.files("MODIS/", pattern=glob2rx("*MCD15A2H*"),full.names=T)
length(n)
```

Here, Quality information available in Table 5 of the user guide is applied and AOI files for FPAR/LAI saved to the defined directory.

```
from <- c(2,3,5)
to <- c(2,4,7)
reject <- c("1", "01", "100")
qa_bits <- cbind(from, to, reject)
qa_bits
```

```
##      from to reject
## [1,] "2"  "2"  "1"
```

```
##      [2,] "3"  "4"  "01"
## [3,] "5"  "7" "100"
```

```
for(i in 1:length(n)){
  path <- paste0(root,'processed/')
  filename <- paste0(path,gsub(".hdf","",basename(n[i])),'.tif')
  if(!file.exists(filename)){
    r <- rast(n[i])
    qc <- r[[3]]
    quality_mask <- modis_mask(qc, 8, qa_bits)
    #FPAR
    sf <- 100
    temp <- r[[1]]*sf
    fpar <- mask(temp, quality_mask)
    names(fpar) <- "FPAR"
    #LAI
    sf <- 10
    temp <- r[[2]]*sf
    lai <- mask(temp, quality_mask)
    names(lai) <- "LAI"
    temp <- c(fpar, lai)
    #Crop to AOI
    out <- crop(temp, poly)
    writeRaster(out,filename,overwrite=TRUE)
  }
}
```

Finally, in a similar fashion Quality information can applied be to MODIS GPP (**MOD17A2H**) product to obtain monthly GPP. The QA bits in this case are similar to those in FPAR/LAI.

```
n <- list.files("MODIS/", pattern=glob2rx("*MOD17A2H*"),full.names=T)
length(n)
```

```
for(i in 1:length(n)){
  path <- paste0(root,'processed/')
  filename <- paste0(path,gsub(".hdf","",basename(n[i])),'.tif')
  if(!file.exists(filename)){
    r <- rast(n[i])
    qc <- r[[3]]
    quality_mask <- modis_mask(qc, 8, qa_bits)
    temp <- r[[1]]
    gpp <- mask(temp, quality_mask)
    names(gpp) <- "GPP"

    #Crop to AOI
    out <- crop(gpp, poly)
    writeRaster(out, filename, overwrite=TRUE)
```

```
  }
}
```

Spatial-temporal index computation

This section illustrates how to aggregate the already pre-computed vegetation indices (**NDVI/EVI**, **FPAR/LAI** and **GPP**) over the entire analysis period (i.e. 2000–2020). The mean is adopted as an aggregation function.

To start off relevant files are loaded.

```
rm(list = ls(all=TRUE))
unlink(".RData")
root <- 'MODIS/'
path <- paste0(root,'processed/')
#16 day NDVI & EVI composite from Terra
n <- list.files(path, pattern=glob2rx("*MOD13Q1*"),full.names=T)
#8 day 500 m FPAR & LAI composite from Terra & Aqua
f <- list.files(path, pattern=glob2rx("*MCD15A2H*"),full.names=T)
#8 day GPP composite from Terra
g <- list.files(path, pattern=glob2rx("*MOD17A2H*"),full.names=T)
```

Get the study area boundary re-project it to MODIS's sinusoidial coordinate reference system.

```
library(terra)
library(raster)

sz <- getData("GADM", country="SWZ", level=0)
temp <- rast(n[1])
prj <- crs(temp)
poly <- project(vect(sz),prj)
```

The next step is to aggregate over the maize growing season (January–March) of each corresponding year. Therefore, relevant files in each have to be selected. This can be done using this function.

```
startSeason <- "01-01"
endSeason <- "03-31"
selectModisFiles <- function(files, startdate, enddate) {
 base_names <- basename(files)
 dates <- MODIS::extractDate(base_names, asDate = TRUE)$inputLayerDates
 i <- (dates >= as.Date(startdate)) & (dates <= as.Date(enddate))
 files[i]
}
```

The next function is applied for temporal aggregation of vegetation indices

```
spatialTempAgg <- function(files, startyear, endyear){
 st_v <- c()
 for(year in startyear:endyear) {
  season <- selectModisFiles(files, paste0(year, "-", startSeason), paste0(year, "-", endSeason))
```

```
  if(length(season) > 0){
   vi <- rast(season)
   temporal <- tapp(vi, index = names(vi), fun = "mean", na.rm = T)
   st <- extract(temporal, poly, fun=mean, na.rm=TRUE)
   st$ID <- year
   st_v <- c(st_v, st)
   #filename <- paste0(path, sub("\\..*", "", basename(n[1])), '_',year,"_",index ,'.tif')
   #writeRaster(temporal, filename = filename , overwrite=TRUE)
  }else{
   print(paste(year,"growing season image is not available!"))
  }
 }
 return(st_v)
}
```

Use spatialTempAgg function to compute spatial-temporal indices for all products.

```
startyear <- 2000
endyear <- 2020

#NDVI_EVI
vi_st <- spatialTempAgg(n, startyear, endyear)

## [1] "2000 growing season image is not available!"

vi_st <- data.frame(matrix(unlist(vi_st), nrow=length(startyear:endyear), byrow=TRUE))

rows

names(vi_st) <- c('Year','NDVI','EVI')
saveRDS(vi_st, paste0(root,'outputs/2000_2020_NDVI_EVI.rds'))

#FPAR/LAI
fpar_st <- spatialTempAgg(f, startyear, endyear)

fpar_st <- data.frame(matrix(unlist(fpar_st), nrow=length(fpar_st$ID:endyear), byrow=TRUE))
names(fpar_st) <- c('Year','FPAR','LAI')
saveRDS(fpar_st, paste0(root,'outputs/2000_2020_FPAR_LAI.rds'))

#GPP
gpp_st <- spatialTempAgg(g, startyear, endyear)

gpp_st <- data.frame(matrix(unlist(gpp_st), nrow=length(startyear:endyear), byrow=TRUE))

names(gpp_st) <- c('Year','GPP')
saveRDS(gpp_st, paste0(root,'outputs/2000_2020_FPAR_GPP.rds'))
```

Once the spatio-temporal index aggregation is complete, the next step is to standardize the indices using Z-score standardization in order to capture long-term deviations of an index from the average. Z-score is computed in terms of standard deviations σ from the mean μ. If a Z-score is 0, it indicates that the data point's score is identical to the mean score. A Z-score of 1.0 indicates a value that is one standard deviation

from the mean. These scores can be positive or negative which indicates that the score is above the mean or below the mean respectively.

```
zscore <- function(y){
 (y - mean(y, na.rm=TRUE) ) / (sd(y, na.rm=TRUE))
}
```

Finally, compute Z-score values of all indices.

```
#Combine Indices
index <- Reduce(function(x,y) merge(x = x, y = y, all =TRUE), list(vi_st, fpar_st, gpp_st))
scores <- apply(index[,-1], 2, zscore)
scores <- cbind(index["Year"], scores)
colnames(scores)[1] <- "Year"
saveRDS(scores, paste0(root,'outputs/2000_2020_MODIS_st_indices.rds'))
```

Maize yield prediction

Maize yield information from FAOSTAT is used in this section to design a model for yield prediction based on remotely sensed Z-scored spatial-temporal indices computed previously.

Load necessary packages and data (MODIS indices and reference yields).

```
rm(list = ls(all=TRUE))
unlink(".RData")
library(dplyr)

library(reshape2)
root <- root <- 'MODIS/outputs/'
filename <- paste0(root, "2000_2020_MODIS_st_indices.rds")
#Indices
index <- readRDS(filename)
index <- as.data.frame(index)

filename <- paste0(root, "outputs/faostat.csv")

#Yields

ref <- read.csv(filename, stringsAsFactors = F)
```

Merge yield refence data with satellite indices for model training.

Year	NDVI	EVI	FPAR	LAI	GPP	Yield_tonnes
2000	0.7411606	0.4212527	NA	NA	0.4953546	112779
2001	0.2562051	-0.0524735	NA	NA	0.1678476	82536
2002	-0.8384683	-0.6522269	NA	NA	-0.0020507	67639

Year	NDVI	EVI	FPAR	LAI	GPP	Yield_tonnes
2003	-0.4130928	-0.2029017	-0.0499667	-0.1897696	-1.3033065	69273
2004	0.3985244	-0.1499997	-0.3330661	-0.4115298	-0.5767296	68087
2005	0.5200565	0.3024980	0.0452522	0.1304741	-0.2504898	74540
2006	0.0471496	0.6077305	0.5025639	0.4582647	0.6186566	67127
2007	-1.2828916	-1.0719244	-0.7466142	-0.9988909	-1.3969325	26170
2008	-0.4744662	-0.9791409	-0.9984130	-1.0110070	-0.4620659	60012
2009	0.7286867	0.3894363	0.0913193	0.1342706	0.3988854	75068
2010	0.3278463	0.5995387	-0.0228007	0.0389736	0.2838685	84685
2011	1.3804522	0.3092396	0.2728595	0.8178207	-0.2355459	75418
2012	0.2716715	0.3085555	0.3331407	0.0599877	-0.0508391	81934
2013	0.7041746	0.5348404	0.9638229	0.9420392	0.4789121	118871
2014	0.4316308	0.7035212	0.8211876	0.9991961	1.5665477	119000
2015	-1.0552476	-0.5846196	-0.2758198	-0.2954577	-0.3370502	82000
2016	-3.1728263	-3.5066937	-3.3533974	-3.1888528	-2.5380942	33000
2017	0.0503048	0.3766478	0.8494430	0.8072019	2.2484281	84000
2018	-0.1531849	0.5785767	0.4927239	0.3289629	0.2613869	113000
2019	0.2521144	1.1465457	0.7457823	0.7345936	0.6511760	95000

Once the yield reference data is merged with satellite indices, plot the timeseries to check if there is any trend

```
plot(Yield_tonnes~Year, data=df, xlab="Year", ylab = "Yield (MT)", type='l')
```

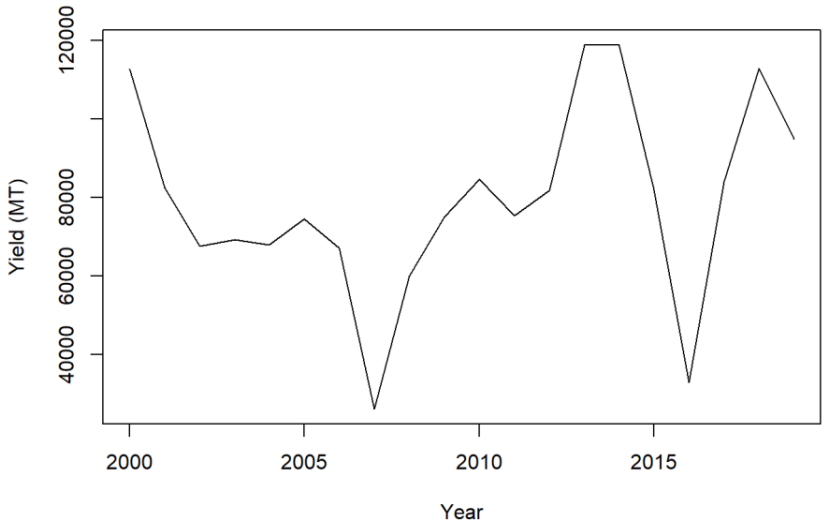

Check for any relationship between indices and maize yield from FAOSTAT in metric tones per hectare?

```
par(mfrow=c(2,2),                                                    mai=c(0.75,0.75,0.1,0.1))
plot(Yield_tonnes~NDVI, data=df, pch=16, ylab= "Yield(MT)", xlab="NDVI", cex=0.9, cex.axis=1.2, ce
x.lab=1.2)
plot(Yield_tonnes~EVI, data=df, pch=16, ylab= "Yield(MT)", xlab="NDMI", cex=0.9,cex.axis=1.2, cex.l
ab=1.2)
plot(Yield_tonnes~GPP, data=df, pch=16, ylab= "Yield(MT)", xlab="GPP", cex=0.9, cex.axis=1.2, cex.la
b=1.2)
plot(Yield_tonnes~FPAR, data=df, pch=16, ylab= "Yield(MT)", xlab="FPAR", cex=0.9, cex.axis=1.2, ce
x.lab=1.2)
```

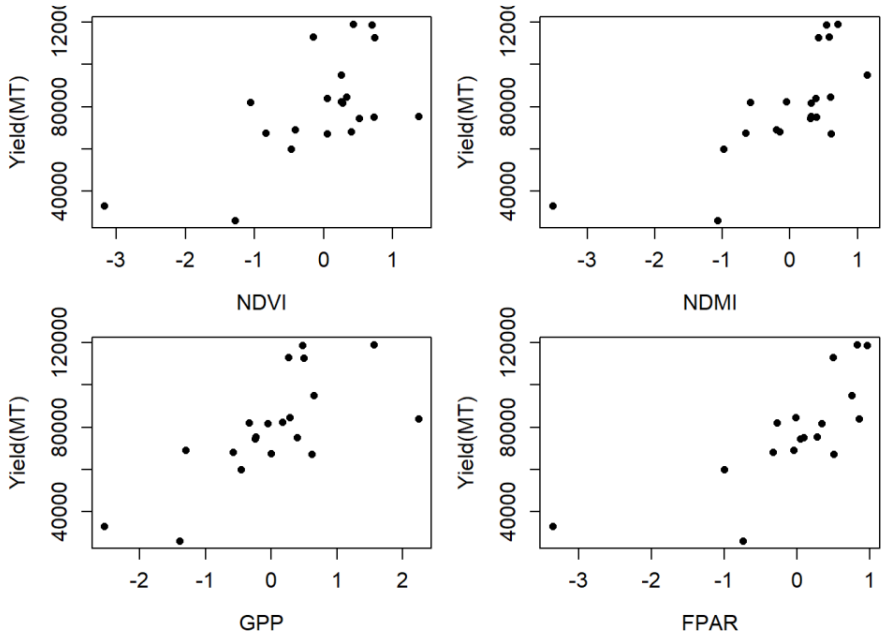

Figure 1: Relationship between maize yields and satellite metrics.

Before the yield modelling process is started, we first use random forest to check the significance of the satellite indices for maize yield prediction.

```
library(randomForest)

train <- df
data <- na.omit(df)
rf = randomForest(Yield_tonnes~., data=data[, -1], importance=TRUE, ntree = 500)
importance <- importance(rf)
importance
```

```
##          %IncMSE  IncNodePurity
## NDVI     2.023014    1598126228
## EVI 7.126598      1709219119
## FPAR     7.355854    1753478416
## LAI 7.348654      1896365793
## GPP 6.589853      1772987638
```

Next is to calculate vegetation index importance and rank

```
varImportance <- data.frame(Variables = row.names(importance),
                            Importance = round(importance[ ,'%IncMSE'],2))
```

```
rankImportance <- varImportance %>%
  mutate(Rank = paste0('#',dense_rank(desc(Importance))))
```

Plot the vegetation indices importance using ggplot2

```
library(ggthemes)
library(ggplot2)


ggplot(rankImportance, aes(x = reorder(Variables, Importance),
                           y = Importance, fill = Importance)) +
  geom_bar(stat='identity') +
  geom_text(aes(x = Variables, y = 0.5, label = Rank),
            hjust=0, vjust=0.55, size = 4, colour = 'red') +
  labs(x = 'Remote sensing metrics') +
  coord_flip() +
  theme_few(base_size = 14)
```

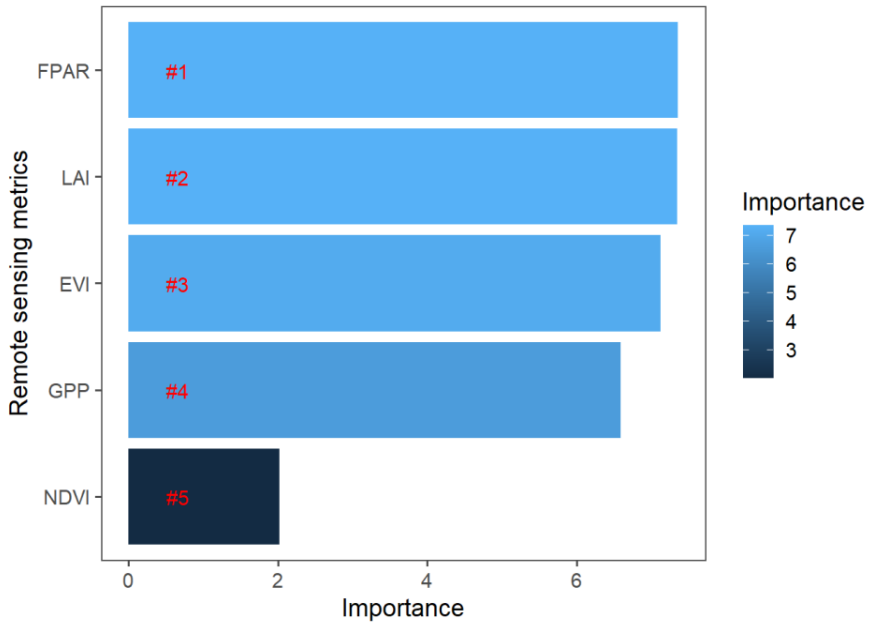

Figure 2: Importance of vegetation indices with yield

So let us predict 2020 yields using 2003-2019 indices and reference yields by training using Linear (LM), Random Forests (RF) and Support Vector Machine (SVM) machine learning models

```
train <- data[data$Year <= 2013, ] #Training data
newdata <- data[data$Year > 2013, ]
#poly model
train <- train[, -1]
```

```
#test using LM
p.lm <- lm(Yield_tonnes~., data=train)
summary(p.lm)


#test using RM

rf = randomForest(Yield_tonnes~., data=train, importance=TRUE, ntree = 500)
importance(rf)


#test using SVM

library(e1071)

svm = svm(Yield_tonnes~., data=train, kernel="radial")
svm
```

After testing the different models, the results are tuned using SVM method

```
#tune result
tuneResult <- tune(method="svm", Yield_tonnes~., data = train, ranges = list(epsilon = seq(0,1,0.1), cost
= (seq(0.5,8,.5))), kernel="radial"
)
tuneResult


#plot svm tuning results

plot(tuneResult)
```

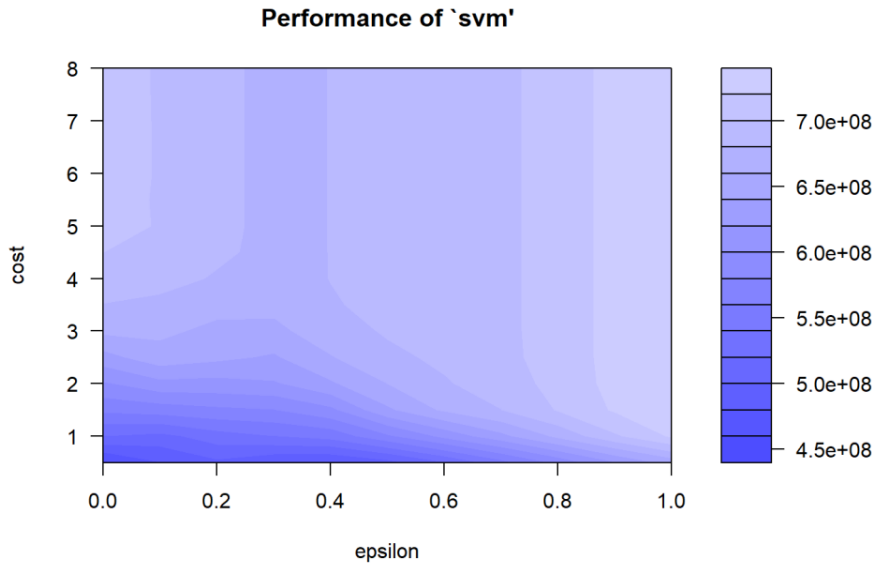

Figure 3: Tunes results from SVM model

From the SVM tuning graph we can see that the darker the region is the better our model is (because the RMSE is closer to zero in darker regions).

Model evaluation

We can use the Root Mean Square Error (RMSE) and mean absolute percentage error (MAPE) to evaluate the models' accuracies.

```
#RMSE

rmse <- function(error){
  sqrt(mean(error^2))
}


#MAPE
MAPE <- function(y_pred, y_true){
   MAPE <- mean(abs((y_true - y_pred)/y_true))
   return(MAPE*100)
}
```

Next step is to predict maize yield in the years we left out using the indices based on the models (LM, RF, SVM).

```
lm_y <- predict(p.lm, newdata[,-c(1,7)])
rf_y <- predict(rf, newdata[,-c(1,7)])
svm_y <- predict(svm, newdata[,-c(1,7)])
svm_tuned <- predict(tuneResult$best.model, newdata[,-c(1,7)])
```

Compute RMSE and MAPE from the predicted results

```
observed_y <- newdata[, "Yield_tonnes"]
#RMSE & MAPE from LOESS
rmse(observed_y-lm_y)

MAPE(observed_y, lm_y)

rmse(observed_y-rf_y)

MAPE(observed_y, rf_y)

#RMSE & MAPE from SVM not tuned
rmse(observed_y-svm_y)

rmse(observed_y-svm_tuned)

#RMSE & MAPE for tuned SVM
MAPE(observed_y,svm_tuned)
```

From the results choose a model with the lowest RMSE and MAPE and subsequently use it to predict yields in 2020. In this case RF model did better and we can use it.

```
rf <- randomForest(Yield_tonnes~., data=na.omit(df[,-1]), importance=TRUE, ntree = 500)
newdata <- index[index$Year==2020, ]
rf_y <- predict(rf, newdata)
rf_y
```

References

[1] Catherine Nakalembe, Inbal Becker-Reshef, Rogerio Bonifacio, Guangxiao Hu, Micheal Lawrence Humber, Christina Jade Justice, John Keniston, Kenneth Mwangi, Felix Rembold, Shraddhanand Shukla, Ferdinando Urbano, Alyssa Kathleen Whitcraft, Yanyun Li, Mario Zappacosta, Ian Jarvis, and Antonio Sanchez. A review of satellite-based global agricultural monitoring systems available for Africa. *Global Food Security*, 29:100543, 2021.

[2] Jayme Garcia Arnal Barbedo. A review on the use of unmanned aerial vehicles and imaging sensors for monitoring and assessing plant stresses. *Drones*, 3(2):1–27, 2019.

[3] Arnab Kumar Saha, Jayeeta Saha, Radhika Ray, Sachet Sircar, Subhojit Dutta, Soummyo Priyo Chattopadhyay, and Himadri Nath Saha. IOT-based drone for improvement of crop quality in agricultural field. In *2018 IEEE 8th Annual Computing and Communication Workshop and Conference (CCWC)*, pages 612–615. IEEE, 2018.

[4] Nadia Delavarpour, Cengiz Koparan, John Nowatzki, Sreekala Bajwa, and Xin Sun. A technical study on UAV characteristics for precision agriculture applications and associated practical challenges. *Remote Sensing*, 13(6):1–25, 2021.

[5] Luana Mendes dos Santos, Brenon Diennevan Souza Barbosa, and Alan Delon Andrade. Use of remotely piloted aircraft in precision agriculture: a review. *Dyna*, 86(210):284–291, 2019.

[6] Sebastian Siebert and Jochen Teizer. Mobile 3D mapping for surveying earthwork projects using an Unmanned Aerial Vehicle (UAV) system. *Automation in construction*, 41:1–14, 2014.

[7] Caroline Dookie, Yianna Lambrou, and Hajnalka Petrics. *A tool for gender-sensitive agriculture and rural development policy and programme formulation: Guidelines for Ministries of Agriculture and FAO.* Food and Agriculture Organization of the United Nations (FAO), 2013.

[8] Tasokwa Kakota, Dickson Nyariki, David Mkwambisi, and Wambui Kogi-Makau. Gender vulnerability to climate variability and household food insecurity. *Climate and development*, 3(4):298–309, 2011.

[9] Christian Nellemann, Ritu Verma, and Lawrence Hislop. Women at the frontline of climate change: Gender risks and hopes. *A Rapid Response Assessment. United Nations Environment Programme, GRID-Arendal*, 2011.

[10] Cheryl R Doss, Caren Grown, and Carmen Diana Deere. Gender and asset ownership: A guide to collecting individual-level data. *World Bank policy Research working paper*, (4704), 2011.

[11] Terri Raney. The state of food and agriculture. *Women in Agriculture: Closing the Gap for Development*, 2, 2011.

[12] Valerie Nelson and Tanya Stathers. Resilience, power, culture, and climate: a case study from semi-arid Tanzania, and new research directions. *Gender & development*, 17(1):81–94, 2009.

[13] Amber Peterman, Agnes Quisumbing, Julia Behrman, and Ephraim Nkonya. Understanding the complexities surrounding gender differences in agricultural productivity in Nigeria and Uganda. *Journal of Development Studies*, 47(10):1482–1509, 2011.

[14] Amelia H X Goh. A literature review of the gender-differentiated impacts of climate change on women's and men's assets and well-being in developing countries. *International Food Policy Research Institute, CAPRi Work*, pages 1–44, 2012.

[15] Y Carvajal-Escobar, M Quintero-Angel, and M Garcia-Vargas. Women's role in adapting to climate change and variability. *Advances in Geosciences*, 14:277–280, 2008.

[16] Agnes R Quisumbing, Ruth Meinzen-Dick, Terri L Raney, André Croppenstedt, Julia A Behrman, and Amber Peterman. Gender in agriculture. *Springer*, 102072:444, 2014.

[17] Ruth Meinzen-Dick, Nancy Johnson, Agnes R Quisumbing, Jemimah Njuki, Julia A Behrman, Deborah Rubin, Amber Peterman, and Elizabeth Waithanji. The Gender Asset Gap and Its Implications for Agricultural and Rural Development BT - Gender in Agriculture: Closing the Knowledge Gap. In Agnes R Quisumbing, Ruth Meinzen-Dick, Terri L Raney, André Croppenstedt, Julia A Behrman, and Amber Peterman, editors, *Gender in Agriculture*, pages 91–115. Springer Netherlands, Dordrecht, 2014.

[18] Julia A Behrman, Ruth Meinzen-Dick, and Agnes R Quisumbing. Understanding gender and culture in agriculture: the role of qualitative and quantitative approaches. In *Gender in Agriculture*, pages 31–53. Springer, 2014.

[19] K Chung. Using qualitative methods to improve the collection and analysis of data from LSMS household surveys. *Designing household survey questionnaires for developing countries: Lessons from 10 years of LSMS experience*, 2000.

[20] Ali Ahmad, Javier Ordoñez, Pedro Cartujo, and Vanesa Martos. Remotely piloted aircraft (RPA) in agriculture: A pursuit of sustainability. *Agronomy*, 11(1), 2020.

[21] Cheryl R. Doss. Designing agricultural technology for African women farmers: Lessons from 25 years of experience. *World Development*, 29(12):2075–2092, 2001.

[22] Agnieszka Jenerowicz, Katarzyna Siok, Malgorzata Woroszkiewicz, and Agata Orych. The fusion of satellite and UAV data: simulation of high spatial resolution band. (November 2017):76, 2017.

[23] Thierry Ranchin and Lucien Wald. Data fusion in remote sensing of urban and suburban areas. In *Remote Sensing of Urban and Suburban Areas*, pages 193–218. Springer, 2010.

[24] Harvey B Mitchell. *Image fusion: theories, techniques and applications*. Springer Science & Business Media, 2010.

[25] Yujiao Zou, Guangming Li, and Shuai Wang. The fusion of satellite and unmanned aerial vehicle (UAV) imagery for improving classification performance. In *2018 IEEE International Conference on Information and Automation (ICIA)*, pages 836–841. IEEE, 2018.

[26] Mohamed R Metwalli, Ayman H Nasr, Osama S Farag Allah, and S El-Rabaie. Image fusion based on principal component analysis and high-pass filter. In *2009 International Conference on Computer Engineering & Systems*, pages 63–70. IEEE, 2009.

[27] Licheng Zhao, Yun Shi, Bin Liu, Ciara Hovis, Yulin Duan, and Zhongchao Shi. Finer classification of crops by fusing UAV images and Sentinel-2A data. *Remote Sensing*, 11(24):3012, 2019.

[28] Teja Kattenborn, Javier Lopatin, Michael Förster, Andreas Christian Braun, and Fabian Ewald Fassnacht. UAV data as alternative to field sampling to map woody invasive species based on combined Sentinel-1 and Sentinel-2 data. *Remote sensing of environment*, 227:61–73, 2019.

[29] Claudia Kuenzer, Stefan Dech, and Wolfgang Wagner. Remote sensing time series revealing land surface dynamics: Status quo and the pathway ahead. In *Remote Sensing Time Series*, pages 1–24. Springer, 2015.

[30] Robert Beach, Daniel Lapidus, Meghan Hegarty-Craver, Maggie O'Neil, James Rineer, and Dorota Temple. Crop mapping using Sentinel-1 and Sentinel-2 imagery and UAV-acquired ground truth data. *Gates Open Res*, 4, 2020.

[31] Anna Chlingaryan, Salah Sukkarieh, and Brett Whelan. Machine learning approaches for crop yield prediction and nitrogen status estimation in precision agriculture: A review. *Computers and Electronics in Agriculture*, 151:61–69, 2018.

[32] Andreas Kamilaris and Francesc X Prenafeta-Boldú. Deep learning in agriculture: A survey. *Computers and electronics in agriculture*, 147:70–90, 2018.

[33] Leo Breiman. Random Forests. *Machine Learning*, 45(1):5–32, 2001.

[34] Ministry of Tourism and Environmental Affairs. Eswatini Third National Communication to the UNFCCC. Technical report, 2016.

[35] The World Bank Group. Climate Risk Country Profile - Eswatini. 2021.

[36] Shraddhanand Shukla, Denis Macharia, Gregory J Husak, Martin Landsfeld, Catherine Lilian Nakalembe, S Lucille Blakeley, Emily Caitlin Adams, and Juliet Way-Henthorne. Enhancing Access and Usage of Earth Observations in Environmental Decision-Making in Eastern and Southern Africa Through Capacity Building , 2021.

[37] Inbal Becker-Reshef, Christina Justice, Brian Barker, Michael Humber, Felix Rembold, Rogerio Bonifacio, Mario Zappacosta, Mike Budde, Tamuka Magadzire, Chris Shitote, Jonathan Pound, Alessandro Constantino, Catherine Nakalembe, Kenneth Mwangi, Shinichi Sobue, Terence Newby, Alyssa Whitcraft, Ian Jarvis, and James Verdin. Strengthening agricultural decisions in countries at risk of food insecurity: The GEOGLAM Crop Monitor for Early Warning. *Remote Sensing of Environment*, 237(December 2019):111553, 2020.